VOT 74511

DEVELOPMENT OF ZEOLITE CATALYST FOR THE CONVERSION OF NATURAL GAS TO ULTRACLEAN LIQUID FUEL
(PEMBANGUNAN MANGKIN ZEOLITE UNTUK PENUKARAN GAS ASLI KEPADA CECAIR BAHAN API YANG ULTRABERSIH)

PROF DR NOR AISHAH SAIDINA AMIN
KUSMIYATI
SOON EE PENG
SRI RAJ AMMASI

PUSAT PENGURUSAN PENYELIDIKAN
UNIVERSITI TEKNOLOGI MALAYSIA

2007

UNIVERSITI TEKNOLOGI MALAYSIA

BORANG PENGESAHAN
LAPORAN AKHIR PENYELIDIKAN

TAJUK PROJEK : DEVELOPMENT OF ZEOLITE CATALYST FOR THE CONVERSION OF NATURAL GAS TO ULTRACLEAN LIQUID FUEL

Saya _____PROF NOR AISHAH SAIDINA AMIN_____
(HURUF BESAR)

Mengaku membenarkan **Laporan Akhir Penyelidikan** ini disimpan di Perpustakaan Universiti Teknologi Malaysia dengan syarat-syarat kegunaan seperti berikut :

1. Laporan Akhir Penyelidikan ini adalah hakmilik Universiti Teknologi Malaysia.
2. Perpustakaan Universiti Teknologi Malaysia dibenarkan membuat salinan untuk tujuan rujukan sahaja.
3. Perpustakaan dibenarkan membuat penjualan salinan Laporan Akhir Penyelidikan ini bagi kategori TIDAK TERHAD.
4. * Sila tandakan (/)

[ ]	SULIT	(Mengandungi maklumat yang berdarjah keselamatan atau Kepentingan Malaysia seperti yang termaktub di dalam AKTA RAHSIA RASMI 1972).
[ ]	TERHAD	(Mengandungi maklumat TERHAD yang telah ditentukan oleh Organisasi/badan di mana penyelidikan dijalankan).
[√]	TIDAK TERHAD	

_____
TANDATANGAN KETUA PENYELIDIK

PROF. DR. NOR AISHAH SAIDINA AMIN
Nama & Cop Ketua Penyelidik

Tarikh : _17 Ogos 2007___

CATATAN : ***** *Jika Laporan Akhir Penyelidikan ini SULIT atau TERHAD, sila lampirkan surat daripada pihak berkuasa/organisasi berkenaan dengan menyatakan sekali sebab dan tempoh laporan ini perlu dikelaskan sebagai SULIT dan TERHAD.*

VOT 74511

DEVELOPMENT OF ZEOLITE CATALYST FOR THE CONVERSION OF NATURAL GAS TO ULTRACLEAN LIQUID FUEL
(PEMBANGUNAN MANGKIN ZEOLITE UNTUK PENUKARAN GAS ASLI KEPADA CECAIR BAHAN API YANG ULTRABERSIH)

PROF DR NOR AISHAH SAIDINA AMIN
KUSMIYATI
SOON EE PENG
SRI RAJ AMMASI

Jabatan Kejuruteraan Kimia
Fakulti Kej Kimia dan Kej. Sumber Asli
Universiti Teknologi Malaysia

2007

DEVELOPMENT OF ZEOLITE CATALYST FOR THE CONVERSION OF NATURAL GAS TO ULTRACLEAN LIQUID FUEL

ABSTRACT

The use of crude oil as the feedstock for gasoline production has a major drawback due to depleting oil deposits. On the contrary, natural gas is available in abundance; therefore, it is considered to be a more attractive alternative source for gasoline production. Extensive research efforts have been devoted to the direct conversion of methane to higher hydrocarbons and aromatics. The transformation of methane to higher hydrocarbons and aromatics has been studied under oxidative and non-oxidative conditions. The chemical equilibrium compositions of methane oxidation to higher hydrocarbons have been calculated using the minimum total Gibbs energy approach. The results showed that the conversion of methane increased with oxygen concentration and reaction temperature, but decreased with pressure. In term of catalyst development, it was found that the W-H_2SO_4/HZSM-5 catalyst prepared with acidic solution showed the highest activity for the conversion of methane to gasoline in the absence and presence of oxygen. The performance of the Li modified W/HZSM-5 catalyst was improved which was attributed to the suitable amount of Brönsted acid sites in the catalyst. The dual reactor system which consisted of OCM and oligomerization reactors was also investigated. The result yielded liquid fuels comprising of C_5-C_{10} aromatics and aliphatics hydrocarbons. In another approach dual bed system was studied and it was found that Ni/H-ZSM-5 was a suitable catalyst for the conversion of methane to gasoline products. Kinetic studies on methane conversion in the presence of co-feeds ethylene and methanol to produce higher hydrocarbons in gasoline range was performed. The reaction rate increased when methane concentration in the feed mixture decreased. The correlation between experimental and calculated reaction rate indicates that the model fits the data well.

ABSTRAK

Penggunaan minyak mentah sebagai bahan mentah dalam penghasilan gasolin mempunyai satu kelemahan kerana pengurangan deposit minyak. Sebaliknya, gas asli terdapat dalam jumlah yang banyak; oleh itu, ia menjadi satu sumber alternatif yang menarik bagi penghasilan gasolin. Usaha penyelidikan yang meluas telah ditumpukan kepada penukaran secara langsung metana kepada hidrokarbon tinggi dan aromatik. Penukaran metana kepada hidrokarbon tinggi dan aromatik telah dikaji di bawah keadaan beroksigen dan tanpa oksigen. Komposisi kesetaraan kimia pengoksidaan metana kepada hidrokarbon dikira menggunakan pendekatan minimum jumlah tenaga Gibbs. Keputusan menunjukkan penukaran metana meningkat dengan peningkatan kepekatan oksigen dan suhu tindakbalas, tetapi menyusut dengan tekanan. Dalam pembangunan katalis, didapati bahawa katalis W-H_2SO_4/HZSM-5 yang disediakan dengan larutan berasid menunjukkan aktiviti tertinggi bagi penukaran metana kepada gasolin dalam kehadiran dan ketiadaan oksigen. Prestasi katalis W/HZSM-5 terubahsuai Li telah diperbaiki yang mana telah menyumbang kepada jumlah tapak aktif Brönsted yang sesuai di dalam mangkin. Sistem dwi-reaktor yang mengandungi OCM dan reaktor pengoligomeran juga dikaji. Keputusan memberikan hasil larutan bahan api yang terdiri daripada hidrokarbon alifatik dan aromatik $C_5 - C_{10}$. Dalam pendekatan yang lain, sistem dwi lapisan telah dikaji dan didapati bahawa Ni/H-ZSM-5 merupakan mangkin yang sesuai bagi penukaran metana kepada produk gasolin. Kajian kinetik bagi penukaran metana dalam kehadiran bahan mentah sokongan etelena dan metanol untuk menghasilkan hidrokarbon tinggi dalam julat gasolin telah dijalankan. Kadar tindakbalas meningkat apabila kepekatan metana dalam campuran bahan mentah berkurang. Kaitan antara eksperimental dan kadar tindakbalas yang telah dikira menunjukkan bahawa model adalah menepati data.

TABLE OF CONTENTS

OF CO-FEEDING

LIST OF TABLES

LIST OF FIGURES

LIST OF SYMBOLS/ABBREVIATIONS

Calc	Calculated
Eq.	Equation
Exp	experimental
E_a	activation energy, J/mol
F	objective function
ΔG	Gibbs free energy, J/mol
ΔH_{ads}	adsorption enthalpy, J/mol
ΔH_i	heat of reaction i, J/mol
k_o	frequency factor
k_{rs}	surface reaction rate constant (controlling step), kmol/kg_{cat}.h atm
K_i	equilibrium constant
P_j	partial pressure of component j, atm
r_i	reaction rate, kmol/kgmol.h
R	constant of ideal gas, 8.314 J/mol.K
ΔS_{ads}	adsorption entropy, J/mol.K
ΔS	entropy of reaction i, J/mol.K
T	temperature, K
W	mass of catalyst, kg
X_{CH4}	methane conversion
$\sum$	n-ary summation
+	plus
λ	Lagrange multiplier of element k
υ	the total stoichiometric number
Φ_i	fugacity coefficient of species i in solution. The Φ_i are all unity if the assumption of ideal gases is justified in all cases

CHAPTER 1

DUAL EFFECTS OF SUPPORTED W CATALYSTS FOR DEHYDROAROMATIZATION OF METHANE IN THE ABSENCE OF OXYGEN

Abstract

The screening of a series of W-based catalysts on different supports i.e. HZSM-5, Hβ, USY and Al_2O_3 for the dehydroaromatization of methane (DHAM) revealed that HZSM-5 emerged as the best support. Next, the performance of W/HZSM-5 and W-H_2SO_4/HZSM-5 catalysts for the DHAM reaction was compared to study the effect of acidic treatment in the impregnation method. The results showed that the optimum activity of W-H_2SO_4/HZSM-5 catalyst exceeded that of W/HZSM-5 catalyst. Finally, the influence of Si/Al ratio in the W-H_2SO_4/HZSM-5 catalyst was studied and the catalyst with Si/Al ratio=30 was found to be the most promising for the DHAM reaction. The remarkable activity of the catalyst is attributed to the presence of dual effects: suitable content of octahedral polymeric and tetrahedral monomeric tungstate species accompanied by proper amount and strength of acid sites in the catalyst.

Keywords: DHAM, W-based catalyst, dual effects

1.1 Introduction

DHAM to aromatics have received considerable attentions [1-18] in the study of catalytic reactions. The most common catalysts reported to be promising for DHAM are HZSM-5 supported Mo and also W catalysts [2-18]. Some of the characteristics of an active DHAM catalyst include a highly dispersed active metal species on the surface and also a proper amount of acidity for the support [1-12]. Mo-based catalysts supported on HZSM-5 have been used for catalytic reaction of DHAM in the absence of oxygen. By using *in situ* FT-IR pyridine technique the acid sites of Mo/HZSM-5 and the interaction between Mo species and HZSM-5 were investigated [2]. By combining FT-IR study with catalytic evaluation, it was concluded that Mo/HZSM-5, which had a 60% remaining number of original Brönsted acid sites exhibited a good catalytic performance. In addition, Naccache et al. (2002) [3] reported that the formation of Mo_2C species in Mo/HZSM-5 under methane stream was responsible for the formation of aromatics. The reaction mechanism for the production of aromatics proceeded via the formation of acetylene from methane on Mo_2C and the acetylene subsequently oligomerized into aromatics. ^{27}Al and ^{29}Si MAS NMR were employed to investigate the interaction between Mo species and HZSM-5 [13]. The results revealed that strong interaction occurred between the metal species and HZSM-5 on Mo/HZSM-5 with relatively higher amount of Mo species and caused the framework aluminum to be extracted into the extra framework. As a consequence, the catalytic activity dropped dramatically.

Recently, many authors reported that the activity and stability of a HZSM-5 supported W catalyst for DHAM increased at a relatively high temperature [4-7, 14]. Improved active and heat-resisting catalysts for DHAM have also been developed by the incorporation of Zn (or Mn, La, Zr) into W/HZSM-5 [4-6]. The present work studies the dehydroaromatization of methane over a series of 3 wt %W based catalysts prepared with different supports, under different preparation conditions and several Si/Al ratios. The relationship between the nature of tungsten species and the acidic sites of the catalysts with the catalytic activity is reported.

1.2 Experimental Procedure

1.2.1 Catalyst preparation

A series of 3 % W-based catalysts with different supports were prepared by aqueous impregnation of support materials (HZSM-5 ; Hβ ; USY ; Al_2O_3) with ammonium meta tungsten ($(NH_4)_6W_{12}O_{40}.H_2O$) solution, followed by drying at 393 K for 2 h and calcining at 773 K for 5 h. Another set of a series of 3 % W-H_2SO_4/HZSM-5 catalysts with different Si/Al ratios were prepared by impregnating HZSM-5 with ($(NH_4)_6W_{12}O_{40}.H_2O$) and H_2SO_4 solution (pH =2-3) followed by drying and calcining at the same previous conditions. All the catalysts were pressed, crushed, and sieved to a size of 30-60 mesh.

1.2.2 Catalyst Characterization

The BET surface area and the pore volume of the samples were obtained by means of nitrogen adsorption determined at 77 K in a Thermo Finnigan surface area analyzer. The acidity of the catalysts was measured by means of TPD-ammonia using a Micromeritics TPD/TPR/O analyzer. The samples were pretreated in flowing nitrogen at 15 K/min. up to 873 K and then cooled to 383 K. Next, the samples were saturated with pure ammonia followed by flushing the physically adsorbed ammonia in helium stream at 373 K for 1 h. Finally, the sample was heated up to 873 K in a heating rate of 15 K/min. The recorded spectra represent the number and strength of the catalyst acidity. The nature of W species on the catalysts was determined by means of UV diffuse reflectance spectra. UV DRS spectra were performed on a Perkin-Elmer Lamda-900 spectrometer. The scanning wavelength range was 198-500 nm and the scan speed was 120 nm/min.

1.2.3 Catalyst Evaluation

The catalyst test was conducted in a micro fixed-bed quartz reactor with internal diameter of 9 mm and length of 300 mm under atmospheric condition. In each run, the catalyst charge was 1 g. Prior to the catalytic testing, the catalysts were pretreated in nitrogen stream for 1 h at 823 K. Feed gas containing CH_4+ 10 % N_2 were passed through over the catalyst bed at WHSV of 1800 $ml.g^{-1}.h^{-1}$. Nitrogen was used as an internal standard for calculating the methane conversion and selectivity of the reaction products. The reaction products were analyzed by a Hewlett-Packard 5890 on-line GC equipped with TCD using Porapak Q, molecular sieve 5A, UCW 982, and DC 200 columns.

1.3 Results and discussion

1.3.1 Catalytic performance of supported W catalysts

Figures 1.1 (A)-(C) show the methane conversion and product selectivity as a function of time on stream over W/USY, W/Al_2O_3, W/Hβ, W/HZSM-5 and W-H_2SO_4/HZSM-5 catalysts. It can be seen that methane conversion decrease gradually with increasing time on stream over all the catalysts. Without considering the acidified effect of W supported on HZSM-5 catalyst, the data on conversion reveal that W/HZSM-5 catalyst, prepared using a neutral solution in the impregnation method, is the most active. The effect of preparation condition using H_2SO_4 solution with pH=2 – 4 for the impregnation method was studied by comparing the activities of W/HZSM-5 and W-H_2SO_4/HZSM-5. The result shows that W-H_2SO_4/HZSM-5 gives higher methane conversion than W/HZSM-5 catalyst at the initial time on stream (within 100 min) and exhibits a maximum value of 9.59 % at 973 K and

GHSV =1800 ml/g.h., but decreases very rapidly beyond that. The rapid deactivation observed for W-H_2SO_4/HZSM-5 catalyst after reaching its maximum conversion at temperature of 1073 K, pressure of 0.1 MPa, and GHSV of 1500 ml/h.g-cat, respectively is similar to the work reported by Zeng et al. [4]. Figure 1.1 (B) exhibits the corresponding aromatics selectivity for DHAM over 3 % W-based catalysts with different supports. Obviously, the aromatics selectivity over all the catalysts decreases steadily with time on stream after reaching maximum. Over the whole time on stream, it can be seen that W-H_2SO_4/HZSM-5 displays the highest aromatics selectivity having maximum at 99.5 % whereas the lowest aromatics selectivity on stream is observed over W/Al_2O_3 catalyst.

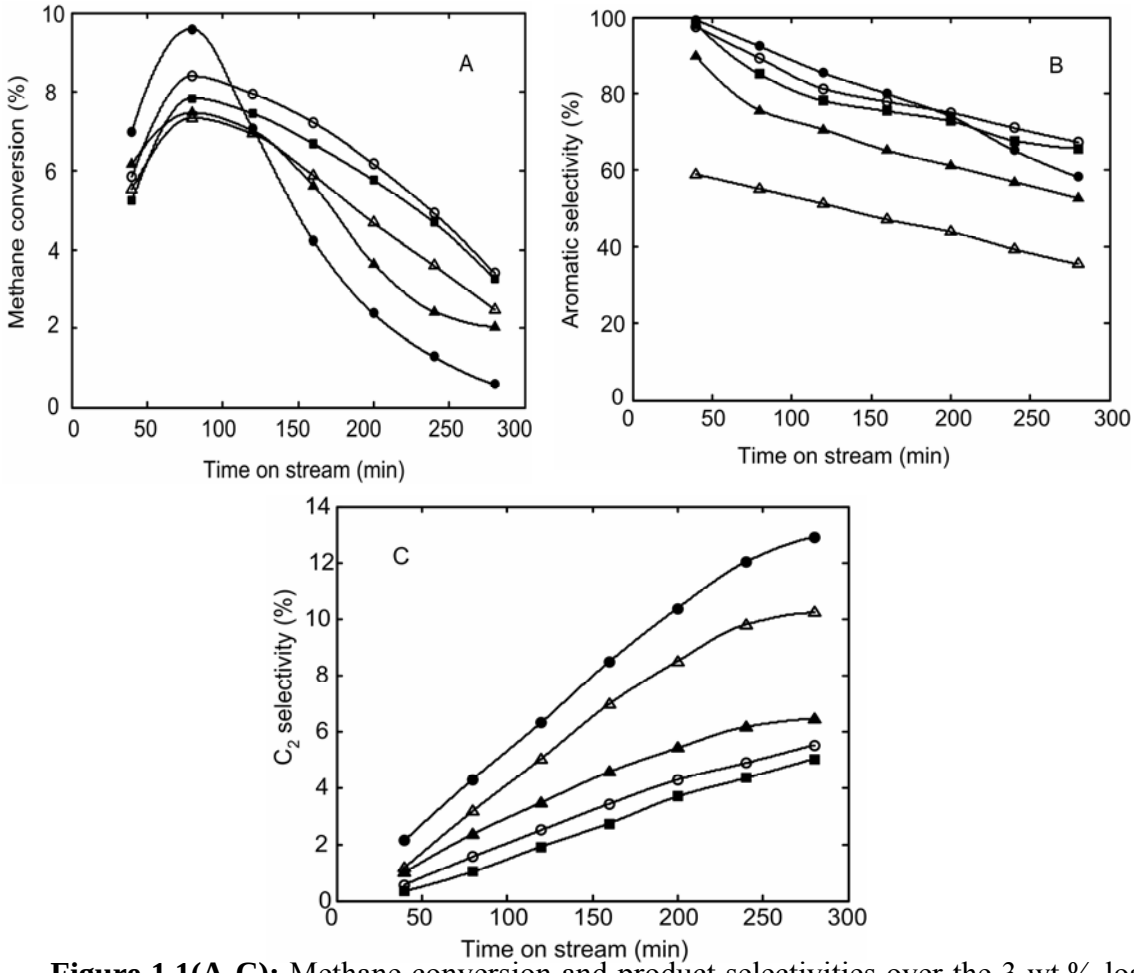

Figure 1.1(A-C): Methane conversion and product selectivities over the 3 wt.%-loading W catalysts with various supports for DHAM at 973 K , GHSV=1800 ml/g.h , Feed Gas = CH_4 + 10% N_2, 1 atm. Catalysts: (●)W-H_2SO_4/HZSM-5 (Si/Al=30); (○)W/HZSM-5 (Si/Al=30 ; (■)W/Hβ(Si/Al=25); (▲)W/USY(Si/Al=5.1); (△)W/Al_2O_3.

In addition to aromatics, the products also contain C_2 hydrocarbons, but to a lesser extent. The selectivity of C_2-hydrocarbons (C_2H_4 and C_2H_6) over the 3 wt. %-loading W catalysts with various supports is given in Figure 1.1 (C). As can be seen, considerable amount of C_2 is produced over W/Al_2O_3 catalyst compared with other W supported catalysts. Between the W/HZSM-5 and $W\text{-}H_2SO_4$/HZSM-5 catalysts, the C_2-hydrocarbons selectivity is higher over the latter than that the former. Meanwhile, the selectivity of C_2-hydrocarbons over W/Hβ and W/USY catalysts are lower than that over the $W\text{-}H_2SO_4$/HZSM-5 and W/Al_2O_3 catalysts.

Next, the effect of Si/Al ratio in the acidified W based catalyst using HZSM-5 as a support was determined. Several $W\text{-}H_2SO_4$//HZSM-5 catalysts with different Si/Al ratios were prepared by the impregnation method in acidic solution with pH 2-3. The variation of methane conversion over 3% wt. $W\text{-}H_2SO_4$/HZSM-5 with different Si/Al ratios is presented in Figures 1.2(A). The results indicate that methane conversion is dependent on the Si/Al ratio of the HZSM-5 support. The higher is the Si/Al ratio, the lower the methane conversion will be. A methane conversion over 3 wt.% $W\text{-}H_2SO_4$/HZSM-5 catalyst with Si/Al =30 approaches a maximum at 22.08 %, and further increases in the Si/Al ratio leads to a decline in the methane conversion. Meanwhile, the selectivity of aromatics over 3 wt. % $W\text{-}H_2SO_4$/HZSM-5 with different Si/Al ratios is presented in Figure 1.2 (B). A maximum in the aromatics selectivity of 97.49 % is achieved over the 3% $W\text{-}H_2SO_4$/HZSM-5 (Si/Al ratio=30) catalyst. On the other hand, the C_2 selectivity over 3% $W\text{-}H_2SO_4$/HZSM-5 with various Si/Al ratios increase with an increase in the time on stream, as seen in Figure 1.2 (C). A gradual but significant increment in the on stream C_2 selectivity from 2.69 % to 12.19 % was observed over the 3% $W\text{-}H_2SO_4$/HZSM-5 catalyst with Si/Al=30.

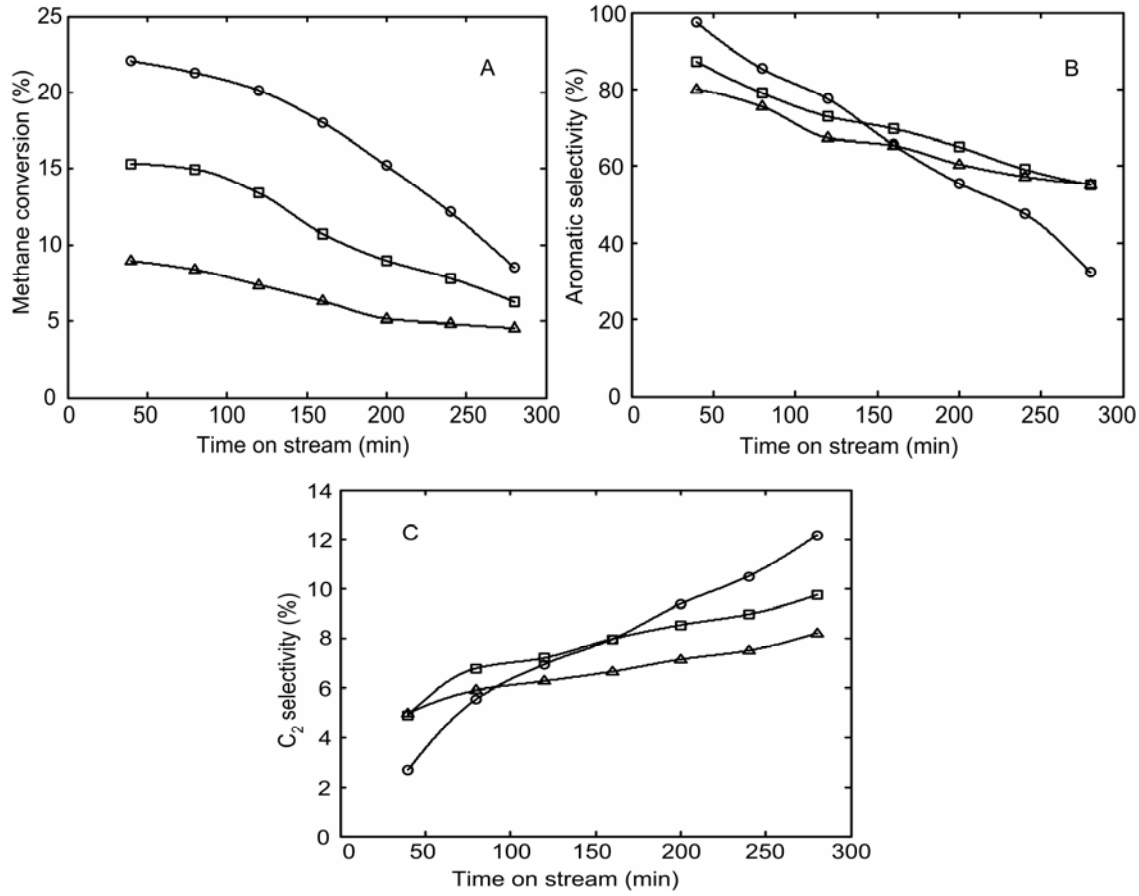

Figure 1.2 (A-C): Effect of Si/Al ratio on the methane conversion and product selectivities over 3 wt.% W-H_2SO_4/HZSM-5 catalysts for dehydroaromatization of methane at 1073 K , GHSV=1800 ml/g.h Feed Gas = CH_4 + 10% N_2, 1 atm. Catalysts : (O)W-H_2SO_4/HZSM-5 (Si/Al=30); (□)W-H_2SO_4/HZSM-5 (Si/Al=50); (△) W-H_2SO_4/HZSM-5 (Si/Al=80).

Further investigation was carried out to study the effect of GHSV on the catalytic activity over W-H_2SO_4/HZSM-5 catalysts with different Si/Al ratios. The results are presented in Figures 1.3 (A), (B), (C) for the dependence of GHSV on methane conversion, aromatic selectivity and C_2-hydrocarbons, respectively. The influence of GHSV on the catalysts activity for non oxidative DHAM reaction has been studied in various range of the GHSV [6, 18]. In the present work, GHSV in the range of 3000 – 9000 ml/g/h was applied. The results show that methane conversion and aromatic selectivity decrease significantly, while C_2 hydrocarbons selectivity increase obviously with increasing GHSV

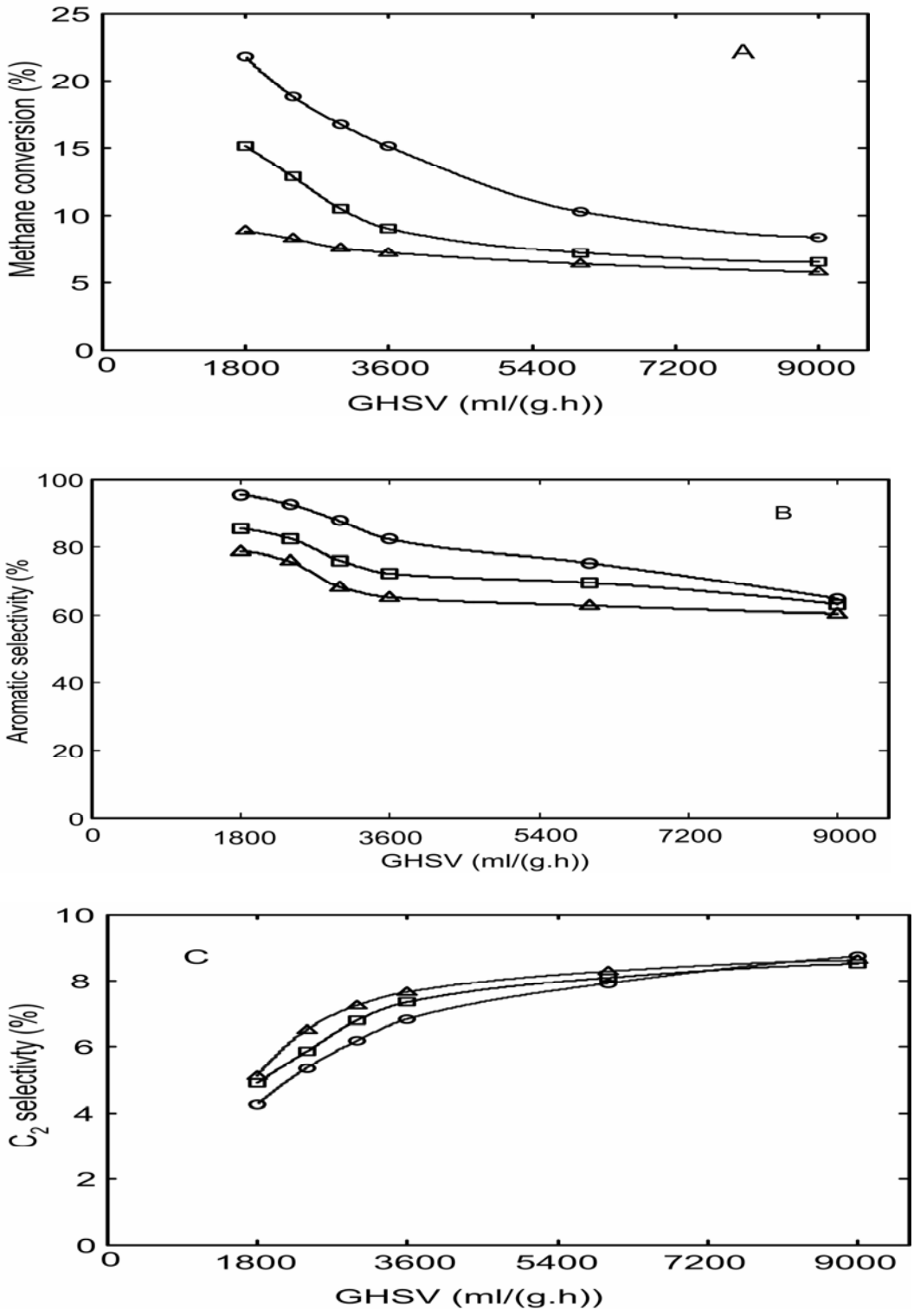

Figure 1.3 (A-C): Effect of GHSV on: (A) methane conversion, (B) aromatics selectivity and (C) C_2 hydrocarbons. Catalysts: (O) W-H_2SO_4/HZSM-5 (Si/Al=30); (□) W-H_2SO_4/HZSM-5 (Si/Al=50); (△) W-H_2SO_4/HZSM-5 (Si/Al=80). Reaction conditions: 1073 K, feed gas: CH4 + N_2, 1 atm, the data taken at 1 h after the reaction starts.

As can be seen in Figure 1.3, the decreasing activity with time on stream over all the 3 % W-H_2SO_4/HZSM-5 catalysts with different Si/Al ratios exhibits a similar trend indicating that GHSV is unfavorable to methane conversion and formation of aromatics product. A similar observation has been confirmed previously [6]. Furthermore, from Figure 1.3 it can be seen the rapid decline in methane conversion and selectivity of aromatics of 3 %W-H_2SO_4/HZSM- 5 catalyst with Si/Al =30, while, a gradual decrease over both the catalysts with Si/Al = 50 and 80 are observed. The trend could be attributed to coke formation. In addition, study on the effect of adding O_2 into methane feed gas for DHAM reaction over 3W-H_2SO_4/HZSM-5 (Si/Al=30) catalyst was performed to enhance the catalyst activity.

The result in Figure 1.4 shows that the activity of catalyst is improved significantly after introducing 2 % O_2 in methane feed. It has been reported by several authors [1, 6,8,17,19] that the addition a suitable amount of oxidants such as CO, CO_2 and O_2 into methane feed resulted in remarkable enhancement in the catalyst activity and stability due to suppression of coke deposited in the catalyst. In the oxidative condition, the aromatics and C_2-hydrocarbons products accompanied by COx (CO and CO_2) as side-products were detected. Meanwhile, in the non oxidative condition, the aromatic and C_2-hydrocarbons were detected with negligible amount of COx. The results of activity testing reveal that, in the presence of O_2 in methane feed, methane conversion decreases by 40.1 % of its initial value (17.59 %) and the corresponding selectivity to aromatics decrease slightly from 85.29 % to 63.25 % within 360 minute time on stream. In the non oxidative condition, the reduction of methane conversion is 81.75 % of its initial value (15.46 %) accompanied by a quick decline in the aromatic selectivity from 75.94 % to 16.27 % after 360 minute of reaction. On the contrary, the C_2-hydrocarbons increase with increasing time on stream from 3.67 to 11.74 % for the oxidative condition. In the presence of oxygen, C_2-hydrocarbons, initially, increase then decrease with increasing time probably due to deposition of coke leading to diminishing C_2 hydrocarbons selectivity.

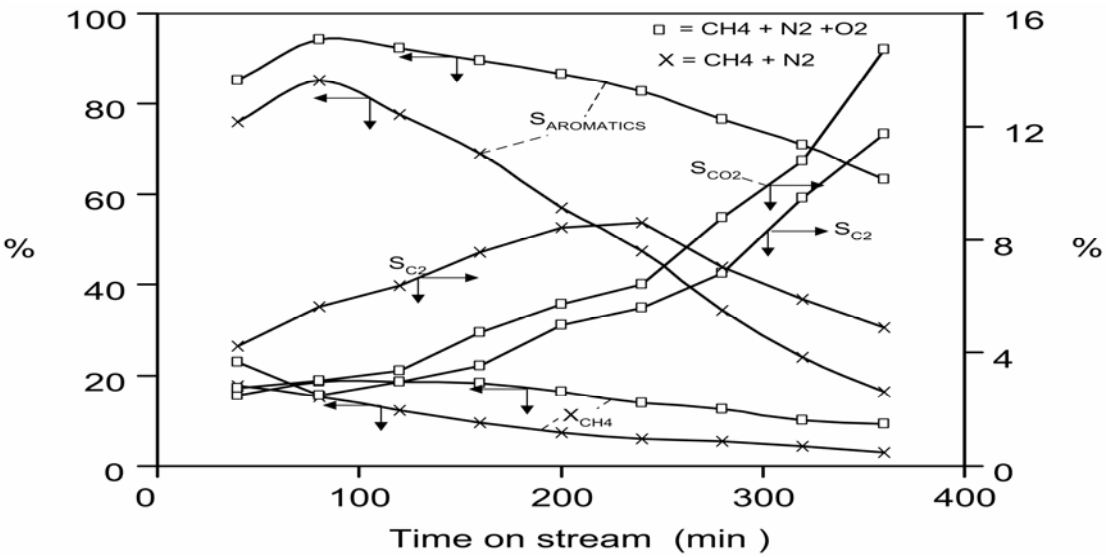

Figure 1.4: Comparison between oxidative and non oxidative of DHAM reactior 3 %W-H_2SO_4/HZSM-5. (Si/Al=30) at 1073 K, GHSV=3000 ml/g/h, 1 atm.

1.3.2 Correlation between activity and characterization of supported W catalysts

The different activities and stabilities exhibited by a series of the 3 % W-based catalysts with different supports in the DHAM suggest that the physico-chemical properties of the catalyst support affect the performance of the catalysts. HZSM-5 possesses two-dimensional pore structure with a 10-membered ring. Its pore system consists of a straight channel with pore diameter of 5.3 x 5.6 Å. Hβ has a two-dimensional pore structure which consists of 12-membered rings with diameter of 7.6 x 6.4 whilst USY is a large-pore zeolite, with a three-dimensional straight channel with supercage pore system [15].

The BET surface area and micropore volume of supported W based catalysts are given in Table 1.1. It can be seen that the BET surface area decrease in the following order W/USY>W/Hβ>W/HZSM-5>WAl_2O_3 while the micropore volume

of the catalysts decrease in the sequence of W/USY>W/Hβ>WAl_2O_3>W/HZSM-5. The BET surface area and micropore volume of the 3%W/HZSM-5 catalyst is slightly larger than the 3 % W-H_2SO_4/HZSM-5 catalyst. The results may be attributed to the difference in the nature of W species present over the catalysts as a consequence of the acidic treatment used for the impregnation method. Meanwhile, the BET surface area and micropore volume do not change significantly with increasing Si/Al ratio.

Table 1.1 BET surface areas and micropore volumes of W supported catalysts

Catalyst	**BET surface area (m^2/g)**	**Micropore volume (cm^3/g)**
W/Hβ	484	0.319
W/USY	611	0.596
W/Al_2O_3	124	0.283
W/HZSM-5	363	0.232
W-H_2SO_4/HZSM-5 (Si/Al=30)	321	0.195
W-H_2SO_4/HZSM-5 (Si/Al=50)	356	0.201
W-H_2SO_4/HZSM-5 (Si/Al=80)	358	0.186

The performances of the W/USY, W/HZSM-5, and W/ Hβ catalysts all prepared with neutral impregnation solution are slightly different at the initial stage of the reaction. Among them, the activities of the W/HZSM-5 and W/Hβ are relatively more stable with time on stream than W/USY. Moreover, HZSM-5 was found to be the best support as evident from the highest activity displayed while USY relatively had the lowest stability. The high activity of a catalyst may be related to its pore diameter which is shape selective to the diameter of a benzene molecule. In contrast, a catalyst exhibiting relatively low performance is associated to aromatics type carbon condensed ring deposited on the catalyst surface. The carbon is easily formed over the large pore zeolite which has three-dimensional structure and cages such as USY. Therefore, the channel is blocked rapidly leading to low aromatics selectivity [15]. This is evident from the aromatics selectivity results over the W/USY catalyst which is shown to decrease significantly whereas the C_2-hydrocarbons selectivity increased rapidly with time on stream. The lowest aromatics selectivity is displayed over the W/Al_2O_3 catalyst. If the acidified effect of

W/HZSM-5 is not considered, the highest C_2 hydrocarbons selectivity is exhibited over the W/Al_2O_3 catalyst indicating that Al_2O_3 is less selective toward aromatics molecule.

The relationship between the acidity of the supports and the activity of the catalysts for DHAM is investigated further. The amount and the strength of the catalysts acidity were determined by means of TPD-ammonia. The number of acid sites of the supports and W supported on HZSM-5 catalysts are given in Table 1.2, while the NH_3- TPD curves of the catalysts supports, i.e. USY, Hβ, HZSM-5 (Si/Al =30), and Al_2O_3 are shown in Figure 1.5.

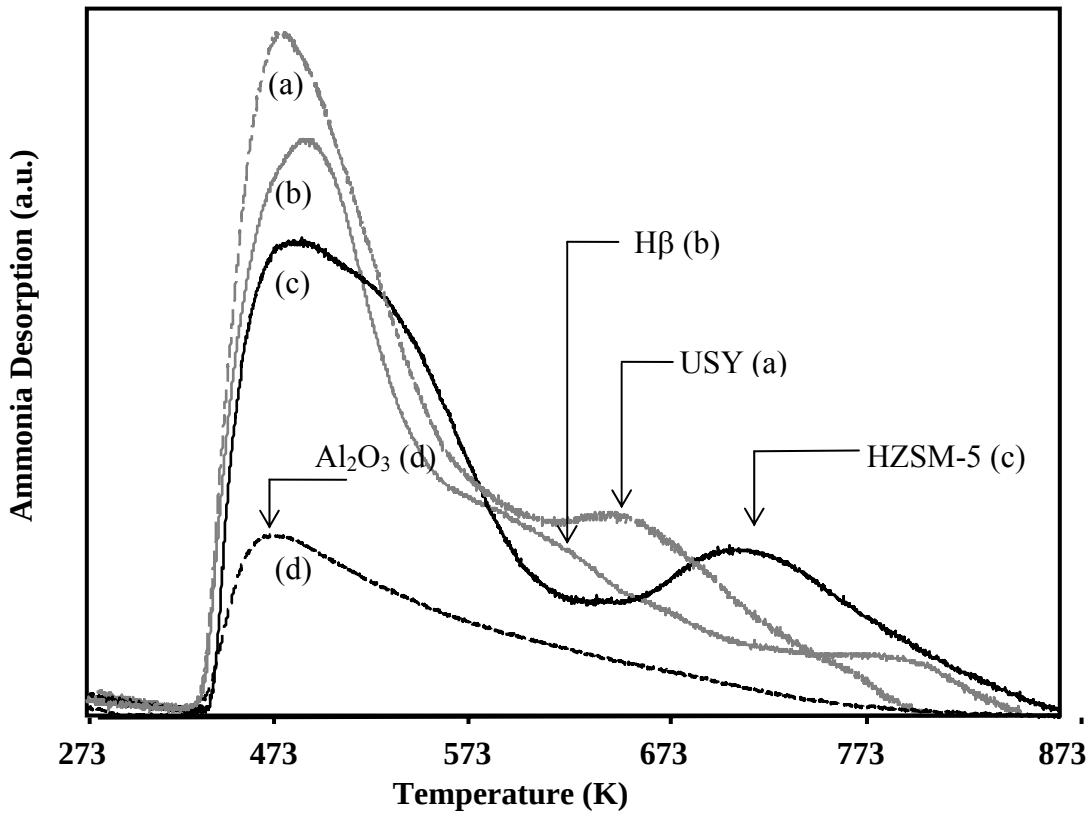

Figure 1.5: Ammonia-TPD profile of catalyst supports used in the present study: (a) USY (b) Hβ (c) HZSM-5 (Si/Al =30) (d) Al_2O_3.

The amount of desorbed ammonia and desorption temperature are directly associated to the amount and strength of catalyst acidity, respectively. The NH_3-

TPD curve of HZSM-5, exhibits two separate peaks at 523 K and 743 K attributed to weak and strong acid sites. The existence of the peaks has been reported for the acid characterization of HZSM-5 by the NH_3-TPD method [16, 17]. Unlike HZSM-5, the TPD curves of Hβ and USY show a major peak at temperature 523 K and a shoulder peak at temperature around 623 K and 653 K for Hβ and USY, respectively. The major peak at lower temperature can be assigned to weak acidity, while a shoulder peak can be attributed to medium acidity. Both Hβ and USY possess relatively high amount of total acid sites, as presented in Table 1.2. The highest amount of ammonia-desorbed shown on USY zeolite is probably due to its high specific surface area. Meanwhile, the TPD-peak of W/Al_2O_3 mainly shows at low temperature indicating the absence of medium and strong acid sites. And also, as seen in Table 1.2, it has low amount of acid sites. Furthermore, the number of acid sites of W supported on HZSM-5 catalysts is also presented in Table 1.2. As can be seen, the amount of acid sites on $W\text{-}H_2SO_4$/HZSM-5 catalysts prepared with the addition of H_2SO_4 in the impregnation solution is reduced compared with the W/HZSM-5 catalyst prepared with neutral solution in the impregnation method. The results in Table 1.2 show that the amount of acid sites on $W\text{-}H_2SO_4$/HZSM-5 decreases with increase in Si/Al ratio of HZSM-5.

Table 1.2: The number of weak (peak L) and strong (peak H) acid sites of the supports and HZSM - 5-supported W catalysts. Peak L at T ~523 K; Peak H at T ~743 K.

Catalyst	**Amount of NH_3-desorbed (mmol/g.cat)**		**Total number of acid sites (mmol/g.cat)**
	Peak L	**Peak H**	
Hβ	1.311 *(L+M)	-	1.311
USY	2.329 ** (L+M)	-	2.329
Al_2O_3	0.348	-	0.348
HZSM-5	0.844	0.407	1.251
W/HZSM-5 (Si/Al=30)	0.698	0.363	1.062
$W\text{-}H_2SO_4$/HZSM-5 (Si/Al=30)	0.614	0.240	0.854
$W\text{-}H_2SO_4$/HZSM-5 (Si/Al=50)	0.561	0.127	0.687
$W\text{-}H_2SO_4$/HZSM-5 (Si/Al=80)	0.356	0.111	0.467

* (L+M) = Peak L at T~523 K and peak M at T~623 K associated to weak and medium acid sites, respectively.

** (L+M) = Peak L at T~523 K and peak M at T~653 K associated to weak and medium acid sites, respectively.

Based on the activity results, it is found that 3% W-H_2SO_4/HZSM-5 (Si/Al=30) exhibits a maximum aromatics selectivity which decrease significantly with time on stream as presented in Figure 1.2(B). Moreover, the effect of GHSV ranging from 1800 – 9000 ml/g.h on the activity of 3 %W-H_2SO_4/HZSM-5 catalysts with different Si/Al ratios indicates that the maximum activity appears on the catalyst with Si/Al =30 as shown in Figure 1.3(A) and Figure 1.3(B) for methane conversion and aromatics selectivity, respectively. It seems that in addition to the pore structures being shape selective, the strength of the acid sites in the HZSM-5 catalyst also contribute to achieving optimum catalyst activity in DHAM reaction as has been reported by several authors [1-12, 16]. The decrease in aromatic selectivity after reaching a maximum value suggested the event of coke deposition in the catalyst. This fact might be due to the presence of extensive amount of strong Brönsted acid sites in the 3% W-H_2SO_4/HZSM-5 (Si/Al=30) catalyst. It has been reported that Brönsted acid sites on the catalyst were responsible for the formation of aromatics, however, an excess of the Brönsted acid sites led to severe coke formation [2]. The deactivation of the catalyst yielded the decreased in the selectivity for aromatics, whereas the C_2 selectivity increased markedly as evident from the results illustrated in Figure 1.2(B) and Figure 1.2(C). This result suggests that the coke formation in the catalyst could reduce the amount of Brönsted acid sites and the catalyst pore size which may lead to the suppression of C_2-hydrocarbons oligomerization to form benzene. Meanwhile, a low amount of acid sites and the absence of strong acid sites on W/Al_2O_3 lead to a low DHAM activity. Likewise, Figure 1.3(C) displays the increase in the C_2 hydrocarbons selectivity with increase in GHSV. Similar result has been reported [6], indicating C_2- species as the primary intermediates which are oligomerized subsequently to aromatics. In order to improve the activity and stability of 3 %W/HZSM-5 (Si/Al=30) catalyst, 2 % O_2 was added into the methane feed, in this case GHSV of 3000 ml/(g.h) was applied. The activity of the catalysts enhance significantly with the presence of oxygen in methane feed as can be seen in Figure 1.4. The same effect are observed on Mo/HZSM-5, Re/MCM-22, and W/HZSM-5 catalysts as has been reported by previous authors for DHAM reaction with co-feed such as CO, CO_2, and O_2 in the methane feed [1, 5, 7, 8, 17-19]. The enhancement of the catalyst activity in the presence of oxidant is due to the partial removal of coke in the catalyst.

The UV-DRS method was performed to investigate the nature of tungsten species in different supports and the results are shown in Figure 1.6. The wavelengths for the supported W species are reported to be at 220 nm, between 250-325 nm, and between 375-400 nm which could be assigned to tetrahedral monomeric tungstate species, octahedral polymeric tungstate species and WO_3 crystallites, respectively [20-22]. As portrayed in Figure 1.6(A), the UV-DRS spectra of W loaded on different supports show a major band at 220 nm and a shoulder at 275 nm for zeolites as supports. In contrast, the W/Al_2O_3 catalyst shows a band at 220nm only and the results are consistent with the work reported for Al_2O_3 supported catalyst [20].

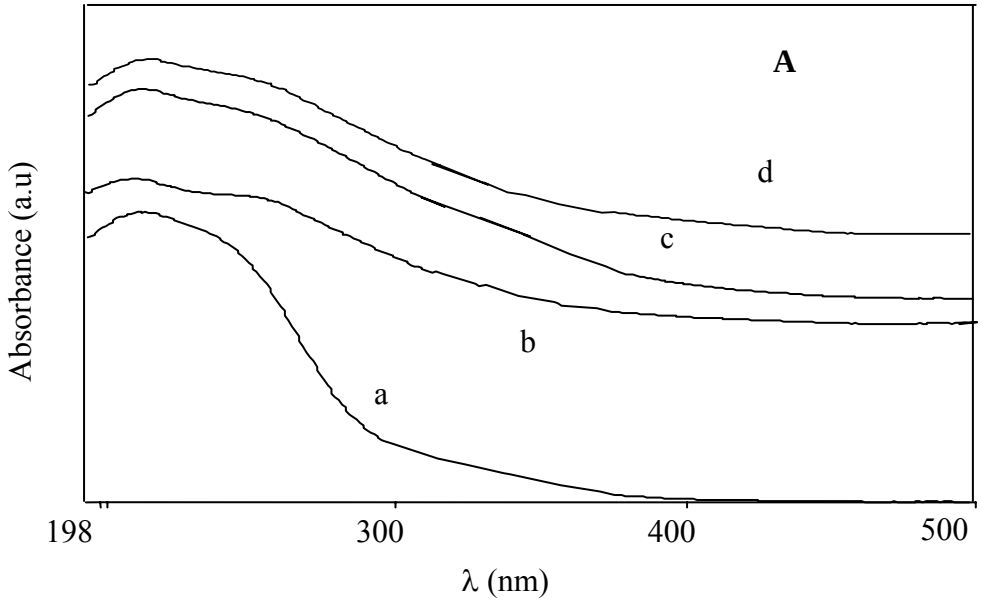

Figure 1.6(A): UV-DRS of 3 % W based catalyst on different supports: (a) Al_2O_3; (b) USY; (c) Hβ ; (d) HZSM-5 (Si/Al=30).

The different behavior exhibited by the W/HZSM-5 and W-H_2SO_4/HZSM-5 (Si/Al =30) catalyst was probably due to the change in the nature of W species caused by the different preparation conditions employed in the impregnation of W on the HZSM-5. The UV-DRS characterization was carried out to provide the evidence for the existence of different kinds of tungsten species and the result is shown in Figure 1.6(B). The UV-DRS spectrum of W-H_2SO_4/HZSM-5 consists of two major bands at around 220 nm and 310 nm

which correspond to the presence of tetrahedral monomeric and octahedral polymeric tungstate species, respectively. Meanwhile, a major band at 220 nm and a shoulder at 275 nm appear on W/HZSM-5 indicating that tetrahedral monomeric tungstate species are predominant while octahedral polymeric tungstate species exist in a minor extent. The addition of H_2SO_4 in the impregnation solution can enhance the formation of polytungstate in the precursor which is in accordance with the work reported by several authors [15, 20-22]. As reported in the literatures the structure of aqueous tungstate anions exist in two forms: a tetrahedrally coordinated WO_4^{2-} anion and an octahedrally coordinated $W_{12}O_{42}^{12}$. The equilibrium between these two species is described by:

$$12WO_4^{2-} + 12\ H^+ \Leftrightarrow W_{12}O_{42}^{12-} + 6\ H_2O$$

Based on the reaction above, the polymeric tungstate species is the predominant species in acidic pH due to the shift of equilibrium to the right. In contrast, the tungstate monomer is predominant in the neutral or alkali solution. Thus, the catalyst prepared with the addition of H_2SO_4 in the impregnation solution exhibited considerable amount of polymeric tungstate present in the W supported catalyst whereas the catalyst prepared in neutral solution had polymeric tungstate in minor amount. The higher activity obtained over the W-H_2SO_4/HZSM-5 catalyst than the W/HZSM-5 catalyst can be attributed to the existence of a considerable amount of octahedral polymeric tungstate species which promote the activity of the W-H_2SO_4/HZSM-5 catalyst. This result seems to be in good agreement with the results reported by Zeng *et al*. [4] who observed that octahedral polymeric tungstate species promoted the reducibility of W-H_2SO_4/HZSM-5 and as a consequence led to a high DHAM activity.

However, the rapid decreased in the methane conversion and aromatic selectivity over W-H_2SO_4/HZSM-5 (Si/Al of HZSM-5=30) as appeared in Figure 1.2 may be attributed to the heavily deposited carbon that covered the acidic and metal active sites which led to the deactivation of the catalyst. Coke deposition also caused a severe drop in the selectivity to aromatics and at the same time the selectivity of C_2 increased substantially. Moreover as shown in Figure 1.2, it was demonstrated that

methane conversion and aromatic selectivity over the W-H_2SO_4/HZSM-5 catalyst were higher than that over W/HZSM-5 at the initial reaction stage. However, the activity of the W-H_2SO_4/HZSM-5 catalyst decreased quickly with time on stream.

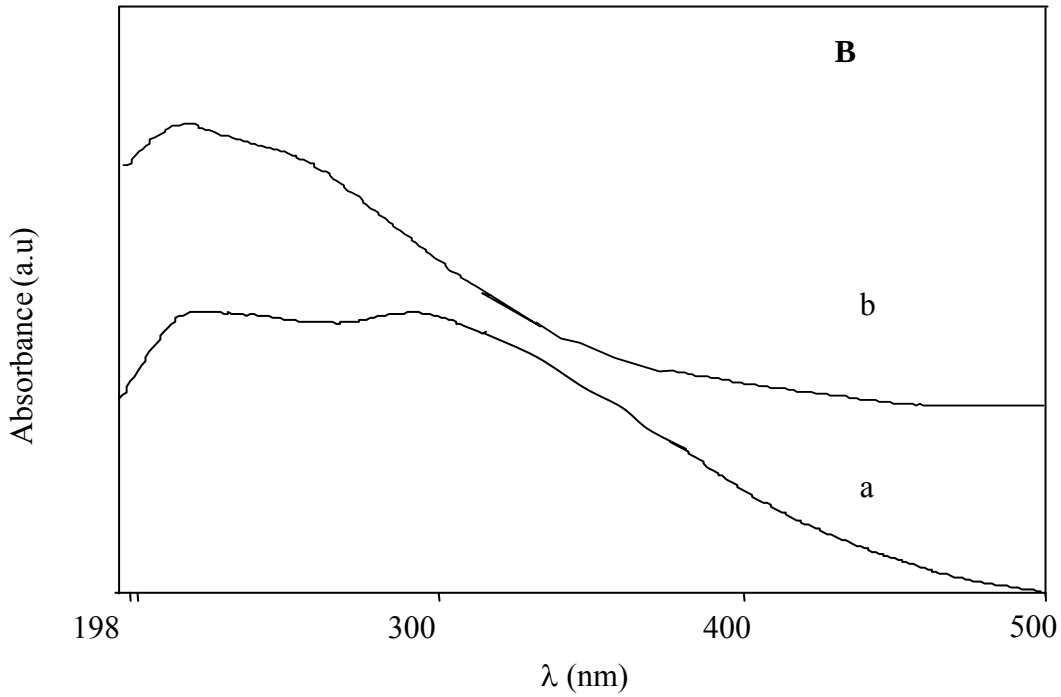

Figure 1.6(B): UV- DRS of (a) 3 % W-H_2SO_4/HZSM-5 (Si/Al=30) and (b) 3 % W/HZSM-5 (Si/Al=30).

The effect of Si/Al ratio on the W-H_2SO_4/HZSM-5 catalysts is to elucidate the correlation between the acidity of HZSM-5 and the nature of W species on the catalytic performance of the catalysts. The NH_3-TPD results reveal that as the Si/Al ratio increases, the amount and the strength of the acid sites on the catalysts decrease which can be seen in Table 1.2. Meanwhile, the UV-DRS spectra demonstrated that all the samples show two kinds of bands at 220 nm and 310 nm associated to tetrahedral monomeric and octahedral polymeric W species respectively as shown in Figure 1.6(C). The increase in Si/Al ratio for HZSM-5 has not affected the monomeric and polymeric concentration ratio of W species as indicated by the ratio in Figure 1.7. The ratio implies a considerable amount of active polymeric W species are present over the three catalysts. However, the results of the activity

testing shown in Figure 1.2 and Figure 1.3 indicate that as the Si/Al ratio increases, the acidic strength weakens and the activity of the catalyst decreases. The same observation was confirmed in a previous study that correlated the activity of benzene formation in methane aromatization with the Brönsted acid sites for the Mo/HZSM-5 catalyst [10]. It was found that benzene formation on the Mo/HZSM-5 is substantially dependent on the SiO_2/Al_2O_3 ratios of the HZSM-5 used. Among the Mo/HZSM-5 catalysts series, the one having SiO_2/Al_2O_3 ratio between 30-45 contains maximum Brönsted acid sites and corresponds to maximum benzene formation.

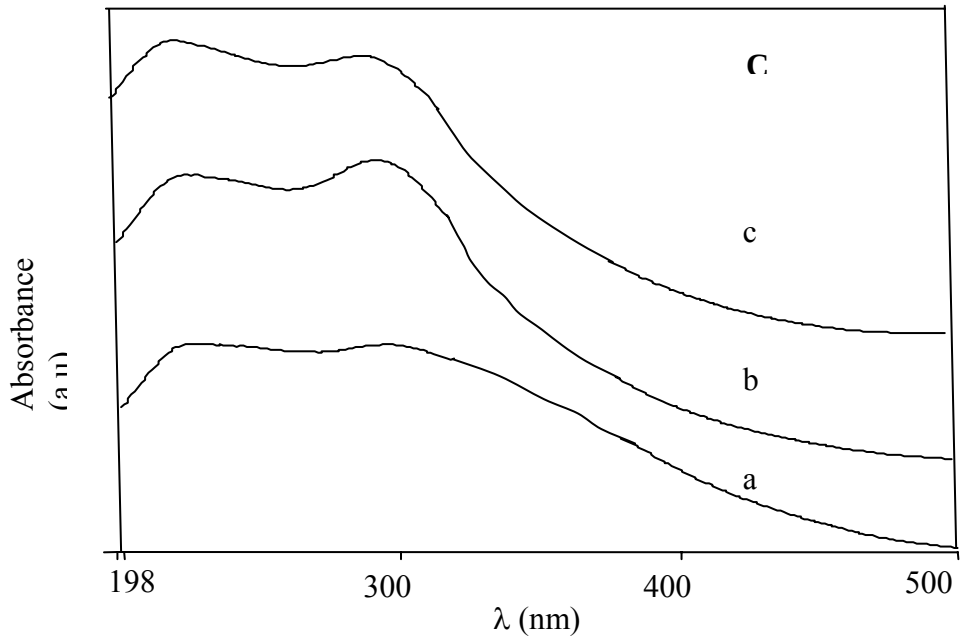

Figure 1.6(C): UV-DRS of 3 %W-H_2SO_4/HZSM-5 with different Si/Al ratios: (a) 30; (b) 50; (c) 80.

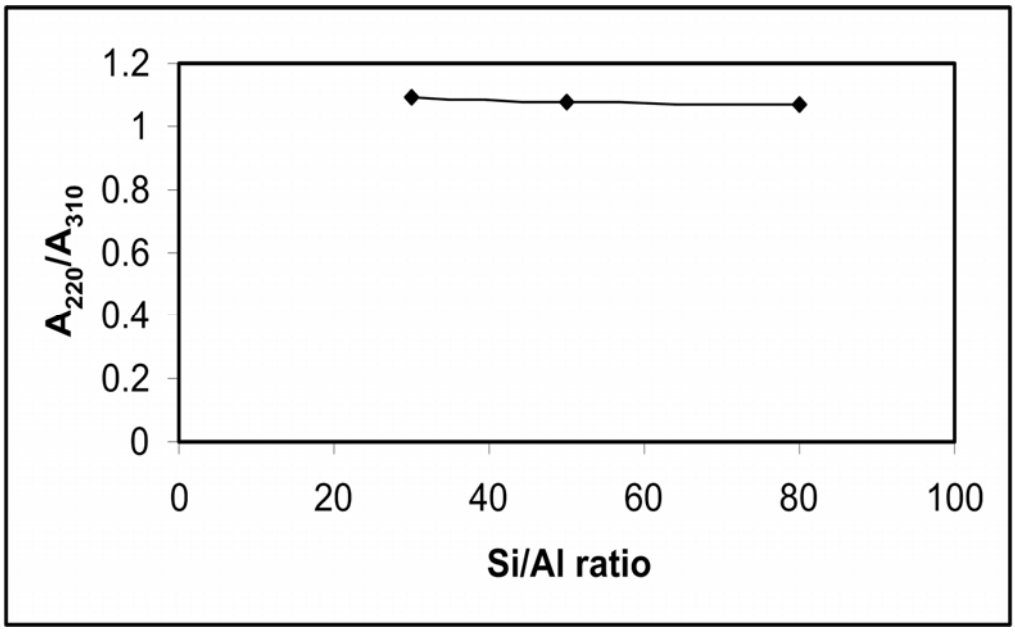

Figure 1.7: Effect of Si/Al ratio of HZSM-5 on A_{220} and A_{310} ratio attributed to monomeric and polymeric concentration of tungsten species

This result of the activity testing for the catalysts with different Si/Al ratios indicates that the activity of W-H_2SO_4/HZSM-5 catalysts is not only affected by the existence of octahedral polymeric W species, but also by the catalyst acidity. Moreover, the result concludes that the optimum activity of W based catalysts for DHAM are dependent on the balanced amount between the two active sites in the catalyst, i.e. acidity and existence of octahedral polymeric and tetrahedral monomeric tungstate species.

1.4 Conclusions

Dehydroaromatization of methane (DHAM) was studied over a series of 3 wt% W based catalysts prepared with different supports (HZSM-5, USY, Hβ, and Al_2O_3), under different preparation conditions and a variety of Si/Al ratios. HZSM-5

catalyst was found to be the best catalyst support. The W-H_2SO_4/HZSM-5 catalyst prepared by acid treatment emerged as the most promising catalyst by exhibiting the maximum catalytic activity which is higher than that over W/HZSM-5 prepared by impregnating the HZSM-5 precursor with a neutral solution of ammonium tungstate. Further investigation on the activity of W-H_2SO_4/HZSM-5 with different Si/Al ratios revealed that W-H_2SO_4/HZSM 5 catalyst with Si/Al =30 showed an optimum methane conversion and aromatic selectivity. However, a significant decrease in the activity of the 3 %W-H_2SO_4/HZSM-5 (Si/Al=30) catalyst was observed with increasing time on stream and GHSV suggesting the deposition of coke in the catalyst. The activity and stability of 3 %W-H_2SO_4/HZSM-5 (Si/Al=30) catalyst improved after introducing 2 % O_2 into the methane feed. The relationship between the activity and the characteristics of the catalyst revealed that suitable content of octahedral polymeric and tetrahedral monomeric tungstate species accompanied by proper amount and strength of acid sites in the catalyst contributed to the highest catalytic performance for DHAM

CHAPTER 2

CONVERSION OF METHANE TO GASOLINE RANGE HYDROCARBONS OVER W/HZSM-5 CATALYST: EFFECT OF CO-FEEDING

Abstract

The conversion of methane in the presence of co-feedings into hydrocarbons in gasoline range over W/HZSM-5 catalyst has been studied in a fixed bed reactor at atmospheric pressure. The effect of CH_4/C_2H_4 ratio in the methane and ethylene feed shows that the fraction of gasoline hydrocarbon (C_5^+ aliphatics and aromatics) in the product distributions increased with high ethylene concentration. The effect of loading W into HZSM-5 catalyst for the conversion of methane and ethylene (ratio CH_4/C_2H_4=86/14) shows that W/HZSM-5 has higher conversion and higher resistance towards deactivation than HZSM-5. The influence of temperatures (250-450 °C) on the conversion of methane and ethylene feed shows that increasing temperature, the selectivity to aromatic products increased. In addition, the conversion of methane with co-feeding of methanol and mixtures of ethylene and methanol were also studied. The result shows that the production of C_5^+ aliphatics increase with the introduction of ethylene and methanol into the methane feed.

Keywords: methane, gasoline, W/HZSM-5 catalysts, co-feeding

2.1. Introduction

The catalytic activation of methane, the main component of natural gas is important since it can be converted into higher hydrocarbons. The formation of synfuels from natural gas appears to be interesting. Current process available is by indirect process in a large commercial scale [23] The first is the trans-formation of natural gas into synthesis gas ($CO + H_2$), by a steam reforming process, autothermal reforming or partial oxidation. The synthesis gas undergoes a Fischer–Tropsch reaction, forming hydrocarbons in the diesel and petrochemical naphtha range, in a route known as traditional gas-to-liquid (GTL), as it transforms gas into liquid derivatives. The second is the transformation of natural gas into synthesis gas, as in the previous example, but this, however, reacts to form other gases, i.e. methanol. Then methanol is transformed to gasoline by using a methanol-to-gasoline (MTG). The MTG process yields high octane gasoline that is rich in aromatics [28].

A few studies have been reported on the direct conversion of methane into higher hydrocarbons or motor fuels. The direct conversion transformation of methane to aromatics has attracted increasing attention. However, the process has limitation due to serious coke formation leading to deactivation of the catalyst at a temperature as high as 973 K and under non oxidative condition [30]. Conversion of methane in the presence of small amounts of light hydrocarbons into higher hydrocarbons rich in aromatics under non-oxidizing conditions over Mo-zeolite at low pressures (1–2 atm) has been reported by Pierella *et al.* (1997) [29]. In the previous study, Alkhawaldeh *et al.* (2003) [24] converted methane into higher molecular weight hydrocarbons. Methane is first converted into acetylene. Acetylene is then either mixed with methane and converted directly into higher molecular weight hydrocarbons over metal-loaded zeolites or hydrogenated into ethylene over HZSM-5 where ethylene in a feed mixture comprising methane is then reacted over a catalyst to produce higher molecular weight hydrocarbons.

In the present study, the conversion of methane in the presence of ethylene and methanol respectively was investigated for the production of higher hydrocarbon products in the gasoline range. The introduction of co-feeding methanol and ethylene into the methane feed is also reported.

2.2. Experimental Procedure

2.2.1. Catalyst preparation

The 2 wt. % W/HZSM-5 catalyst was prepared by impregnation method. The HZSM-5 zeolite (SiO_2/Al_2O_3=30) (commercially available from Zeolyst international Co. Ltd) was impregnated with a calculated amount of the aqueous solution of ammonium tungstate $(NH_4)_5H_5[H_2(WO_4)_6].H_2O$ (A. R.). The sample was dried at 110 ^oC overnight and calcined at 550 ^oC for 5 h. The catalyst was crushed and sieved into the size of 35-60 mesh for catalytic testing.

2.2.2 Catalytic activity

The catalytic reaction was carried out in a fixed bed continuous-flow system. The schematic diagram of the experimental setup is shown in Figure 1. The reactor was 15 cm long, 9 mm internal diameter made up of stainless steel. The reactor was heated up by means of an electric furnace at the temperature range between 250 and 450 ^oC at p=101 kPa. The catalyst was placed in the middle of the reactor and supported by quartz wool. Prior to the catalytic reaction, the catalyst was preheated

in situ in a flow of nitrogen for one hour at reaction temperature to activate the catalyst. A feed consisting of methane and ethylene mixtures was flowed into the reactor at a GHSV of 1200 ml/g h with a CH_4/C_2H_4 molar ratio of 80/20 and 14/86, respectively. In the case of methanol as co-feed, the methanol was added at a flow rate of 5 ml/h into methane-ethylene feed by using a syringe pump (model A-99 EZ Razel Scientific Instrument, Inc.). In another case, the reaction was carried out using methane and methanol as a feed. The GHSV of methane was 1200 ml/g.h and flow rate of methanol was 5 ml/h. The gases leaving the reactor were cooled in a water bath. The uncondensed gaseous products were analyzed by means of an on-line gas chromatograph (GC) type HP 5890 series II using a TCD. The GC equipped with two columns Porapak Q and molecular sieve 5A for separation of N_2, CH_4, C_2H_4, while UCW 982 12 % and DC 200 26 % columns were used to separate the lower hydrocarbons including C_3-C_5 hydrocarbons. The liquid products which accumulated over a reaction time comprising of C_5^+ aliphatics and aromatics hydrocarbons were analyzed on a flame ionization detector (FID) chromatograph using HP-1 capillary column.

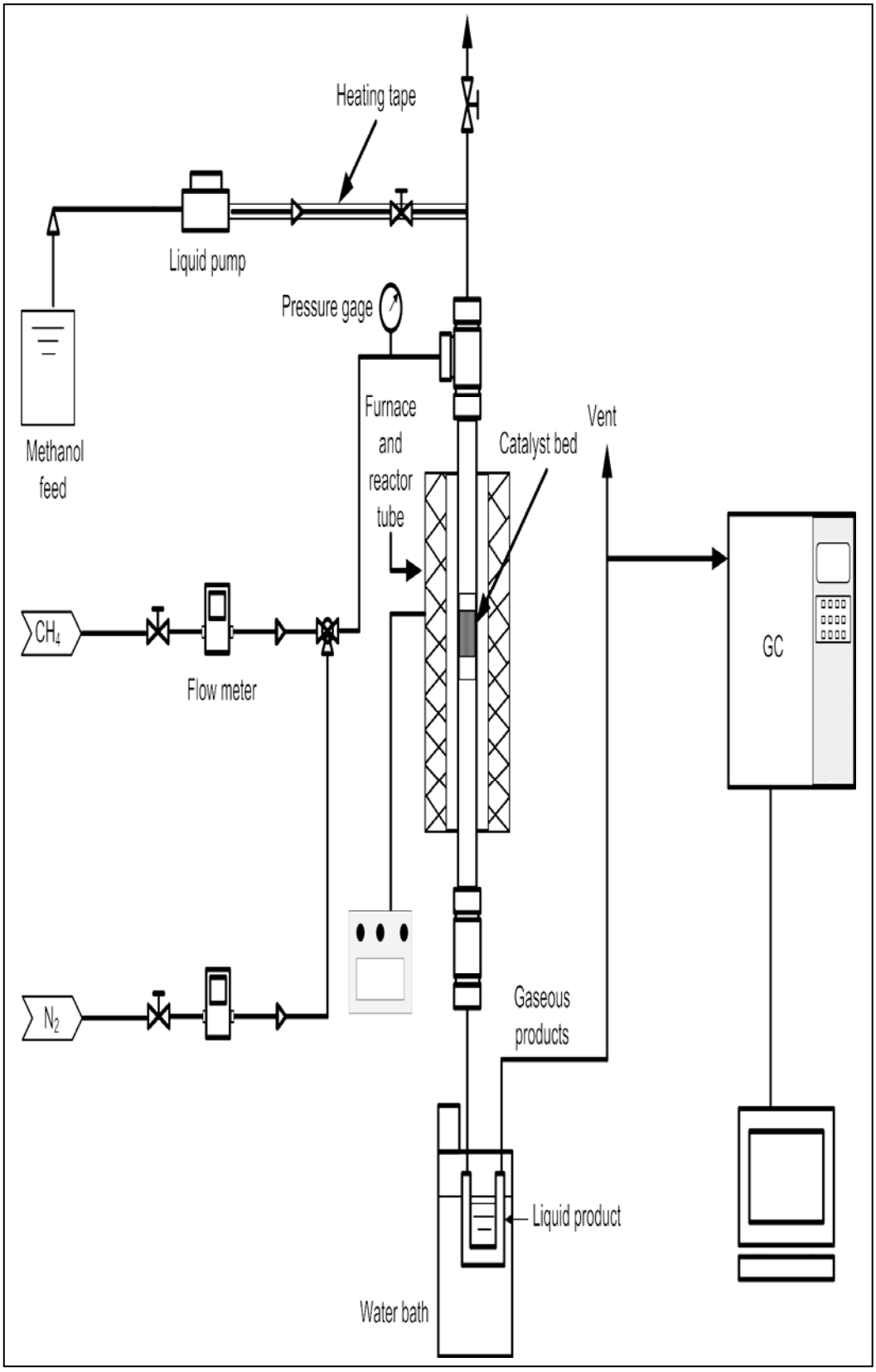

Figure 2.1: Experimental rig set up

2.3. Results and Discussion

Table 2.1 shows a comparison of products distribution obtained from reacting methane and ethylene in the feed at high ethylene concentration (molar ratio CH_4/C_2H_4 :10/80) and low ethylene concentration (86/14), respectively over W/HZSM-5 catalysts at 400 ^oC and atmospheric pressure. As can be seen, the products reaction consisted of C_2-C_4 alkanes (ethane, propane, butane,); C_2-C_4 alkenes (ethylene, propylene); C_5^+ aliphatics and aromatics including benzene, toluene, ethyl benzene, trimethyl benzene, isopropyl benzene, and xylene.

Table 2.1: Conversion and hydrocarbon distribution at two different CH_4/C_2H_4 molar ratios: 10/80 and 86/14, respectively

Compound	**CH_4 : C_2H_4= 10:80 (v/v)**	**CH_4 : C_2H_4 = 86:14 (v/v)**
Conversion, ethylene %	96.6	97.5
C_2-C_4 alkanes	24.1	33.01
C_2-C_4 alkenes	5.7	19.2
C_5^+ aliphatics	49.67	7.31
Aromatics	20.53	40.3

Reaction condition: T=400 ^oC, 1 atm, GHSV= 1200 ml/g.h.

The effect of CH_4/C_2H_4 ratio on the distribution of products shows that a decrease of ethylene concentration in the feed decreases the fraction of higher hydrocarbons (C_5^+ and aromatics) content in the product. When high ethylene concentration (CH_4/C_2H_4 ratio of 10/80) was fed, the percentage of higher hydrocarbons (C_5^+ and aromatics) and lighter hydrocarbons (C_2-C_4 alkenes and alkanes) products were 70.20 % and 29.8 %, respectively. At low ethylene concentration in the feed (CH_4/C_2H_4 molar ratio=86/14), the percentage of higher hydrocarbons was lower to 47.61 % while the lighter products increased to 52.9 %. The result is in agreement with the results reported by Anunziata *et al.* (1999) [25].

They reported the C_1 + LPG conversion to higher hydrocarbon and aromatic products over Zn-ZSM-11 at GHSV (LPG) = 810 ml/g h and 450 and 550 ^oC, respectively. The results of the reaction of methane and methanol over W/HZSM-5 catalyst are summarized in Table 2.2.

Table 2.2 Conversion and hydrocarbon distribution for methane+ethylene, methane+methanol, and methane+ethylene+methanol feed

Compound	**CH_4 :C_2H_4 = 86:14(v/v)**	**CH_4 / CH_3OH***	**CH_4 /C_2H_4 / CH_3OH****
Conversion, ethylene %	97.5	-	98.5
C_2-C_4 alkanes	33.01	25.4	26.2
C_2-C_4 alkenes	19.2	6.7	15.9
C_5^+ aliphatics	7.31	12.3	20.7
Aromatics	40.3	55.6	37.2

Reaction condition: T=400 ^oC, 1 atm , GHSV (CH_4+C_2H_4)= 1200 ml/g.h, *GHSV CH_4=1200 ml/g.h + CH_3OH = 5 ml/h, ** GHSV (CH_4+C_2H_4)= 1200 ml/g.h + CH_3OH = 5 ml/h.

As can be seen from Table 2.2, the gasoline range hydrocarbon, aromatics were the major products from the conversion of methane and methanol. In the presence of ethylene, the heavy hydrocarbons of 47.61 % were obtained while the introduction of methanol to the feed increased the fraction of heavy hydrocarbons (67.9 %). The fraction of C_5^+ aliphatics (12.3 %) was observed from the reaction of methane and methanol, with the presence of ethylene in the methane feed, the fraction of C_5^+ aliphatics was lower (7.31 %).

The proposed mechanism of the transformation of methane and methanol to gasoline boiling range might be explained by the following mechanisms. Methanol is first dehydrated to dimethyl ether (DME) which is then converted to light olefins [31]. Then, methane and light olefins react to form C_2^+ carbenium ions which undergo the formation of higher hydrocarbons as has been proposed by Pierella *et al* (1997) [29]. The reaction of ethylene with methane yielded propylene which is an

intermediate molecule for the production of higher hydrocarbons as suggested by Baba and Abe (2003) [26].

The percentage of C_5^+ aliphatics of 20.7% was observed with the adding of methanol to methane and ethylene feed. When methane and ethylene was used as feed, C_5^+ aliphatics was 12.3 %. This results suggest that the introduction of methanol to the mixture of methane and ethylene is intend to generate the carbenium ions which help to initiate the reaction and produce heavier components that is in accordance with the result reported by Alkhawaldeh *et al.* (2003) [24].

The influence of temperature on the products distribution at GHSV (CH_4+C_2H_4) =1200 ml/g h and a molar ratio of CH_4: C_2H_4 in the feed = 86:14 (v/v), over W/HZSM-5 is shown in Figure 2.2. The C_2H_6, C_4H_{10} and C_5^+aliphatics selectivity remained very low with the temperature increase whereas the C_3H_8 and aromatics selectivity increased. The C_2H_4 and C_4H_8 decreased with increasing temperature. Higher hydrocarbons product in the gasoline range mainly contains aromatic hydrocarbons in the whole range of the temperature studied. The activation of methane with LPG using zinc-loaded ZSM-11 zeolite has been studied over Zn-ZSM-11 [25]. The influence of temperature on the products distribution at GHSV (LPG) = 810 ml/g h and LPG molar fraction in the feed LPG/ (LPG + C_1) = 0.15 showed that the C_2 and C_5–C_6 yield remained very low with the temperature increase whereas the C=2 and aromatic hydrocarbons yield increased. Aromatic hydrocarbons were the main products in the whole range of temperatures studied, reaching a total of 12 % at 550 ^oC.

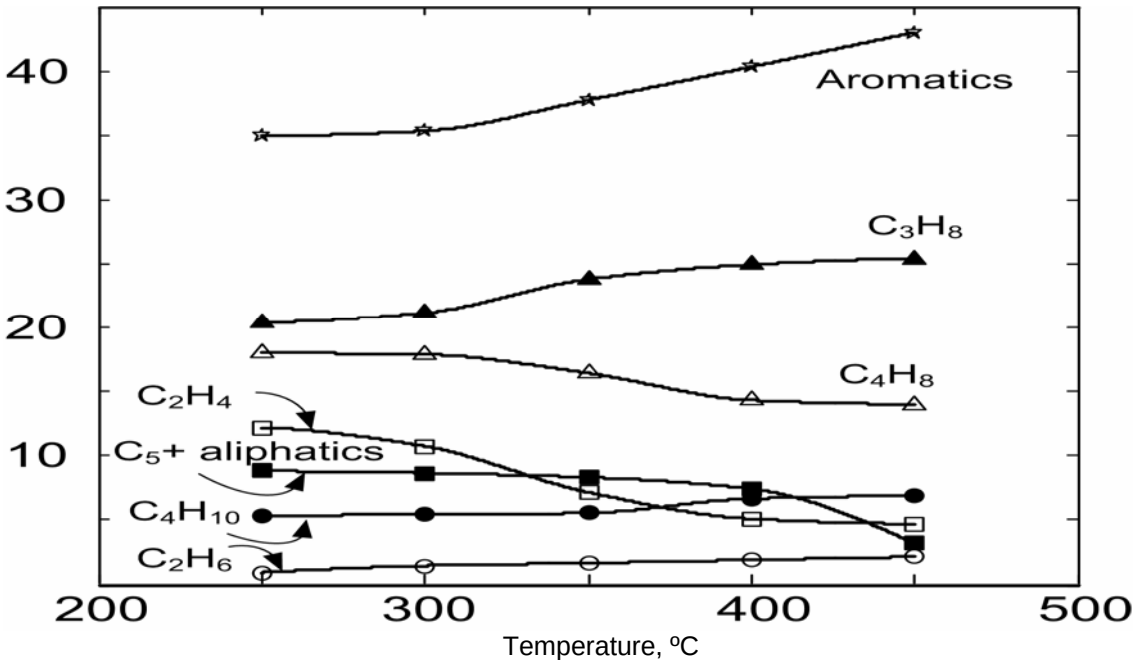

Figure 2.2: Hydrocarbons products distribution as a function of reaction temperature with methane and ethylene as a feed. GHSV(CH_4+C_2H_4) =1200 ml/g h, CH_4:C_2H_4 molar ratio=86:14.

Figure 2.3 shows the comparison of the conversion of dilute ethylene over time on stream for the HZSM-5 and W/HZSM-5 catalysts at T = 400 ^{o}C, P = 1 atm. The W/HZSM-5 shows relatively prolonged time of high conversion. For the first 2 hour the ethylene conversion was almost 100 % over W/HZSM-5 catalyst, whereas this number decreased to 75.91 % for W-loaded ZSM-5. On the other hand non-loaded HZSM-5 shows a high conversion (100 %) at the second hour of operation then it decreases gradually to reach 45.4 % at the end of the reaction. The W/HZSM-5 catalyst shows increased resistance towards deactivation as compared to the HZSM-5 catalyst. Among the catalysts used, Pd/ZSM-5 showed an improved performance in terms of the product distribution and conversion over all the other loaded and non-loaded HZSM-5 catalysts [24].

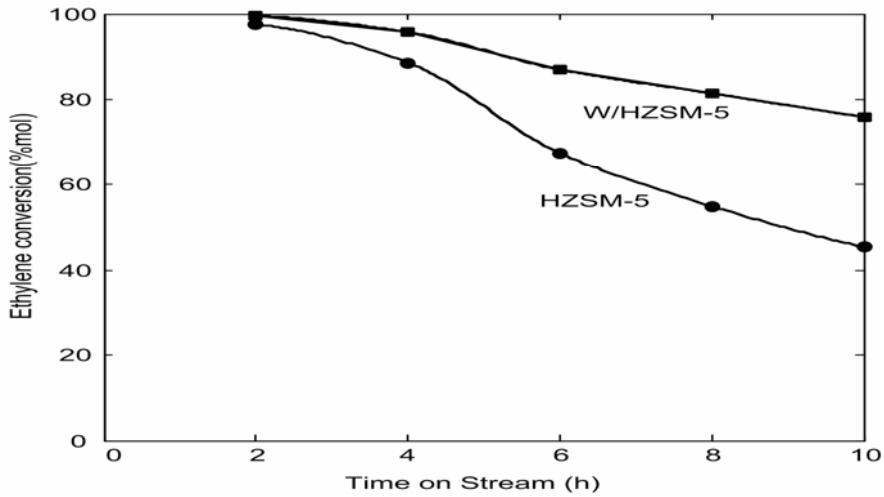

Figure 2.3 Ethylene conversion with time on stream for the reaction of methane and ethylene over W/HZSM-5 and HZSM-5 catalysts. Reaction condition : T=400 ^{o}C, GHSV(CH_4+C_2H_4) =1200 ml/g h, CH_4:C_2H_4 molar ratio=86:14

The aromatic content over the HZSM-5 catalyst was 14.93 mol % and W/HZSM-5 catalyst results in an increase in aromatic content up to 36.5 mol % as can be seen in Figure 2.4. As can be seen in Figure 2.4, C_5^+ production is observed over W/HZSM-5 and HZSM-5 catalysts. The production of C_5^+ liquid from CH_4 over metal-containing ZSM-5 catalyst has been reported by Han *et al.* (1994) [27]. They suggested that the C_5^+ could be produced from methane and O_2 via an MTG mechanism. They proposed mechanisms for the C_5^+ production from CH_4 are as follows: the methane is first converted to CH_3OH which is further transformed to olefins, the initiation for the C_5^+ production.

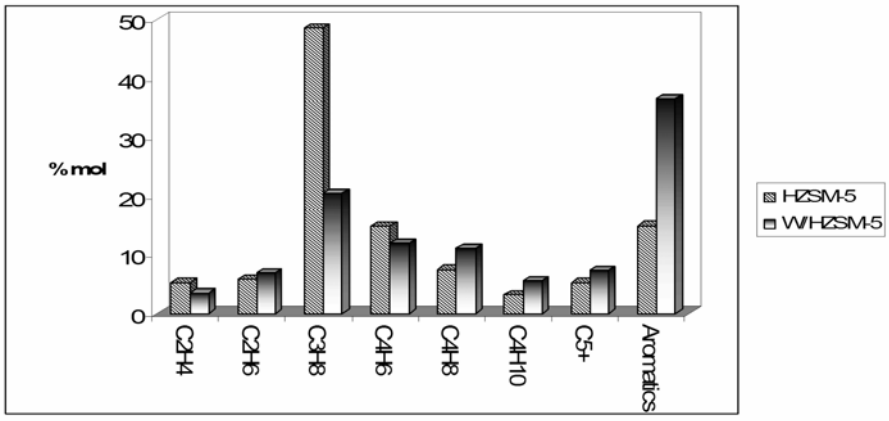

Figure 2.4: Product distribution for the reaction of methane and ethylene over HZSM-5 and W/HZSM-5 catalysts, T = 400 ˚C, and GHSV(CH_4+C_2H_4) =1200 ml/g h, CH_4:C_2H_4 molar ratio=86:14.

2.4. Conclusions

Methane containing ethylene or methanol, respectively, can be converted to higher hydrocarbons in the gasoline boiling range at low temperatures of 250 - 450 ^{o}C. Ethylene or methanol, respectively, was used as co-feeding to activate methane to form higher hydrocarbons. The aromatic hydrocarbons are the main reaction products obtained from the reaction of methane-ethylene and methane-methanol, respectively. The effect of CH_4/C_2H_4 ratio on the distribution of products shows that a decrease in ethylene concentration in the feed decreases the fraction of higher hydrocarbons (C_5^+ and aromatics) content in the product. The effect of adding co-feeding methanol to the methane and ethylene feed on the distribution of hydrocarbons was also studied. The production of C_5^+ aliphatics increase significantly with the introduction co-feeding methanol to methane and ethylene feed. The influence of temperature on the products distribution shows that with increasing temperature, the selectivity to aromatic products increased. The reaction of methane and ethylene was also studied over the parent HZSM-5 and W/HZSM-5

catalysts. As compared to HZSM-5, W/HZSM-5 has an improved performance in terms of the product distribution and conversion.

CHAPTER 3

PRODUCTION OF GASOLINE RANGE HYDROCARBONS FROM CATALYTIC REACTION OF METHANE IN THE PRESENCE OF ETHYLENE OVER W/HZSM-5

Abstract

The catalytic conversion of a methane and ethylene mixture to gasoline range hydrocarbons has been studied over W /HZSM-5 catalyst. The effect of process variables such as temperature, % vol. of ethylene in the methane stream, and catalyst loading on the distribution of hydrocarbons was studied. The reaction was conducted in fixed-bed quartz - micro reactor with i.d 9 mm in the temperature range of 300 to 500 ^{o}C using % vol. of ethylene in methane stream between 25 – 75 % and catalyst loading of 0.2 – 0.4 gram. The catalyst showed good catalytic performance yielding hydrocarbons consisting of gaseous products along with gasoline range liquid products. The mixed feed stream can be converted to higher hydrocarbons containing a high liquid gasoline product selectivity (>42%). Non-aromatics C_5 - C_{10} hydrocarbons selectivity in the range of 12 – 53% was observed at the operating conditions studied. Design of experiment was employed to determine the optimum conditions for maximum liquid hydrocarbon products. The distribution of the gasoline range hydrocarbons (C_5-C_{10} non-aromatics and aromatics hydrocarbons) was also determined for the optimum conditions.

3.1 Introduction

An excess consumption of petroleum resources has become significantly critical problems that may lead to acute energy crisis. Utilization of natural gas and coal has been considered as an effective way to reduce the dependence on liquid oil consumption. The transformation of methane (the main component of natural gas) to useful higher hydrocarbons and fuel can be performed by indirect and direct process, which proceeds with and without passing through the syngas formation, respectively. Recently, the manufacture of synfuels from natural gas is available for large scale as demonstrated by the MTG plant and the Fischer–Tropsch (FT) by using indirect process technologies. Nevertheless, many attempts are being made to covert natural gas into liquid hydrocarbons by the direct method without passing through the intermediate syngas formation [32]. The direct conversion of methane to C_2 hydrocarbons via OCM has attracted the academic and industrial interests due to their potential as an effective method to utilize natural gas for industrial feedstock. However, the usefulness of this process has been limited so far as it has low methane conversion and/or low hydrocarbons selectivity [33]. An approach to overcome the limitation of OCM process was reported and it consisted of a two-step process [34]. In the first step, methane or natural gas is converted into lower olefin which is transformed directly into gasoline range hydrocarbons over a pentasil zeolite catalyst. More recently, Alkhawaldeh *et al*. [24] reported the conversion of methane into higher molecular weight hydrocarbons. In their study, methane is first converted into acetylene which is followed by hydrogenation into ethylene. Then, the ethylene in a feed mixture comprising of methane was reacted over a catalyst to produce higher molecular weight hydrocarbons. It is therefore of great practical interest to convert dilute ethylene without it being separated from the methane streams into a much less volatile product(s) such as gasoline hydrocarbons. In another development, the conversion of methane to higher hydrocarbons in the presence of ethylene proceeded over silver cations-loaded H-ZSM-5 (Ag/H-ZSM-5) [26]. Due to the increasing interest in the production of sulfur-free transportation fuels via lower olefins oligomerization, the optimization study on oligomerization of feed mixture containing methane and ethylene to produce higher hydrocarbons in the

gasoline range over W/HZSM-5 is reported in this paper. The effect of process variables such as temperature, % vol. of ethylene in the methane stream, and catalyst loading on the distribution of hydrocarbons was studied according to statistic method with the application of design of experiment utilizing the STATISTICA software (version 6.0; Statsoft Inc).

3.2 Experimental Procedure

3.2.1 Catalyst preparation

The 2 wt. % W/HZSM-5 catalyst was prepared by impregnation method. NH_4ZSM-5 (SiO_2/Al_2O_3=30; Zeolyst international Co. Ltd.) was converted to HZSM-5 by calcinations at 500 ^oC for 4 h. It was then impregnated with calculated amount of the aqueous solution of ammonium tungstate $(NH_4)_5H_5[H_2(WO_4)_6]\cdot H_2O$ (A. R.). The sample was dried at 110 ^oC overnight and calcined at 550 ^oC for 5 h. The catalyst was crushed and sieved into the size of 35-60 mesh for catalytic testing.

Table 3.1 Properties of HZSM-5 zeolite and W/HZSM-5 catalysts.

Properties	**HZSM-5**	**W/HZSM-5**
Si/Al ratio	30	30
BET surface area (m^2/g)	400	372
Pore size (nm)	0.53 x 0.56	
Acidity (mmol NH_3/g)	1.251	1.164

3.2.2 Activity testing

Catalytic testing was carried out at atmospheric pressure in a fixed-bed continuous flow system with a quartz reactor of 9 mm i.d. and length of 300 mm. Before reaction, the catalyst was pretreated in a flow of nitrogen at 100 ml. min^{-1} for 1 h at 550°C. A gas mixture comprised of CH_4, C_2H_4 and N_2 (N_2 was used as internal standard), was introduced into the reactor containing the catalyst. Catalytic reactions were performed with different reaction variables based on Central Composite Design (CCD) method. The gaseous products was analyzed by an on-line HP 5890 series II GC-TCD equipped with Porapak Q and molecular sieve 5A columns for separation of N_2, CH_4, C_2H_4, while UCW 982 12 % and DC 200 26 % columns were used to separate the lower hydrocarbons including C_3-C_5 hydrocarbons. The liquid products comprised of C_{5+} non aromatics and aromatics hydrocarbons were analyzed on flame ionization chromatograph equipped with HP-1 capillary column.

3.3. Results and discussion

The study was performed based on design of experiment (DOE) method. The statistical method of factorial DOE eliminates the systematic errors with an estimate of the experimental error and minimizes the number of experiments [35, 36]. A central composite design (CCD) with three process variables was used. Each variable consists of three different levels from low (−1), to medium (0) and to high (1). According to the CCD, the total number of experiments conducted was 16 experiments including a 2^3 of the two-level factorial design, central points, and star points [37]. The independent variables used in the statistical study were temperature, ethylene concentration in the feed mixture containing methane and ethylene, and catalyst loading. Table 3.2 presents the independent variables with the

operating range of each variable. The levels of the independent variables were chosen based on a previous study reported in the literature [26].

Table 3.2 Independent variables with the operating range of each variable.

Independent Variables		-α	-1	0	+1	+α
Temperature (ºC)	X_1	271	300	400	500	529
Ethylene concentration in a Methane-Ethylene Mixture	X_2	0.19	0.25	0.50	0.75	0.82
Catalyst loading	X_3	0.17	0.2	0.3	0.4	0.43

The reaction of methane and ethylene mixture over W/HZSM-5 catalyst produced liquid hydrocarbons with high selectivity to gasoline range. The outlet reactor stream comprised of gaseous products (C_3-C_5) and liquid products including C_5-C_{10} non-aromatics and aromatics in addition to heavy hydrocarbons (C_{11}^+). The compositions of aromatics were benzene, toluene, ethylbenzene, xylene, tri-methyl benzene, tri-ethyl benzene. A series of statistically designed studies were performed to investigate the effect of independent variable i.e. temperature, ethylene concentration in a methane – ethylene mixture, and catalyst loading to optimize the liquid hydrocarbons, C_5-C_{10} non-aromatics hydrocarbons, and aromatics products. In this study, a full central composite design (CCD) with six star points and two replicates at the center point was used. Based on CCD with a 2^3 design, 16 sets of experiments were performed. Table 3.3 shows the experimental design and the results (observed and predicted values) of the three observed responses.

Table 3.3: An experimental plan based on CCD and the three responses.

Run	Variables					
	X_1	X_2	X_3	Y, S_{C5+}	Y, $S_{C5\text{-}10\ non\text{-}aromatics}$	Y, $S_{aromatics}$
1	300	0.25	0.20	63.62	20.63	17.97
2	300	0.25	0.40	65.89	25.54	18.06
3	300	0.75	0.20	80.13	57.15	19.86
4	300	0.75	0.40	75.53	54.35	18.42
5	500	0.25	0.20	45.60	12.57	20.21
6	500	0.25	0.40	42.60	14.79	24.58
7	500	0.75	0.20	43.80	24.57	18.12
8	500	0.75	0.40	49.10	29.77	19.90
9	271	0.50	0.30	85.70	59.53	29.57
10	529	0.50	0.30	70.40	12.59	47.54
11	400	0.18	0.30	60.31	20.73	11.34
12	400	0.82	0.30	70.67	49.67	20.53
13	400	0.50	0.17	66.62	31.99	22.49
14	400	0.50	0.43	76.69	39.70	25.54
15	400	0.50	0.30	83.60	53.25	30.26
16	400	0.50	0.30	83.60	53.32	30.27

X1= Temperature (ºC), X2= Ethylene concentration in a methane-ethylene mixture, X3= Catalyst loading, SC5+ = Sel. of C5+ hydrocarbons, SC5-10 non-aromatics= Sel. of non aromatics (NA), Saromatics = Sel. of aromatics.

The relationship between the independent variables and response variable was estimated by using regression analysis program. A central composite is designed to estimate the coefficients of a quadratic model. Eq. (3.1) presents a quadratic model for predicting the optimal point for the selectivity of C_5^+ liquid hydrocarbons.

$$Y_1 = -105.330 + 0.326\ X_1 + 257.391\ X_2 + 515.267\ X_3 - 201.014\ X_2^2 - 884.270\ X_3^2 - 0.107\ X_1X_2 + 0.058\ X_1X_3 + 7.150\ X_2X_3 \quad (3.1)$$

The regression equation (Eq. (3.2)) for the selectivity of C_5-C_{10} non-aromatics hydrocarbons is expressed as follows:

$$Y_2 = -163.783 + 0.498\,X_1 + 246.383\,X_2 + 417.049\,X_3 - 0.001\,X_1^2 - 116.781\,X_2^2 - 690.965\,X_3^2 - 0.912\,X_1X_2 + 0.066\,X_1X_3 - 23.650\,X_2X_3 \quad (3.2)$$

The regression equation obtained for the selectivity of aromatics hydrocarbons is:

$$Y_3 = -12.271 - 0.268\,X_1 + 187.086\,X_2 + 288.98\,X_3 - 0.045\,X_1X_2 + 0.094\,X_1X_3 - 20.600\,X_2X_3 - 160.282\,X_2^2 - 514.11\,X_3^2 \quad (3.3)$$

where Y_1,Y_2, Y_3 are the response variables corresponding to selectivity of C_5^+ liquid hydrocarbons, C_5-C_{10} non-aromatics, and aromatics, respectively and X_1, X_2, and X_3, represent the temperature, concentration of ethylene in a mixture methane-ethylene in the feed and catalyst loading, respectively as independent variables.

Table 3.4 shows the analysis of variance (ANOVA) to check the significance of the second-order model equation. The statistical significance of the second-order model equation was determined by *F*-value. Generally, the calculated *F*-value should be several times the tabulated value, if the model is good predictor of the experimental results [38]. The calculated F-value which is higher than the tabulated F-value ($F_{0.05}(9, 6) = 4.10$) provides evidence that the model fit the experimental data adequately.

Table 3.4: ANOVA for the second order model equations.

	Sum of squares	**Degree of freedom**	**Mean square**	**F value**	**$F_{0.05}$ (table)**	**R^2**
C_5^+ hydrocarbon selectivity						
SS regression	3033.92	9	337.10	10.29	4.10	0.9392
SS error	196.374	6	32.73			
SS total	3230.28	15				
C_5-C_{10} non-aromatics selectivity						
SS regression	4158.53	9	462.06	10.16	4.10	0.9384
SS error	272.79	6	45.47			
SS total	4431.32	15				
Aromatics selectivity						
SS regression	887.83	9	98.65	4.44	4.10	0.8694
SS error	133.35	6	22.22			
SS total	1021.18	15				

Figure 3.1 shows the comparison between the observed values with the predicted values. The value of R^2 was determined to evaluate the correlation between experimental and predicted value which yield 0.9392; 0.9384; 0.8694 for the selectivity of C_5^+ liquid hydrocarbons, C_5-C_{10} non-aromatics (NA), and aromatics hydrocarbons, respectively. These results indicated that the predicted values show a good agreement with the experimental results.

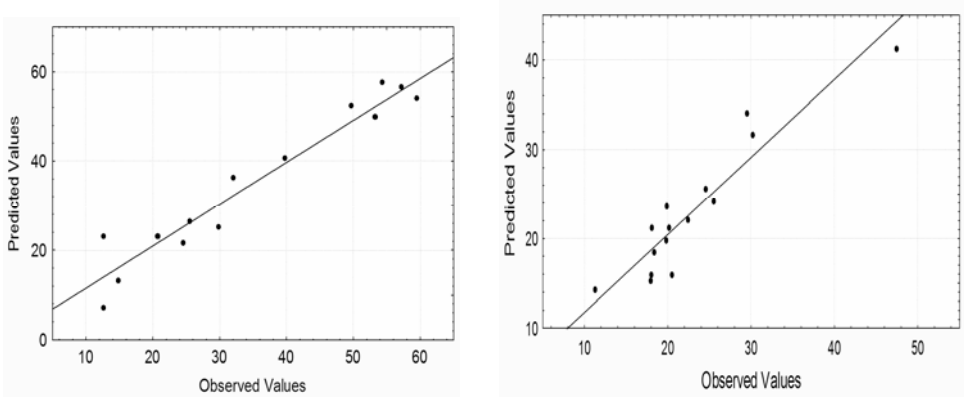

(a) (b)

Figure 3.1. Correlation of the observed and predicted value for (a) selectivity of C_5-C_{10} non-aromatics hydrocarbons (b) selectivity of aromatics hydrocarbons.

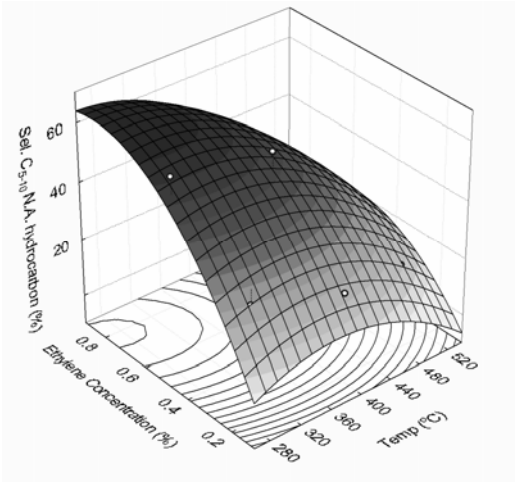

Figure 3.2 Response surface methodology for the $C_{5\text{-}10}$ non-aromatics hydrocarbons selectivity.

Finally, a Response Surface Methodology (RSM) was performed to optimize the operating conditions and maximize the selectivity to C_5-$_{10}$ hydrocarbons. The three-dimensional graph obtained from the calculated response surface is presented in Figure 3.2. Three-dimensional response surface plots of reaction temperature and ethylene concentration against $C_{5\text{-}10}$ hydrocarbons can further explain the results of the statistical and mathematical analyses [39]. It is evident from the plot that $C_{5\text{-}10}$

non-aromatics hydrocarbons selectivity reached its maximum at reaction temperature being 268 ^{o}C with the concentration of ethylene in the methane-ethylene feed being 80.43 % (v/v) and catalyst loading being 0.30 g. The maximum value for the C_{5-10} non-aromatics hydrocarbons selectivity predicted from the model is 64.78%.

3.4. Conclusions

The reaction of methane-ethylene feed over W/HZSM-5 produced organic liquid product rich in gasoline fraction in the range of C_5-C_{10} non-aromatics and aromatics hydrocarbon. Central composite design coupled with response surface can be used to predict the relationship between reaction variables to selectivity of the liquid hydrocarbons. The model equation obtained was statistically checked by ANOVA and the second order polynomial equation presents the experimental results adequately. The optimum predicted value for the selectivity to C_{5-10} non-aromatics hydrocarbons was 64.78 % obtained at reaction temperature being 268 ^{o}C with the concentration of ethylene in the methane-ethylene feed being 80.43 % (v/v) and catalyst loading being 0.30 g.

CHAPTER 4

DIRECT CONVERSION OF METHANE TO HIGHER HYDROCARBONS OVER TUNGSTEN MODIFIED HZSM-5 CATALYSTS IN THE PRESENCE OF OXYGEN

Abstract

The direct conversion of methane to higher hydrocarbons in the presence of oxygen was studied over the tungsten modified HZSM-5 catalysts. The catalysts were characterized by mean of UV-vis diffuse reflectance spectroscopy. It was found that the W-H_2SO_4/HZSM-5 catalyst, prepared from impregnating HZSM-5 with a H_2SO_4-acidified solution of ammonium meta-tungstate (pH = 2-3), showed the highest activity compared to W/HZSM-5 and WO_3/HZSM-5 catalysts prepared from impregnating HZSM-5 with a neutral solution of ammonium meta-tungstate and physical-mixture of solid WO_3 with HZSM-5 respectively. UV-vis DRS provided evidence for the existence of octahedral polymeric species on the W-H_2SO_4/HZSM-5 catalyst. This result seems to imply that the observed high catalytic activity of W-H_2SO_4/HZSM-5 catalyst was closely correlated with the octahedral coordinated tungsten species as catalytically active species. Over a 2%W-H_2SO_4/HZSM-5 catalyst and under reaction conditions of 823°C, 0.1MPa and F/W =1500 ml/g-cat·hr, the average methane conversion reached ≈ 20% with the average yield to aromatic at ≈ 9% after 200 minutes of experiment. In addition, methane conversion in nonoxidative condition was also carried out and the results showed that the catalytic activity was drastically decreased with time on stream, most probably due to severe coking. Consequently, we concluded that the durability of the catalysts was greatly enhanced in the presence of suitable amount of O_2.

4.1 Introduction

In recent years, the direct conversion of methane to higher hydrocarbons has been widely studied in heterogeneous catalysis. Among them, nonoxidative dehydro-aromatization of methane (DHAM) to aromatic over zeolite catalyst has drawn great attention. This process is more energy efficient compare to conventional indirect conversion since it circumvent the expensive syngas step. The aromatic hydrocarbons product also can be easily separated from the unconverted methane.

Numerous researchers have studied the DHAM over Mo/HZSM-5-based catalysts [3, 30, 40-44]. These catalysts performed reasonably well operating at 700°C. Thermodynamic calculations showed that an operating temperature as high as 800°C is required for methane conversion of DHAM to reach 20% [45, 46]. However, under this temperature, these catalysts are deactivated due to the fouling by coke formation and the losing of Mo component by sublimation [4].

Recently, some efforts have been made to add some oxidants into the gas feed in order to remove the coke deposit on the catalysts. Ohnishi et al. [47] reported that the addition of a few percent of CO and CO_2 to methane feed significantly improves the stability of the Mo/HZSM-5 catalyst. The results of Yuen et al. [19] indicated that small amount of O_2 in gas feed can improve the durability of the catalysts. In addition, Tan et al. [17] have claimed that there are three reaction zones in the catalyst bed for the conversion of methane with O_2, namely oxidation, reforming and aromatization and the H_2 and CO generated in the first two zones are responsible for the improvement of the catalyst's performance.

In an attempt to develop a DHAM catalyst which able to operate at high temperature (800ºC or 1073K), Zeng et al [4] have developed highly active and heat-resisting W/HZSM-5-based catalysts. They found from the experiments that the W–

H_2SO_4/HZSM-5 catalyst prepared from a H_2SO_4-acidified solution of ammonium tungstate (with a pH value at 2–3) displayed high DHAM activity at 1023 K even up to 1123 K. They elucidate that the observed high DHAM activity on the W–H_2SO_4/HZSM-5 catalyst was closely correlated with polytungstate ions with octahedral coordination as the precursor of catalytically active species. Later, Xiong et al [6] tested the W–H_2SO_4/HZSM-5-based catalysts with the addition of minor amount of CO_2 to the feed gas. Their results showed that addition of CO_2 significantly enhance the activity and coke resistant performance of the catalyst.

Therefore, it is interesting to study the catalytic performance of W/HZSM-5-based catalysts with the presence of other oxidant besides CO and CO_2, such as O_2. Out previous studies [48, 49] have shown that with the addition of secondary metals, the selectivity of the liquid hydrocarbons over tungsten modified HZSM-5 was improved significantly. In this paper, the preparation of tungsten modified zeolite constituted of different surface tungsten species was reported and the resulting catalysts were tested in the conversion of methane to aromatics using O_2 as oxidant.

4.2. Experimental Procedure

4.2.1 Catalyst preparation

Ammonium-ZSM-5 zeolite with a SiO_2/Al_2O_3 mole ratio of 30 was supplied by Zeolyst International Co., Ltd., Netherlands. The surface area of the zeolite is 400 m^2/g. This NH_4-formed zeolite was calcined at 500°C for four hours to get the H-formed zeolite before any modification and catalytic evaluation were performed. The W/HZSM-5 catalyst was prepared by impregnating HZSM- 5 with a desired amount of ammonium meta-tungstate in a neutral aqueous solution at room

temperature. The W-H_2SO_4/HZSM-5 catalyst was prepared with a desired amount of ammonium meta-tungstate in a H_2SO_4-acidified aqueous solution at pH 2-3 [15]. All impregnated samples (10 ml of solution per gram zeolite) were dried overnight in an oven at 120°C and then calcined at 550°C for five hours. Tungsten oxide was prepared by directly calcined the ammonium meta-tungstate at 550°C for five hours.

4.2.2 Catalytic evaluation

The catalytic evaluation was performed in a fixed-bed continuous-flow quartz reactor with an inner diameter of 9 mm. The reaction over the catalysts was carried out at 823°C, F/W of 1500 ml/g-cat·hr and atmospheric pressure. 1 g of catalyst was used each time for testing and the catalyst was crushed and sieved to size of 30-60 mesh before loaded into reactor. Prior to reaction, the catalyst was flushed with nitrogen at reaction temperature for 1 hour. A feed gas mixture of 80% methane (of 99.99% purity) and 20% air (with N_2 in the air served as internal standard for GC analysis) was introduced into the reactor through Alicat volumetric flow controllers. The reactor effluent gases were analyzed by an on-line Hewlett Packard Agilent 2000 GC equipped with TCD and 4 columns (UCW 982, DC 200, Porapak Q and Molecular sieve 13A). The liquid products were collected just after the experiments and analyzed using FID and HP-1 capillary column in the same GC.

4.2.3 Catalysts characterization

UV-vis diffuse reflectance spectra (UV-vis DRS) were performed on a Perkin Elmer Lambda spectrometer equipped with diffuse reflectance accessory. The

scanning wave length range was 190-500 nm and the scan speed was 120 nm per min.

4.3. Results and Discussion

4.3.1 Results

The UV-vis diffuse reflectance spectra of the 3%W/HZSM-5, 3%W-H_2SO_4/HZSM-5 and WO_3 are shown in Figure 4.1. A band at 210 nm can be observed for 3%W/HZSM-5 and 3%W-H_2SO_4/HZSM-5 catalysts. 3%W-H_2SO_4/HZSM-5 exhibited an additional band at about 290 nm and a further band at about 363 nm is noted for WO_3. de Lucas et al. [20] analyzed the spectra of tungsten compound with a known geometry, namely sodium tungstate, exclusively constituted of tetrahedral tungsten, and ammonium metatungstate and tungsten oxide, both mainly constituted by octahedral tungsten (tetrahedral species are also present as terminal tungsten atoms). By comparing these with the spectra in Figure 4.1, it can be concluded that the band at 210 nm could be assigned to the tetrahedral W (VI) species while the other bands at about 290 nm and 363 nm could be assigned to octahedral W (IV) species: polytungstate and WO_3 crystallites respectively.

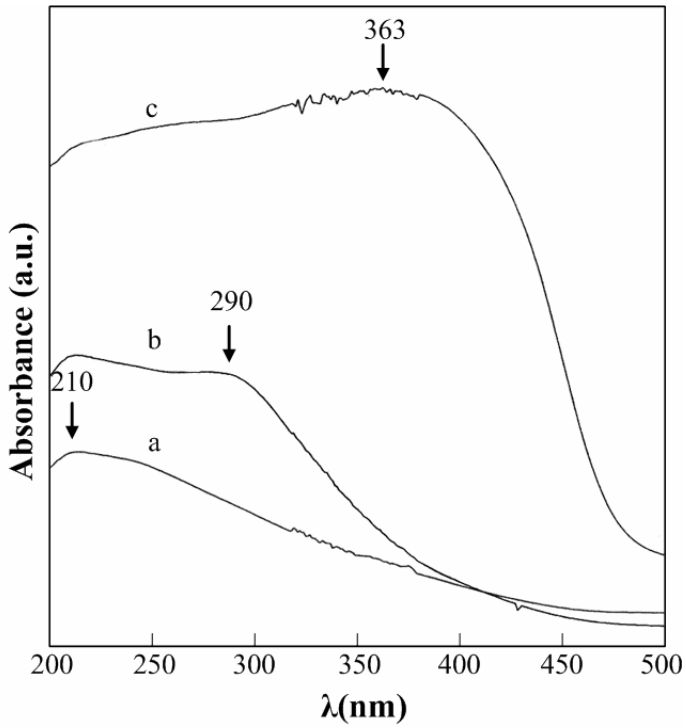

Figure 4.1: UV-vis diffuse reflectance spectra of (a) 3%W/HZSM-5; (b) 3%W-H_2SO_4/HZSM-5; (c) WO_3.

The reaction of CH_4 and O_2 over tungsten modified HZSM-5 catalysts led to the formation of CO, H_2, C_2H_4, C_2H_6 and aromatics. Table 4.1 shows the methane conversion and product yields for the W/HZSM-5-based catalysts, together with the results collected in a non-catalytic reaction using quartz-sand bed and HZSM-5.

In Table 4.1, one can observe that the contribution of the homogeneous reaction could not be neglected in the experimental condition used in this work, since CH_4 conversion as high as 4.5% was obtained with the blank experiment. Likewise, unmodified HZSM-5 zeolite showed a great activity in the oxidation of methane leading to the formation of CO and C_2 hydrocarbons. However, HZSM-5 showed only little DHAM activity in the same experiment.

Table 4.1: Methane conversion and product yields over different tungsten modified HZSM-5 catalysts.

Catalysts	**CH4 conversion (%)**	**Yield (%)**		
		CO_x	**C_2**	**Aromatics**
Blank[a]	4.5	3.1	1.4	-
HZSM-5	12.9	10.7	1.3	0.9
1%W-H_2SO_4/HZSM-5	17.9	10.2	0.9	6.8
2%W-H_2SO_4/HZSM-5	19.9	10.1	0.6	9.0
3%W-H_2SO_4/HZSM-5	17.8	10.2	0.9	6.7
3%W/HZSM-5	13.6	10.2	1.5	1.9
3%WO_3/HZSM-5[b]	15.1	10.4	1.5	3.2
5%W-H_2SO_4/HZSM-5	17.1	10.3	0.9	6.0
10%W-H_2SO_4/HZSM-5	14.6	10.2	0.8	3.6

[a] Quartz-sand bed with a length equal to catalyst bed.

[b] Physical-mixture of solid WO_3 with HZSM-5.

From Table 4.1, it can be seen that the 3%W-H_2SO_4/HZSM-5 catalysts displays rather high DHAM activity in comparison with the 3%W/HZSM-5 and 3%WO_3/HZSM-5. The effect of amount of tungsten loading on DHAM performance of the W-based catalysts was also investigated. It can be seen that both CH_4 conversion and aromatic yield increased initially with increasing amounts of tungsten loading, and reached a maximum at tungsten loading of 2%, whereas it decreased slightly up to 10% tungsten content. These results show that an amount of tungsten loading at ≈2% would be appropriate for the modification of HZSM-5.

Illustrated in Figure 4.2 is the result of DHAM reaction activity over 2%W-H_2SO_4/HZSM-5 with and without oxidant. The results showed that the CH_4 conversion, C_2 hydrocarbons yield and CO yield for oxidative DHAM reaction were higher than that in nonoxidative DHAM reaction. CO was the only detactable oxygen containing product in both cases. In nonoxidative condition, the aromatics

yield reduced drastically from 15.8% at the 40th minute down to 2.6% after 200 minutes of reaction. On the other hand, the aromatic yield in oxidative DHAM reaction was lower than that obtain in nonoxidative reaction but it tended toward stable level after 80 minutes of reactions. The catalysts could retain an aromatics yield more than 8.1% for even more than 200 minutes in oxidative condition.

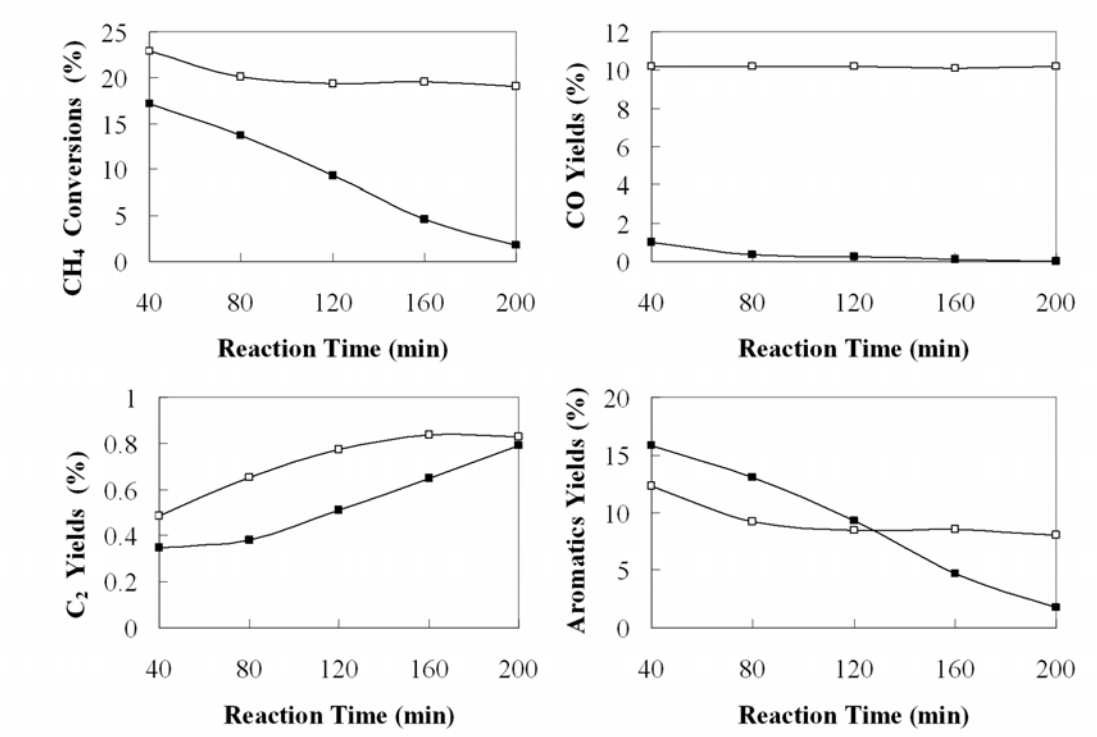

Figure 4.2: Methane conversion activity over 2%W-H_2SO_4/HZSM-5 at 823ºC, feed gas: (□) 80%CH_4 + 20% air; (■) 80%CH_4 + 20%N_2

The aromatics products distribution of 2%W-H_2SO_4/HZSM-5 in oxidative DHAM reaction is shown in Table 4.2. Besides benzene and toluene, trace C_8 aromatics, including ethylbenzene and xylene (dimethylbenzene), and noticeable C_9-C_{12} aromatics could be found in the product.

Table 4.2: Composition of liquid product collected over 2%W-H_2SO_4/HZSM-5 catalysts.

Composition of Liquid Product	**%**
Benzene (C_6)	41.6
Toluene (C_7)	35.8
C_8 aromatics (ethylbenzene, xylene)	4.7
C_9-C_{12} aromatics	17.9

4.3.2 Discussion

The UV diffuse reflectance spectra in Figure 4.1 shows that three tungsten species were formed in the tungsten modified HZSM-5, although the relative amount of each one varies significantly with the modification method. For 3%W/HZSM-5, the monomeric species was predominant. Owing to their small size (<2Å), the presence of tetrahedral species was most likely attributed to the grafting of tungsten oxides species with the Brønsted acid sites located inside the pores of HZSM-5 [20].

On the other hand, the peak corresponding to polytungstate species could be clearly observed on 3%W-H_2SO_4/HZSM-5. This inferred that the addition of H_2SO_4 resulting in formation of the polytungstate species in the precursor solution via the reactions as follows [4]:

$$6(WO_4)^{2-} + 7H^+ \leftrightarrows (HW_6O_{21})^{5-} + 3H_2O$$

or/and

$$12(WO_4)^{2-} + 14H^+ \leftrightarrows (H_2W_{12}O_{42})^{10-} + 6H_2O$$

Lowering the pH value of the precursor solution would shift the equilibria of the above reactions to the right. Since the size of this species is about 2nm, which is bigger than the size of the HZSM-5 pores, this species was expected to be formed on the external surface of the HZSM-5 [20].

The experimental results, together with the UV-vis diffuse reflectance spectra indicated that the present of polytungstate species on the catalysts surface of W-H_2SO_4/HZSM-5 is crucial for oxidative DHAM. This observation is consistent with the previous work for nonoxidative DHAM over W-H_2SO_4/HZSM-5 catalysts and the observed high DHAM activity have been attributed to the pronounced reducibility of polytungstate species on HZSM-5 support [4, 6, 5]. Furthermore, the study on W-H_2SO_4/HZSM-5 by Yang et al. [14] revealed that an induction period exists for nonoxidative DHAM reaction and the tungsten species was reduced to lower oxidation state, most likely W^{4+}, by methane at 973K. The appearance of the DHAM products after the induction period implying that methane was activated with the formation of W^{4+} oxides.

In contrast, for W/HZSM-5 catalysts, tungsten species existed in form of tetrahedral coordination and was difficult to be reduced to W^{4+} state [4, 20], and thus the catalysts had little activity in methane activation. Likewise, the bulk WO_3 on WO_3/HZSM-5 catalyst is more reducible than the tetrahedral W (VI) species [20], and thus had better catalytic performance than W/HZSM-5 catalyst. However, the bulk WO_3 might not be dispersed well on the surface of HZSM-5 through physical mixing. Therefore, the catalytic performance of WO_3/HZSM-5 catalyst was expected not as high as W-H_2SO_4/HZSM-5 catalyst.

The comparison between the catalytic activity of 2%W-H_2SO_4/HZSM-5 in oxidative and nonoxidative condition indicating that deactivation of the catalyst occurred in a certain extent in nonoxidative condition. However, the catalyst was relatively more stable in oxidative condition. This result suggested that the addition

of suitable amount of oxygen greatly improve the catalyst durability; agree well with the work on Mo/HZSM-5 [19, 17].

Yuen et al. [19] attributed the improvement of Mo/HZSM-5 catalysts in oxidative condition to the partial removal of coke deposit on catalysts, and with the catalyst being kept as partially carburized MoO_xC_y/HZSM-5 state. However, according to literature, there was neither reduced metal nor metal carbides formed on W/HZSM-5-based catalyst during methane activation [19, 20]. On the contrary, they pointed out that the W^{4+} species, which is derived from W^{6+} species, is able to activate methane at high temperature. The observed small number of CO in product stream in nonoxidative DHAM reaction was most probably derived from the partial reduction of W^{6+} to W^{4+} by methane.

Therefore, we suggest that the function of O_2 in DHAM reaction over W/HZSM-5-based catalysts is to keep the oxidation state of tungsten species on HZSM-5 as W^{4+}. This added O_2 can partially oxidize the completely reduced tungsten species, and accordingly, the tungsten species can be kept in the state of W^{4+} for a longer time than without O_2, and the durability of the catalyst is improved.

4.4. Conclusions

The W-H_2SO_4/HZSM-5 catalyst, which possesses polytungstate species on the external surface of HZSM-5, showed better catalytic performance in oxidative DHAM reaction compared to W/HZSM-5 and WO_3/HZSM-5 catalysts. The optimum aromatic yield was found at 2% of tungsten loading. The added O_2 in the reactant stream could maintain the active phase possibly, which results in the improvement of the lifetime of the catalyst. The major aromatic products of

oxidative DHAM over 2%W-H_2SO_4/HZSM-5 catalyst are benzene and toluene, and C_8-C_{12} aromatics.

CHAPTER 5

DIRECT CONVERSION OF METHANE TO LIQUID HYDROCARBONS IN A DUAL-BED CATALYTIC SYSTEM: PARAMETER STUDIES

Abstract

A dual-bed catalytic system is proposed for the direct conversion of methane to liquid hydrocarbons. In this system, methane is converted in the first stage to Oxidative Coupling of Methane (OCM) products by selective catalytic oxidation with oxygen over La supported MgO catalyst. The second bed, comprises of HZSM-5 zeolite catalyst, is for the oligomerization of OCM light hydrocarbon products to liquid hydrocarbons. The effects of the temperature (650-800 ^{0}C), methane to oxygen ratio (4-10) and SiO_2/Al_2O_3 ratio of the HZSM-5 zeolite catalyst on the process are studied. At higher reaction temperatures, dealumination of HZSM-5 becomes considerable and thus its catalytic performance is reduced. The acidity of HZSM-5 in the second bed is responsible for the oligomerization reaction to form liquid hydrocarbons. The activity of the oligomerization sites is unequivocally affected by the SiO_2/Al_2O_3 ratio. The relation between the acidity and the activity of HZSM-5 is studied by means of TPD-NH_3 techniques. The rise in oxygen concentration is not beneficial for C_{5+} selectivity where reaction forming carbon oxides ($CO + CO_2$) products from combustion of intermediate hydrocarbon products rather than oligomerization reaction is dominant. The dual-bed catalytic system is highly potential to convert methane directly to liquid fuels.

5.1. Introduction

The direct catalytic conversion of methane into desired chemicals or liquid fuels is still a great challenge in natural gas utilization. The two approaches involved are direct conversion of methane with the assistance of oxidants and direct conversion of methane under non oxidative conditions. However, existing methane conversion methods have proven to be prohibitively expensive and inefficient. Thus, developing a less expensive and more efficient catalytic conversion process is of great interest and technological importance.

The oxidative coupling of methane into ethylene has been extensively studied for the utilization of methane during the past decade. A wide variety of catalysts, mainly metal oxide based catalysts, have been investigated and many types of reaction mechanisms have been proposed. Although significant progress has been achieved in the research and development of the oxidative coupling of methane (OCM) process [51], the technical and economic hurdles have yet to be overcome. One of the more serious limitations of the OCM process is the uneconomical separation of low concentration of ethylene in the product stream. One of the alternatives to overcome this limitation is to convert directly the dilute ethylene present in the OCM product streams into much less volatile product streams, such as aromatics and/or gasoline range hydrocarbons, which can be easily separated. Hence, there is a great need for designing a new concept of catalytic reactor system useful for converting ethylene at very low concentrations or partial pressures into liquid hydrocarbons. The selectivity and yields of higher liquid hydrocarbons are achieved mainly by the development of more selective catalysts, but optimization of reaction conditions, reactor design and operation also provide opportunities for improved performance of the catalytic process.

For that reason, the concept of the double-bed catalytic reactor configuration is proposed. The system comprises of a dual- bed catalytic system for the production

of liquid hydrocarbons from methane gas. In the first bed, methane is converted to OCM light hydrocarbons over La/MgO. Subsequently, the products formed in the first bed oligomerized over HZSM-5 to form liquid hydrocarbons without the needs to separate the OCM light hydrocarbons from the gaseous stream.

The investigation of this type of reactor concept, which combines at least two catalyst or process functionalities, has been the subject of considerable attention in recent literatures. The dual-bed reactor concept enhanced reaction and offers high potential for process simplification and energy conservation. For example, Ramirez et al. [52] proved that a dual-bed catalytic system, consisting of a deNO_x and deN_2O catalyst bed in series, could operate with high and stable activity for successive removal of NO and N_2O. Furthermore, Lee et al. [53] investigated a practical use of a Co-zeolite as a deNO catalyst at a lower temperature in dual-bed system, consisting of deNO and deNO_2 catalyst beds in series. In addition, syngas has been produced from the gasification of various biomasses such as jute stick, bagasse, rice straw, and saw dust of cedar wood using a dual-bed gasifier combined with a novel catalyst. This concept permits the high technology biomass upgrading systems to gaseous and liquid fuels [54]. Recently, Zhu et al. [55] proposed a system with two catalyst beds instead of one single metal catalyst bed for catalytic partial oxidation of methane (CPOM) to synthesis gas. The most important advantage of this approach is the prevention of any contact between oxygen and the metal catalyst, because oxygen is completely converted on the first bed catalyst. Therefore, metal loss via evaporation of oxides can be excluded. Thus, the previous research on the dual-bed catalytic system provides an incentive to develop conceptually this type of catalytic system in the present work (see Figure 5.1).

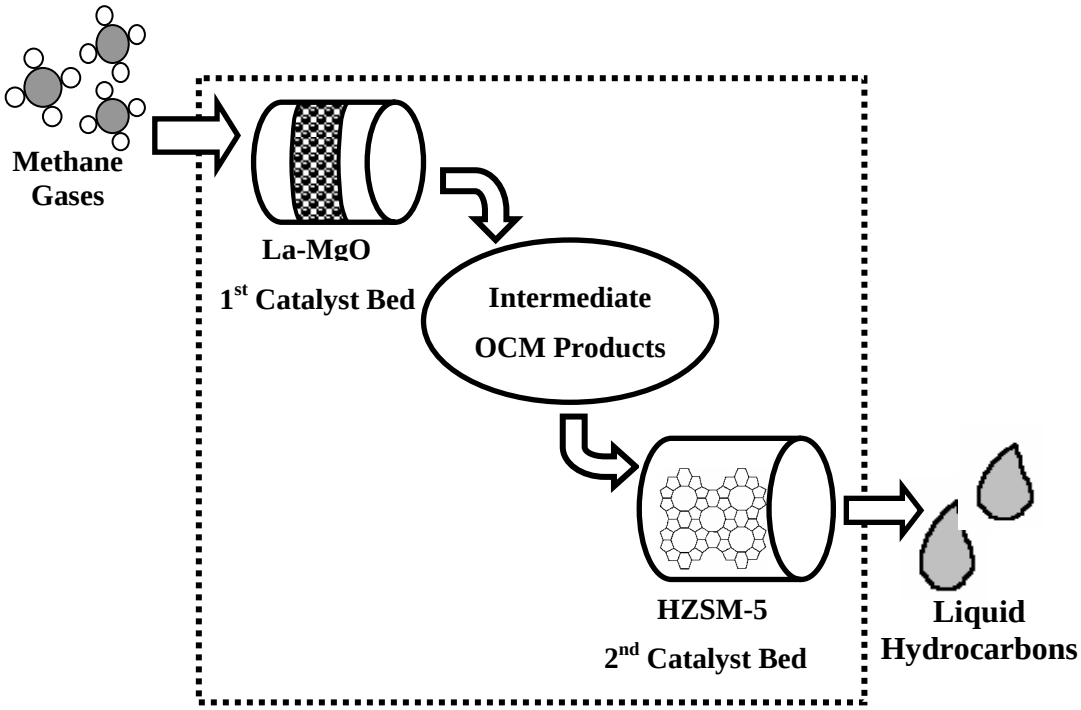

Figure 5.1: Simplified reaction scheme for the dual-bed catalytic system over La/MgO and HZSM-5 catalysts

On the other hand, a number of earlier studies have demonstrated that La promoted MgO is a reasonably good catalyst for the OCM reaction [56-63]. Choudhary *et al.* [60] reported that La–promoted MgO exhibited remarkable activity and high C_2 selectivity (towards C_2H_4+ C_2H_6) and also high catalyst stability in the OCM process. Their study also indicated that the promotional effect by lanthanum doped on MgO was attributed to a large increase in the strong basicity of the catalyst. Hence, La-MgO has been chosen as the viable candidate for the catalyst in the first bed for the dual-bed catalytic system in this study. Subsequently, the function of the second catalytic bed to oligomerize the OCM light hydrocarbons comprising of mainly olefins to higher hydrocarbons is handover to the HZSM-5 catalyst. Earlier studies have demonstrated that acidic HZSM-5 zeolite catalyst is a reasonably good oligomerization catalyst for converting C_2 products to higher hydrocarbons [64-68].

In this work, La-MgO is placed in the first layer whilst HZSM-5 in the second so that the affiliation between basicity and acidity of the catalysts could be explored in order to attain the maximum selectivity of the liquid hydrocarbons. The main objective of this paper is to carry out a systematic research on the effect of important process parameters like the reaction temperature (650-800 ^{0}C), CH_4/O_2 ratio (4-10) and the SiO_2/Al_2O_3 ratio of HZSM-5 (SiO_2/Al_2O_3 = 30, 50, 80 and 280) on the performance of the dual-bed catalytic system. The relation between the acidity and the activity of HZSM-5 are studied by means of TPD-NH_3 techniques.

5.2. Experimental Procedure

5.2.1 Catalysts Preparation

The La promoted MgO catalyst was prepared by mixing powdered magnesium oxide with lanthanum nitrate (La/MgO= 0.1 mol ratio) in deionized water just sufficient to form a thick paste and dried at 120 ^{0}C for 12 h. The resulting dried mass was then calcined at 800 ^{0}C for 10 h in static air. Four HZSM-5 samples, with different SiO_2/Al_2O_3 ratios, were used and designated as HZ (30), HZ (50), HZ (80) and HZ (280), where the parenthesises indicate the SiO_2/Al_2O_3 molar ratio. Zeolytst^{TM} International supplied all the ZSM-5 zeolite in the ammonium form. The ammonium form was converted to HZSM-5 by calcining at 550 ^{0}C for 5 h. In addition, HZSM-5 (SiO/Al_2O_3=30) were also pretreated at different thermal conditions (T=550, 600, 650, 700, 750 and 800 ^{0}C) in order to study the effect of temperature on the acidity of the HZSM-5. These zeolites were coded as HZT-(*X*) [HZT-(550), HZT-(600), HZT-(650), HZT-(700), HZT-(750) and HZT-(800)] where *X* refers to the temperature at which thermal treatment was performed.

5.2.2 Catalyst Characterization

All the catalysts in this study were characterized using temperature-programmed desorption of ammonia (TPD- NH_3). The measurements for this TPD-NH_3 analysis were carried out using a Micromeritics TPD/TPR 2900 Instrument. The catalyst utilized was 300 mg for each experiment. First, the sample was heated up to 773 K under a flow of dry nitrogen and kept at that temperature for 1 h in order to desorb all traces of desorbed water. The sample was then cooled down to ambient temperature. Next, the sample was saturated in ammonia gas flow for 30 min, and subsequently loosely bound ammonia was removed by purging the catalyst with by nitrogen stream at a flow rate of 20 ml/min for 30 min, and finally cooled down to room temperature. The amount of desorbed ammonia was determined by a linear heating rate of approximately 15 K/min from 393 K to 823 K while the evolved ammonia concentration was monitored using thermal conductivity and mass spectrometric detectors.

5.2.3 Catalytic Evaluation

The reaction was performed at atmospheric pressure using a conventional fixed-bed quartz reactor with dimensions of 10 mm inner diameter and 300 mm length (Figure 5.2). In the dual-bed catalytic system, the feed gas mixture was first passed over the La-MgO catalyst in the first bed followed by the HZSM-5 catalyst bed. A plug of glass wool separated the two catalyst beds. A Carbolite tube furnace (Model: MTF 10/15/130) was used to heat up the reactor to the required operating temperature. Inside the reactor tube, a thermocouple was inserted along the axial direction to monitor the temperature of the catalyst beds. The temperatures reported were those for the OCM bed; the temperature of the second bed was about 115 ^{0}C

lower than the OCM bed. The difference of 115 ^{0}C remained constant over the OCM bed temperature range between 650 and 800 ^{0}C.

For catalyst testing, the catalyst was first activated in situ by heating to 550 ^{0}C for 1 h in flowing nitrogen before the flow was switched to the reactant gases. The reactant feed gas used in this study were high purity methane (≥99.9% purity) and oxygen (≥99.99%). The inlet volumetric flow rate of each gas was controlled using the individual volumetric flow controller (Alicat) with a flow rate range from 5-512 ml/min.

The product stream leaving the reactor was separated into liquid and gas fractions using water bath. The reactor effluent gases were analyzed on-line by means of a Hewlett Packard Agilent 6890N gas chromatograph system equipped with thermal conductivity detector (TCD) and four series column (UCW 982, DC 200, Porapak Q and Molecular Sieve 13A). The fraction of collected liquid products was determined by manually injecting the liquid in the same GC. The liquid was then separated by a capillary column and detected by a flame ionization detector (FID). The conversion of CH_4 and the selectivity of the products were calculated on the carbon basis (coke was not taken into account).

.

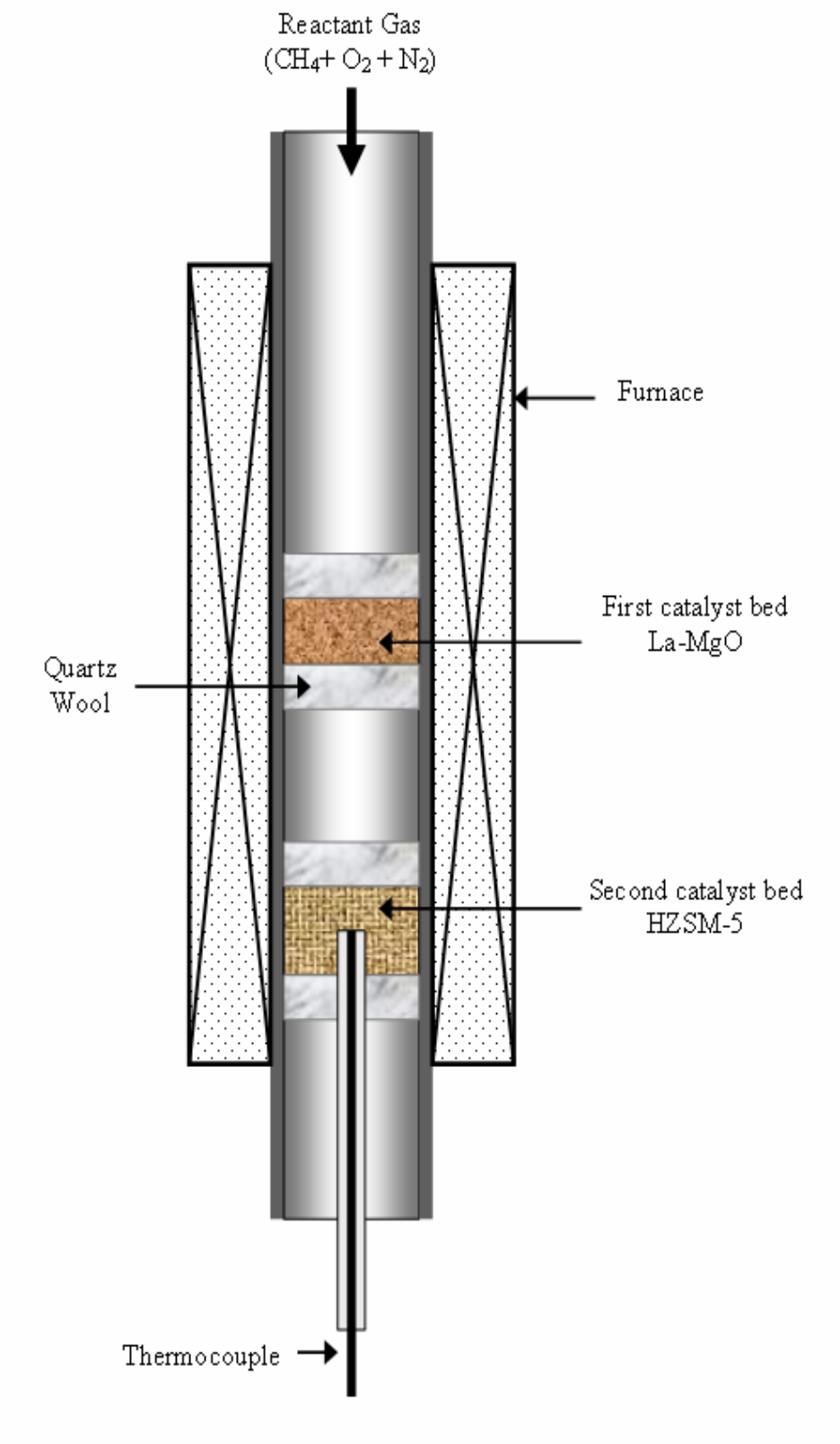

Figure 5.2: Dual-bed catalyst reactor set-up

5.3. Results and Discussion

5.3.1. Catalysts Characterization

5.3.1.1 SiO_2/Al_2O_3 Ratio Effect

The NH_3-TPD profiles of the HZSM-5 catalysts with different SiO_2/Al_2O_3 ratios are depicted in Figure 5.3. All samples exhibit two well resolved desorption peaks: the low desorption temperature peak (α) and the high desorption temperature peak (β) are in good agreement with other previous reports [69-70]. The α peak is assigned to desorption of ammonia from silanol and other weak acidic centers; the β peak is assigned to desorption of ammonia from strong acid sites [64, 71-73]. Based on the peak intensities, the relative areas of these two peaks (α and β) are proportional to the SiO_2/Al_2O_3 ratio.

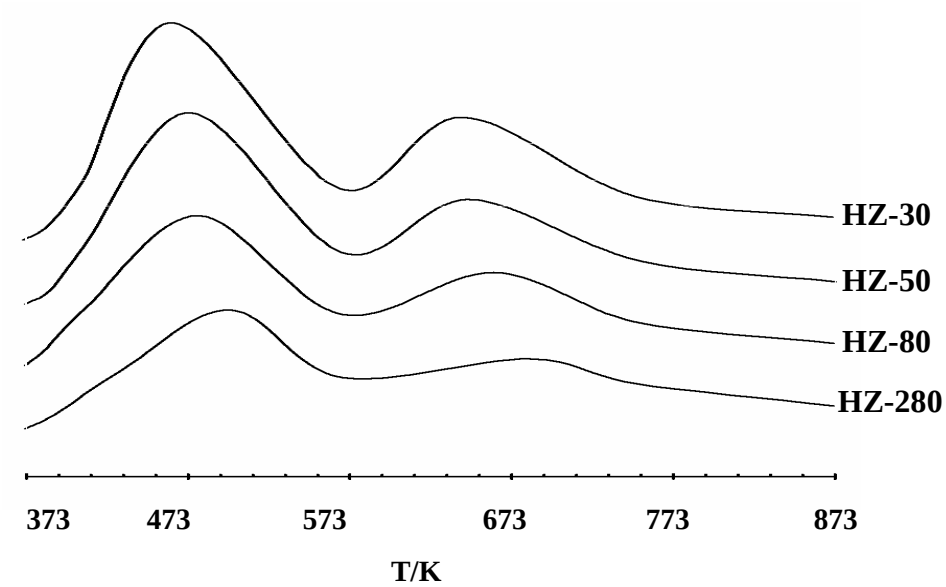

Figure 5.3: Temperature programmed desorption of ammonia from HZSM-5 with different SiO_2/Al_2O_3 ratios

Table 5.1: Acidity of HZSM-5 catalysts with different SiO_2/Al_2O_3 ratios by TPD-NH_3.

Sample	Total acidity (mmol NH_3 $_{gcat-1}$)	Weak Acidity (mmol NH_3 $_{gcat-1}$)	T_d(K)	Strong Acidity (mmol NH_3 $_{gcat-1}$)	T_d(K)
HZSM-5 (30)[b]	1.25	0.41	465	0.84	644
HZSM-5 (50)	1.17	0.37	475	0.80	648
HZSM-5 (80)	0.91	0.31	480	0.60	663
HZSM-5 (280)	0.22	0.09	499	0.13	685

[b]The SiO_2/Al_2O_3 ratio of the materials are given in the parentheses

The results in Table 5.1 show that the total number of acid sites (the strong and the weak acid sites) increases with Al content. A general decrease of the total amount of desorbed ammonia was found for increasing SiO_2/Al_2O_3 ratio, indicating an overall decrease in the concentration of the acid sites. The amount of ammonia (Table 5.1) also allows us to evaluate the concentration of accessible weak and strong acid sites. The strong acid sites increase with Al content. Theoretically, one proton should be introduced for each framework Al^{3+}, and therefore the larger the number of framework aluminum atoms, the higher the potential number of acid sites would be in zeolite [74-75]. Strong acid sites (Brønsted) are generated by tetrahedrally coordinated Al atoms forming Al-O(H)-Si bridges [76]. The increase in the strong acid sites with Al content implies that most of the Al is tetrahedrally coordinated in the framework. Therefore, it is clear that the total number of Brønsted acid sites present in a zeolite catalyst depends on the framework SiO_2/Al_2O_3 ratio, or more generally speaking, on the ratio of framework M^{4+}/M^{3+} cations.

5.3.1.2 Thermal treatment analysis of the HZSM-5 samples

The thermal analysis was carried out to determine the thermal stability of the HZSM-5 (SiO_2/Al_2O_3=30) zeolite and to measure the loss of acidity as a function of temperature. The samples investigated in this work were obtained by heating in air the parent HZSM-5 catalyst at different temperatures. From the intensities of the signals in Figure 5.4, it can be deduced that the amount of available acids depends on the treatment temperature although the samples possess the same SiO_2/Al_2O_3 ratio. The densities of the strong acid sites are significantly reduced, as indicated by the height (or the area under curve) and the temperature of the high temperature peaks, respectively, as shown in Figure 5.2. However, the density and strength of weak acids do not change as significantly as those of the strong acids.

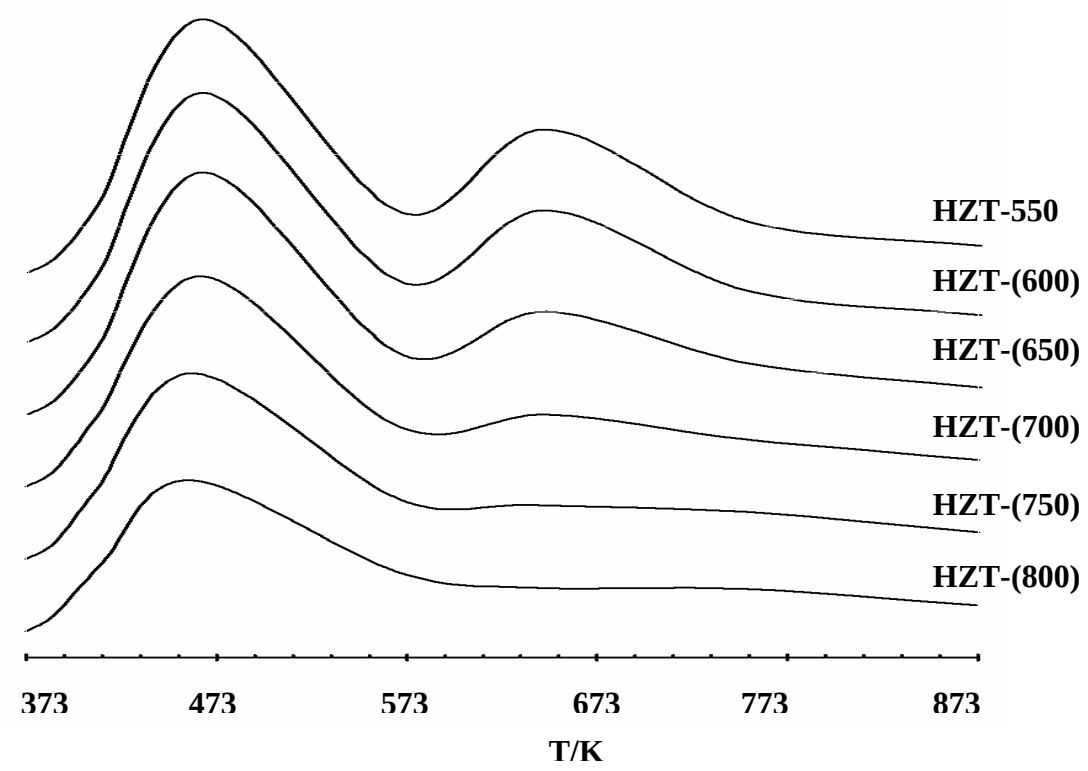

Figure 5.4: NH_3-TPD profiles of HZSM-5 catalysts treated at different temperatures

On the other hand, HZT-550 possesses the largest amount of available strong and weak acid sites among the six samples (Table 5.2). However, the number of both strong and weak acid sites decreases remarkably, when HZSM-5 undergoes heat treatment. Finally the TPD profile of HZSM-5 demonstrates that the heat treatment at above 750 ^{0}C is more likely to decrease the amount of acid sites where only one peak at low temperature (~460 K) is observed, indicating a low acidity.

Table 5.2: NH_3 sorption capacity of the HZSM-5 samples treated at various temperatures.

Sample	Temperature (^{0}C)[a]	Total acid density (mmol/g)	Loss of strong acid sites after thermal treatment(%)[b]
HZT-(550)	550	1.25	-
HZT-(600)	600	1.03	25.57
HZT-(650)	650	0.88	71.87
HZT-(700)	700	0.85	85.68
HZT-(750)	750	0.66	98.03
HZT-(800)	800	0.61	100

[a] temperature of thermal treatment analysis

[b] loss of strong acid sites at each temperature calculated relative to amount of strong acid sites at HZT-(550)

The trend of the acidity values measured by this technique agrees favorably with those obtained by other researchers. According to Xing et al. [77], the increase in calcinations temperature would attribute to the removal of water molecules, resulting in the decrease of Brønsted acid sites with constant increase in Lewis acid sites. Additionally, the reduction of acid sites concentration for the higher temperature desorption peak is much more remarkable at temperatures above 700 ^{0}C as shown in Table 5.2. Campbell et al. [28] pointed out that dealumination of zeolite lattice occurred at T= 725 ^{0}C for HZSM-5 and there would be the breaking of the Si-H-Al bonds and the formation of extralatice aluminum species. At T≥ 750 ^{0}C, Tan et

al. [79] observed dealumination and suggested with the partial destruction of the HZSM-5 structure and the occupancy of the channels by extralatice aluminum, there would be a reduction mainly in the number of strong acid sites. Similar results are also observed in our present study. Ultimately, these results suggest that the total amount of ammonia adsorbed continuously decreased with increasing treatment temperature due to the dealumination of framework alumina of the treated HZSM-5 samples.

5.3.2 Catalytic Performance

5.3.2.1 Effect of Temperature

Figure 5.5(a) displays the variation in the rate of reaction of methane over the dual-bed catalysts and the corresponding product distribution as a function of temperature. A ratio of CH_4 to O_2 about 10:1 (in volume) was selected, and the temperature was varied from 650 ^{0}C to 800 ^{0}C. Figure 5.5(a) exhibits the slight increase in the conversion of methane obtained when the temperature increased from 650 ^{0}C to 800 ^{0}C, but only to a small extent. It is also noted that by increasing the temperature, the ratio of ethylene/ethane ratio increased monotonously. The selectivity of C_{5+} goes through a maximum for a temperature of 700 ^{0}C and then decreased dramatically. At T=800 ^{0}C, HZSM-5 (SiO_2/Al_2O_3=30) catalyst succumbed and failed to function as a catalyst for oligomerization reaction. As the temperature is increased, the selectivity of C_3 remained almost constant. The selectivity of C_4 was constant until 750 ^{0}C, and then leveled-up significantly at 800 ^{0}C. The CO_2/CO ratio was nearly constant over the temperature range of 650-700 ^{0}C but increased to a stable value at higher temperatures.

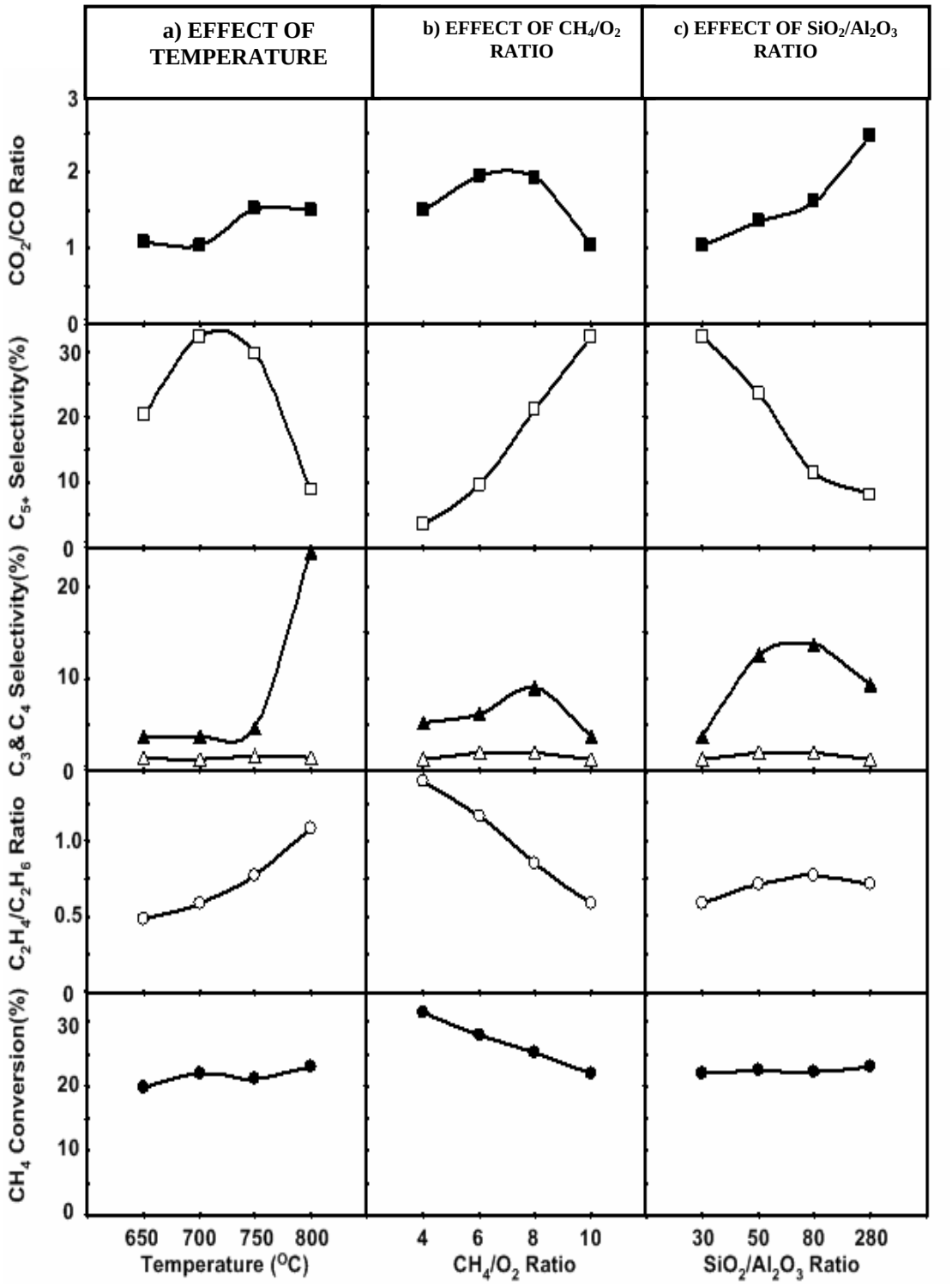

Figure 5.5: Influence of reaction parameters on the catalytic activity and product distribution (● methane conversion, ○ C_2H_4 to C_2H_6 ratio, Δ selectivity of C_3, ▲ selectivity of C_4, □ selectivity of C_{5+} and ■ CO to CO_2 ratio)

The influence of temperature on methane conversion is similar to most of the results investigated for OCM catalysts. With increasing temperature, methane conversion passes through a maximum or reaches a plateau. The temperature of maximum conversion of methane is unique for each catalyst and depends on the partial pressures of reactants as well as on mixing pattern, which are different in various reactor types. However, in the dual-bed reactor system investigated here, numerous simultaneous reactions involved in the complex reaction pathway of methane and intermediate/final products transformation can also produce methane, decreasing the net conversion of methane [80-81] as the temperature increases. In addition to the heterogeneous reactions, a large number of homogeneous free radical reactions [82-85] are also involved, depending upon the process conditions. Hence, the profile of methane conversion as a function of temperature in this study is slightly different compared with those for single bed La/MgO catalysts reported in the literature [56, 57, 60].

The increase in the ethylene/ethane ratio as a function of temperature indicates that the conversion of ethane to ethylene is favored at higher temperatures. It is expected due to the thermal decomposition of ethyl radicals and thermal cracking of ethane at higher temperatures [57]. The increment in the C_2 olefin selectivity with an increase in temperature can be explained on the basis that an increase in temperature increases the rate of dehydrogenation reactions and more C_2 olefins are formed at the expense of C_2 paraffins [86].

Ethylene that is produced in the first stage may be reacting with other intermediate species, undergoing numerous secondary transformations in the second bed catalyst. Thus, the presence of strong acid sites in the HZSM-5 promotes the oligomerization and cyclization reactions in complex mechanism to produce C_{5+} hydrocarbons. Nevertheless, deactivation of HZSM-5 catalysts at high temperatures as proven earlier by TPD-NH_3 characterization analysis in this study, affects the product distribution and trends in the catalytic reaction. Thus, a significant change in the acidic property at higher temperature causes the HZSM-5 catalyst to be less

effective for oligomerization reaction. This phenomenon exerts more negative effect in terms of ethylene oligomerization and it proved that the presence of strong acid sites is essential for ethylene oligomerization. Hence, the ratio of ethylene to ethane increased markedly and the selectivity of C_{5+} decreased drastically above 700 ^{0}C. Based on these inclinations, the effect of thermal deactivation of the HZSM-5 in the second bed catalyst demonstrated that the amount of ethylene formed in the first catalyst bed was greater than the amount of ethylene consumed at higher temperature in the second bed.

In the dual-bed catalytic process, the visible increase in selectivity of C_4 products over the investigated La-MgO and HZSM-5 catalysts is displayed only when the temperatures is elevated to 800 ^{0}C. The enhancement in C_4-hydrocarbon selectivity implies that reaction temperature at above 750 ^{0}C exert an effect more negative on oligomerization reaction than on C_2 activation in the second bed, and the presence of Brønsted acid sites is essential for oligomerization. In addition, the marked increase of C_4-hydrocarbon selectivity coupled with the decrease in the amount of acid sites demonstrates that C_4-hydrocarbons is an initial product in C_2-hydrocarbon activation in the second bed reaction.

On the other hand, the rise of CO_2/CO ratio in the whole investigated temperature range indicates the formation of CO_2 is more favored at higher temperature [87]. This implies that reaction steps that lead to the formation of CO_2 increased at a faster rate with temperatures than those that lead to the formation of hydrocarbons. Accordingly, this observation is consistent with the results reported in the literature and implies a higher rate of carbon oxidation with an increase in temperature and the CO formed is converted to CO_2 at higher temperatures [88-89].

5.3.2.2 Effect of Oxygen Concentration

In the second series of experiments, we studied the effect of varying the methane to oxygen (CH_4/O_2) ratio at a reaction temperature of 700 ^{0}C on the combination of both La/MgO and HZSM-5 (SiO_2/Al_2O_3 =30) catalysts. As shown in Fig. 5.5(b)**,** with increasing CH_4/O_2 ratio, the methane conversion and ethylene to ethane ratio decrease constantly. However, the selectivity of C_4 and the ratio of CO_2/CO go through a maximum for a ratio of CH_4/O_2 about 8 and then decrease dramatically. In contrast, the selectivity of C_{5+} increases remarkably and the selectivity of C_3 remains almost constant with increasing CH_4/O_2 ratio.

Chaundary *et al.* [60] and Davydov *et al.* [90] have reported that the promotional effect of the lanthanum on MgO is attributed to a large increase in the strong basicity of the catalyst. This property is responsible for the La-MgO catalyst to exhibit better catalytic performance in the OCM process, giving higher values of methane conversion and C_2 (C_2H_4 + C_2H_6) selectivity. However, the HZSM-5 catalyst which is tested as an oligomerization function catalyst was reported to have shown lower activities on the methane conversion compared to the OCM catalysts [51, 91]. Based on this understanding, it can be concluded that in our dual-bed catalytic system, La/MgO catalyst is particularly responsible for the methane conversion to produce OCM products at the first stage. Therefore, discussions about the effect on the conversion of methane in dual bed catalytic system as well as about the CH_4/O_2 ratio in the feed will correlate with OCM reactions over the La-MgO catalyst.

Anshits et al. [93] and Takashi et al. [94] have demonstrated that the presence of gas phase oxygen is essential for favorable methane activity in order to achieve a high level methane conversion via OCM reaction. The equilibrium adsorption reaction between gas phase O_2 and the La-MgO catalyst result in a form of surface oxygen that is capable of abstracting a hydrogen atom from methane where methyl

radicals formed on the surface coupled in the gas phase to produce ethane [85, 87-88]. Consequently, oxygen is absolutely required as a key in the formation of methyl radicals. Therefore, the clear correlation between the methane conversion and oxygen concentration could be found in Figure 5.3(b), suggesting that the rate of methyl radical formation (rate determining step of this reaction) is exclusively related to the methane to oxygen ratio, in accordance with previous conclusions drawn from the study of the oxidative coupling over alkali earth metal oxides and rare earth metal oxide catalysts [58, 59, 95].

It is interesting to note that, at least for the selective route leading to C_2 products, methane must be activated into methyl radicals released into the gas phase. Ethylene as well as ethane are primary reaction products from methane, but at higher oxygen concentration ethylene was predominantly produced from ethane in a secondary reaction in accordance with previous studies [51, 88]. The increase in the ethylene/ethane ratio with decreasing CH_4/O_2 ratio, also observed in the earlier studies [57, 60], is most probably due to the availability of oxygen at higher concentration for the subsequent gas phase reactions involved in the formation of ethyl radicals and ethylene from ethane. Therefore, the results in this study indicate that ethylene formation is not a result of dehydrogenation of ethane and suggests that the main production of secondary product ethylene is by oxy-dehydrogenation of the primary product, ethane [56, 96]. This phenomenon explains why the profile of the ethylene to ethane ratio increased with the decrease of the CH_4/O_2 ratio as illustrated in Fig. 5.5(b).

In the presence of oxygen, numerous studies reported the ease of gas phase oxidation of ethylene and this is not surprising owing to the fact that the double bond in ethylene is much more susceptible to be activated to undergo both catalytic and non-catalytic combustion reaction to form CO_x products [81, 97]. In addition, high oxygen concentrations cause some of the intermediate and desired final hydrocarbon products to become more combustible and it is also attributed solely to the lost in selectivity of the products [87]. Therefore, with an increase in oxygen concentration,

the C_4 and C_{5+} formations are curtailed. These outcomes could be reasonably understood by considering that high oxygen concentration improves the storage of oxygen capacity on the catalysts surface and gas phase. As a result, in the high oxygen rich environment, the combustion rate increases faster than the oligomerization rate which caused marked decrement of C_4 and C_{5+} hydrocarbon products. Therefore, the concentration of oxygen should be kept at low levels to minimize the undesired oxidation of ethylene.

The dependence of CO_2/CO ratio on CH_4/O_2 ratio clearly indicates consecutive oxidation of CO to CO_2. From the experimental results, and also based on the data published in the literature, it is possible to make some considerations that the availability of higher oxygen favors the conversion of CO to CO_2 and formation of more CO_2 as compared with that of CO in the process under the oxygen-advantaged conditions. Conversely, at the higher oxygen concentration (CH_4/O_2= 4 and 6), production of both CO and CO_2 involves a complex reaction system, with the reaction steps occurring in series and parallel. In such a situation, the response of CO and CO_2 products to change in CH_4/O_2 ratio does not necessarily produce any definite trends. Thus, summarizing these experiments, it is clear that a rise in oxygen concentration gives a positive effect in terms of methane conversion but is not beneficial for C_{5+} selectivity, which is our main desired product in this study.

5.3.2.3 Effect of Acid Site Concentration

The catalytic properties of HZSM-5 materials with different SiO_2/Al_2O_3 ratios were evaluated for the same reaction conditions at temperature 700 ^{0}C and CH_4/O_2 ratio 10. This study was carried out in an attempt to test the hypothesis that the Brønsted acid sites of HZSM-5 participate actively in the oligomerization reaction step in the dual-bed catalytic system.

It can be seen that the methane conversion and selectivity of C_3 hydrocarbon (Figure 5.5(c)) remain almost constant for the whole SiO_2/Al_2O_3 range studied. The ratio of ethylene to ethane and selectivity of C_4 increase when SiO_2/Al_2O_3 ratio is increased from 30 to 80. Nonetheless, these trends slightly decrease with SiO_2/Al_2O_3 ratio 280. Furthermore, increasing SiO_2/Al_2O_3 ratio of HZSM-5 results in a sharp decrease in selectivity of C_{5+} and a gradual increase in the ratio of CO_2 to CO.

As was presumed, the HZSM-5 catalysts in the second bed are much less active toward unreacted methane molecules from the first bed. Additionally, not much variation in the methane conversion was observed even by changing the acid properties of the second bed by varying the SiO_2/Al_2O_3 ratio of the HZSM-5 zeolite. The results seems to suggest that HZSM-5 used as second bed in this approach is not an active phase to alter the methane molecules and thus methane conversion is independent of the HZSM-5 catalyst. Based on the above consideration, it is evident from this study that acidic HZSM-5 catalyst applied as second bed is less effective to dissociate the C-H bond in methane and the C-H bond activation of methane mainly depends on the first bed of La-MgO catalyst. These results also help us to conclude that the La-MgO catalyst is vital to catalyze the methane reaction.

On the other hand, the knowledge on the structure of the active centres is of prime importance to elucidate the HZSM-5 catalytic activity in the dual bed catalytic system. Schwarz and co-workers [73] reported that the structure of Brønsted acid centres is responsible for the oligomerization reaction and there is a significant change in product distribution with an increase in SiO_2/Al_2O_3 ratio of HZSM-5. As reveal by the TPD-ammonia characterization results, the density of strong acid sites is dependent upon the value of the SiO_2/Al_2O_3 ratio, whereby lower SiO_2/Al_2O_3 relates to higher amount of strong acid sites. In addition, the literature indicates that the chemical uniformity of the Brønsted-type acid sites (framework hydroxyl groups) in the HZSM-5 contents has been proven in the oligomerization test, where the oligomerizing activity is linearly related to Brønsted acid sites content [73,98-99]. Furthermore, Vereshchagin et al.[100] suggested that the reaction of ethylene

oligomerization via HZSM-5 catalyst is a sequence of reactions that include a slow step of active surface species formation followed by a fast process of chain growth. Thus, the Brønsted acid sites of HZSM-5 in the second bed are responsible for oligomerizing the initially formed ethylene by the OCM catalyst in the first bed to produce C_{5+} hydrocarbon products in this catalytic system [64, 66, 73, 100].

Consequently, one can observe a monotonic increase in C_{5+} selectivity with a decrease in the bulk SiO_2/Al_2O_3 ratio. This increase becomes more noticeable for the HZSM-5 with larger aluminum content, namely HZSM-5 with SiO_2/Al_2O_3 of 30 and 50. This trend can be related to the high hydrogen transfer [HT] capability of low SiO_2/Al_2O_3 that results in the increase of the rate of oligomer formation as previously reported [98, 100]. Therefore, it is demonstrated that C_{5+} product selectivity in this study depends strongly on the distribution of Brønsted acid sites, which is related to the extent of hydrogen transfer reactions. The linear correlation between selectivity of C_{5+} hydrocarbon products and concentration of Brønsted acidic site confirms the crucial role of acid sites in oligomerization reaction.
Another interesting observation that has been found in this study is the nearly opposite variation in selectivity of C_4 and C_{5+} hydrocarbon as a function of SiO_2/Al_2O_3 ratio. The results suggest that the C_4 hydrocarbon is produced at the initial stage of the oligomerization reaction due to the coupling of ethyl radicals both on the catalyst surface and in the gas phase reaction [101-103]. The C_4 species hydrocarbon which is more reactive than C_2 species will oligomerize further to produce C_{5+} hydrocarbon products in the dual-bed catalytic system.

One can speculate as to why the ethylene to ethane ratio is quite small at low SiO_2/Al_2O_3 ratio. The most likely hypothesis is that the double bond in ethylene is much more susceptible to be activated than the C-H bonds in ethane. Therefore, HZSM-5 with SiO_2/Al_2O_3 of 30 which has high acid density sites will increase the rate of ethylene consumption which reflects the rate of oligomer formation [73,104-105] and causes the ethylene to ethane ratio to reduce at low SiO_2/Al_2O_3 ratio. For that reason, it can be observed in Figure 5(c) that the increase in the ethylene to

ethane ratio in the final products, coupled with the increase in the SiO_2/Al_2O_3 ratio of the HZSM-5 demonstrated the limited occurrence of oligomerization reaction for the catalyst with a small amount of acid sites.

Changing SiO_2/Al_2O_3 ratios in the range of 50-280 and other reaction parameters do not signify the selectivity of C_3. Therefore, it is not clear whether C_3 species hydrocarbon play any direct or indirect role in the catalytic oligomerization reaction in the second bed HZSM-5 catalyst. Likewise, HZSM-5 zeolite shows a great activity in the oxidation of light hydrocarbons leading to the formation of total oxidation products, mainly carbon oxide. Consequently, the ratio of CO_2 to CO increases as the SiO_2/Al_2O_3 ratio of HZSM-5 increase. This result indicates that HZSM-5 with relatively strong acidity lead to CO formation as observed previously [106].

The results in this study clearly suggests that the active sites for oligomerization is predominantly affected by the SiO_2/Al_2O_3 ratio thus, reflecting a large amount of Brønsted acid sites are mainly responsible for the formation of larger hydrocarbons. HZSM-5 with low SiO_2/Al_2O_3 ratios in the second bed gives higher activity and selectivity to the desired C_{5+} liquid hydrocarbons products.

5.4. Conclusions

The conversion of methane and C_{5+} selectivity in the dual-bed system were strongly dependent on the reaction temperature and oxygen concentration as well as were directly proportional to the number of strong acid sites. The results implied that the Brønsted acid sites of HZSM-5 were the active centers responsible for the oligomerization of primary ethylene products. Oxygen was absolutely necessary for

the formation of the methyl radicals from methane, but it should be provided at a controllable manner in order to avoid undesired oxidation of intermediate OCM products. In addition, the partial destruction and dealumination of HZSM-5 at higher temperature had caused the deactivation of the second bed meant for the oligomerization reaction. The activity of the oligomerization sites was unequivocally affected by the SiO_2/Al_2O_3 ratio. This exploration also suggests that the concept of the dual-bed catalytic system via direct process is an interesting contender for application in the OCM technology that would overcome the separation limitations and permits the process to be more viable from the economic point of view.

CHAPTER 6

KINETIC STUDY FOR CATALYTIC CONVERSION OF METHANE IN THE PRESENCE OF CO-FEEDS TO GASOLINE OVER W/HZSM-5 CATALYST

Abstract

The kinetic of catalytic methane conversion in the presence of co-feeds ethylene and methanol over W/HZSM-5 was studied in a fixed-bed micro reactor at atmospheric pressure and temperatures between 973 -1073 K. Methane concentration in the feed (methane+ethylene+methanol+N_2) was varied from 50% to 90% v/v at constant ethylene and methanol concentrations. The kinetic model based on Langmuir-Hinshelwood reaction mechanism fitted well with the experimental data as the deviations between experimental and simulated data were relatively low. Arrhenius and Van't Hoff equations were used to calculate the kinetic parameters: activation energy (E_a), frequency factor (k_0), adsorption enthalpy (ΔH_{ads}), and entropy (ΔS_{ads}).

Keywords: kinetic, methane, W/HZSM-5 catalysts, co-feeds

6.1 Introduction

The use of crude oil as the feedstock for gasoline production has a major drawback due to depleting oil deposits. On the contrary, natural gas is available in abundance; therefore, it is considered to be a more attractive alternative source for gasoline production. The current technology to convert methane, the main component of natural gas, to desirable chemical products proceeds by indirect process. The first step in the indirect process is the conversion of methane to syngas ($CO + H_2$) via steam reforming or partial oxidation. The second step is the conversion of syngas to desirable chemical products either by Fischer Tropsch (FT) or Methanol to Gasoline (MTG) routes. However, the utilization of methane (the main constituent of natural gas) to desirable chemical products or liquid fuel has limitation due to the stability of methane molecule having four C-H covalent bonds [107].

Extensive research efforts have been devoted to the direct conversion of methane to higher hydrocarbons and aromatics. The transformation of methane to higher hydrocarbons and aromatics has been studied under oxidative and non-oxidative conditions. The reaction of methane in the presence of O_2 has a limitation due to the formation of undesirable product, CO_2. The catalytic conversion of methane under non-oxidative condition over metal loaded catalyst has attracted considerable attention from many researchers [15, 107]. Some metals such as Mo, W, and Re supported on HZSM-5, HZSM-11, and MCM-22 zeolites were found to be active catalysts for the conversion of methane to higher hydrocarbons and aromatics [8, 108]. The correlation between catalytic performance and structure of the catalyst has been studied. Various techniques, such as specific surface area (BET), X-ray diffraction (XRD), NH_3 temperature-programmed desorption (NH_3-TPD), in situ X-ray photoelectron spectroscopy (XPS), Fourier transform infrared spectroscopy (FT-IR), and ^{27}Al and ^{29}Si nuclear magnetic resonance (NMR) have been used to characterize the catalysts. On the basis of these studies the physical and chemical structures of the catalysts materials have been reported. Moreover, the

correlation between the structure of the catalyst and the catalytic performance has been investigated. The active sites of the catalyst were found to be responsible in the activation of methane to form higher hydrocarbons and aromatics.

Although extensive studies have been devoted to understand the mechanism of direct conversion of methane to higher hydrocarbons, there is very little information available about the kinetics of methane to higher hydrocarbons in particularly gasoline range C_5^+ hydrocarbons. Previously, the kinetic study for the reaction of methane to aromatics was carried out over Ru-Mo/HZSM-5 in a conventional fixed-bed reactor in the temperature range of 873 to 973 K [113]. The present work studies the kinetic of methane conversion in the presence of light hydrocarbons as co-feeders to gasoline range hydrocarbons over W/HZSM-5 catalyst at temperatures between 973 to 1073 K. The reaction parameters such as rate constant, activation energy, and adsorption constants were measured based on the proposed model.

6.2 Experimental Procedure

6.2.1 Catalyst preparation

The 2 wt. % W/HZSM-5 catalyst was prepared by incipient wetness impregnation method as described by Wang *et al.* [109]. HZSM-5 (SiO_2/Al_2O_3=30; Zeolyst International Co. Ltd) was impregnated with a calculated amount of an aqueous solution of $(NH_4)_5H_5[H_2(WO_4)_6].H_2O$. The sample was subsequently dried at 383 K overnight and then calcined at 823 K for 5 h. The catalyst was crushed and sieved into the size of 35-60 mesh for catalytic testing.

6.2.2 Reactor system

The kinetic measurements of methane conversion in the presence of co-feeders ethylene and methanol to gasoline range were carried out in a fixed- bed differential reactor. The schematic diagram of the experimental setup is shown in Figure 6.1. The reactor is a 9 mm internal diameter (i.d) and 15 cm length stainless steel tube. The catalyst particles were held on quartz wool plug which was placed in the middle of the reactor. The flow rates of the gaseous feeds (methane, ethylene, nitrogen) were regulated with volumetric flow controllers, while methanol was fed using a syringe pump. The methanol was heated in a heating tape before flowing into the reactor. Five series of runs were carried out at different temperatures i.e, 973, 998, 1023, 1048, and 1073 K. At each temperature, the concentration of methane was varied from 50 to 90% v/v at a constant ethylene concentration of 5%v/v. The total gas hourly space velocity (GHSV) of gaseous feed mixture (methane+ethylene+nitrogen) was kept at 1800 ml/g.h. The flow rate of methanol was constant at 5 ml/h. The total pressure of the reaction was around 1 atm. Nitrogen was used as an internal standard for calculating methane conversion and selectivity of reaction products. The products from the reactor were cooled and separated into gas and liquid products. The gaseous products were analyzed on-line by means of a Hewlett-Packard 5890 automated equipped with a thermal conductivity detector (TCD) while the liquid products were analyzed using a flame ionization detector (FID).

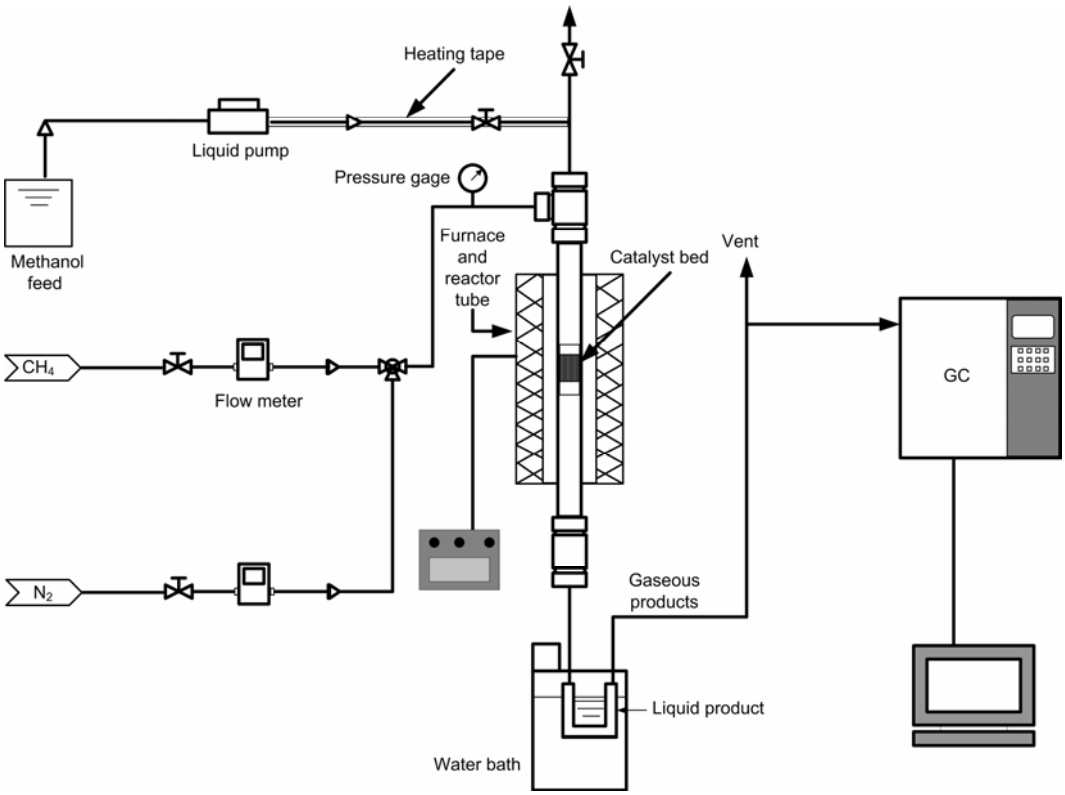

Figure 6.1: Schematic diagram of experimental set up and fixed bed reactor system

6.2.3 Reaction mechanism and kinetic model

Many attempts have been devoted to better understand the possible pathways of the methane reaction to higher hydrocarbons and aromatics. Wang *et al.* [110] suggested that the activation of methane over Mo/HZSM-5 zeolite catalyst was initiated via the carbenium ion mechanism, with Mo_6C species or protonic sites acting as hydride acceptor. Chen *et al.* [111] proposed that methane conversion was catalyzed by the molybdenum species inside the HZSM-5 channels together with the strong acid sites of the zeolite. The process would form CH_3 free radicals, which could dimerize to form ethane and ethylene easily. Then the ethylene aromatized to benzene with the aid of the protons of HZSM-5 zeolite. Ohnishi *et al.* [112] proposed the mechanism for the catalytic conversion of methane to higher

hydrocarbon and aromatics over Mo/HZSM-5. The mechanism proceeded primarily by methane dissociation on Mo/HZSM-5 catalysts to form surface carbon species such as CH_x and C_2H_y (x, y>0) on the Mo site of Mo carbide, which were oligomerized on HZSM-5 support having the proper acidity toward aromatic compounds such as benzene and naphthalene. As described above, the mechanism for methane conversion to higher hydrocarbons and aromatic is being explored. It seems that there is an almost common agreement that ethylene, the primary product of methane activation, undergoes subsequent oligomerization and cyclization reactions on Brönsted acid sites of the zeolite to form non aromatics and aromatics higher hydrocarbons, such as paraffin, benzene, naphthalene, and toluene. It is also generally agreed that the dual active sites: metal active sites and zeolite acid sites are responsible for the reaction. Recently, Iliuta *et al.* [113] proposed the mechanism for methane non-oxidative aromatization based on dual-site mechanism with metal active sites and acidic active sites, respectively. Their proposed mechanism was arranged using single site mechanism with the assumption that all the active sites were identical over the catalyst. In this study, the mechanism for the conversion of methane in the presence of co-feeders to C_5^+ hydrocarbons in gasoline range is proposed as follows: The presence of co-feeds ethylene and methanol is necessary for the formation of active species on the catalyst. The reaction pathway for the conversion of methane containing ethylene and methanol is initiated by the formation of C_2^+ carbenium ions over W/HZSM-5 catalyst (Eq. 6.1). The carbenium ions are converted to form coke which is deposited in the W/HZSM-5 catalyst (Eq. 6.2).

$$C_2H_4 + CH_3OH + \ W/HZSM-5 \ \Rightarrow \ C_2^+ carbenium \ \ ions \qquad (6.1)$$

$$C_2^+ carbenium \ \ ions \ \ \Rightarrow \ Coke \qquad (6.2)$$

$$Coke \ + \ W/HZSM-5 \ \Rightarrow \ C-W/HZSM-5 \qquad (6.3)$$

In this way, C_2^+ carbenium ions (Eq. 6.1) would be more easily formed than C_1 carbenium ions. C_2^+ carbenium ions would be more reactive than CH_4 molecules and would form carbon deposition on the catalyst surface. The deposited coke over the W/HZSM-5 catalyst is the catalyst active sites for the transformation of methane to produce C_5^+ hydrocarbons in gasoline range [29]. According to previous studies [110-112], it is generally agreed that the mechanism of methane conversion to aromatics and higher hydrocarbons consists of two main consecutive reactions of methane to methyl radicals which could dimerize to form ethane and ethylene easily followed by ethylene aromatization to gasoline. Furthermore, the reactions pathways for the production of C_5^+ hydrocarbons in gasoline range from methane over partially coke deposited on the catalyst (C-W/HZSM-5) is arranged based on the above consecutive reactions. [9].

The kinetic model is developed with the following reaction mechanism. A sequence of elementary steps for the formation of C_5^+ hydrocarbons on the catalyst active sites, (C-W/HZSM-5 or S*) is presented in Eqs 6.4 - 6.7 arranged based on Langmuir-Hinshelwood kinetic model.

$$CH_4 + S^* \overset{K1}{\Leftrightarrow} CH_3S^* + \frac{1}{2}H_2 \qquad (6.4)$$

$$CH_3S^* \overset{k_{rs}}{\Rightarrow} CH_2S^* + \frac{1}{2}H_2 \qquad (6.5)$$

$$CH_2S^* \overset{K2}{\Leftrightarrow} \frac{1}{2}C_2H_4 + S^* \qquad (6.6)$$

$$\frac{1}{2}C_2H_4 \overset{K3}{\Leftrightarrow} \frac{1}{6}C_6H_6 + \frac{1}{2}H_2 \qquad (6.7)$$

where S* represents the partially coke catalyst= C-W/HZSM-5.

The sequence steps on the catalyst active sites include adsorption of methane from gas phase on catalyst surface, dissociation of methane to form methyl radical,

formation of ethylene on the catalyst surface, desorption of ethylene to gas phase. The oligomerization of the ethylene to produce C_5^+ hydrocarbons [114] then follows. The step for the conversion CH_3S^* species into ethylene CH_2S^* (Eq. 6.6) is assumed to be non equilibrium. The following assumptions were made to establish the model equation:

1. Surface reaction is the rate-limiting step

2. C_6H_6 represents the C_5^+ hydrocarbons products in gasoline range

3. The limitation due to intraparticle diffusion is negligible.

To exclude the limitation of intraparticle and external diffusion, the kinetics experiments are performed by using small particle sizes and high space velocities. The catalyst particle sizes ranged between 259 and 420 μm and the space velocity maintained at 1800 ml/g.h. The size of the particles used was smaller and the space velocity was larger than those reported for the reaction kinetics of conversion of methane to C_5^+ hydrocarbons [113].

The model has been derived based on the above reaction pathway. The rates for decomposition of methane to methyl radical (Eq. 6.4 of elementary step) is

$$r_1 = k_1 P_{CH4} \theta_v - k_{-1} \theta_{CH_3} \left(P_{H2}\right)^{1/2} \qquad (6.8)$$

Substitute k_{-1} with $k_{-1} = \frac{k_1}{K_1}$, the rate expression for reaction (4) is defined by

$$r_1 = k_1 \left[P_{CH_4} \theta_v - \frac{\theta_{CH_3}}{K_1} \left(P_{H_2}\right)^{1/2} \right] \qquad (6.9)$$

where,

$$K_1 = \frac{k_1}{k_{-1}} \qquad (6.10)$$

Methane can be highly activated on coke deposited catalyst. Wang, *et al.* [12] reported that activation of methane reactant occurred on the coke modified Mo_2C catalyst surface to produce ethylene. Similarly, Pierella, *et al.* [29] reported that coke deposited on Mo catalyst promoted methane activation. In the present work, the cokes are formed from co-feeder molecules, ethylene and methanol in the methane feed. As a result, excess amount of methyl radicals can be produced before the radicals are coupled and oligomerized to higher hydrocarbons. The surface reaction for the conversion of methyl radical to ethylene is considered to be irreversible reaction due to the presence of excess amount of methyl radicals on the catalyst surface**.**

The corresponding expression for rate of reaction is (Eq. 6.5 of elementary step).

$$r_s = k_{rs}\ \theta_{CH3} \qquad (6.11)$$

The corresponding desorption rate of ethylene (6) is defined by

$$r_2 = k_2\theta_{CH2} - k_{-2}\theta_v\left(P_{C2H4}\right)^{1/2} \qquad (6.12)$$

Rearrangement,

$$r_2 = k_2\left[\theta_{CH_2} - \frac{\left(P_{C_2H_4}\right)^{1/2}\theta_v}{K_2}\right] \qquad (6.13)$$

where $K_2 = \frac{k_2}{k_{-2}}$ (6.14)

The rate expression for the oligomerization reaction (6.7) is given as follows:

$$r_3 = k_3\left(P_{C2H4}\right)^{1/2} - k_{-3}\left(P_{C_6H_6}\right)^{1/6}\left(P_{H2}\right)^{1/2} \quad (6.15)$$

Rearrangement

$$r_3 = k_3\left[\left(P_{C_2H_4}\right)^{1/2} - \frac{\left(P_{C_6H_6}\right)^{1/6}\left(P_{H_2}\right)^{1/2}}{K_3}\right] \quad (6.16)$$

For steady state conditions, the rates of each of the reactions (6.9), (6.13) and (6.16) are equal to each other, that is $r_1=r_s=r_2=r_3$. Since r_s is the limiting reaction, k_1, k_2, and k_3 are very large compared with k_{rs}. Therefore, the rate of methane conversion (r_s) is obtained:

$$r_s = \frac{k_{rs}\, K_1\, P_{CH4}\theta_t}{P_{H2}^{1/2}\left(1 + K_1\frac{P_{CH4}}{\left(P_{H_2}\right)^{1/2}} + \frac{P_{C6H6}^{1/6}P_{H2}^{1/2}}{K_2K_3}\right)} \quad (6.17)$$

$$\text{where } K_3 = \exp\left(-\frac{\Delta G_3}{RT}\right) \quad (6.18)$$

The equilibrium constant K_3 was calculated using the following relationships for the Gibbs free energy, heat, and entropy of ethylene to benzene reaction (Eq. 6.7) [113]:

$$\Delta G_3 = \Delta H_3 - T\Delta S_3 \qquad (6.19)$$

Where

$$\Delta H_3 = -12296 + 5.456(T - 298) + 1.516\times10^{-3}\left(T^2 - 298^2\right) - 0.36725\times10^{-5}\left(T^3 - 298^3\right) \qquad (6.20)$$

$$\Delta S_3 = 0.434 + 5.456\ln(T/298) + 3.033\times10^{-3}(T - 298) - 0.55087\times10^{-5}(T^2 - 298^2) \qquad (6.21)$$

6.2.4 Kinetic Parameters Estimation

Non linear regression analysis for Eq. (6.17) using least squares techniques determined the unknown parameters i.e., surface rate reaction constant (k_{rs}) and adsorption equilibrium constants (K_1, K_2). The objective function of the residual sum squares was minimized (Eq. 6.22) to obtain a mathematical fit for the rate of reaction equation (Eq. 6.17):

$$F = \sum_k^n \left(r_k^{calc} - r_k^{\exp}\right)^2 \qquad (6.22)$$

6.3 Results and discussion

6.3.1 Effect of temperature and methane concentration

The effect of temperature on methane conversion presented in Figure 6.2 reveals that methane conversion increases with an increase in temperature from 973 to 1073 K which is in agreement with the results reported by Weckhuysen *et al.* [116]. The methane conversion percentage increased with increasing temperatures was also reported by Shu *et al.* [8] for the methane dehydrocondensation reaction over Re/HMCM-22 at 973, 1023 and 1073 K. However, the formation rates of benzene and naphthalene decreased at temperature as high as 1073 K due to deactivation occurring on the Mo/HZSM-5 catalyst [8]. The result shows that higher CH_4 conversion was obtained with decreasing methane concentration in the feed. The lower methane concentration in the feed (more dilution of N_2 in the feed) leads to mixing and the temperature being distributed more evenly along the catalyst bed. This affects the methane conversion. The presence of inert gas in the methane feed that increased methane conversion was also reported by Iliuta *et al.* [113].

The conversion of methane in the presence of lower hydrocarbon to higher hydrocarbons has been studied in the presence of C_2 and C_4 hydrocarbons [29, 117, 118]. Introduction of a small amount of light hydrocarbons was reported to increase methane conversion compared with pure methane as reactant. The increased conversion in the presence of small amount of lower hydrocarbons was due to C_2^+ additives in the feed which could act as an initiator for the conversion of methane to gasoline range hydrocarbons.

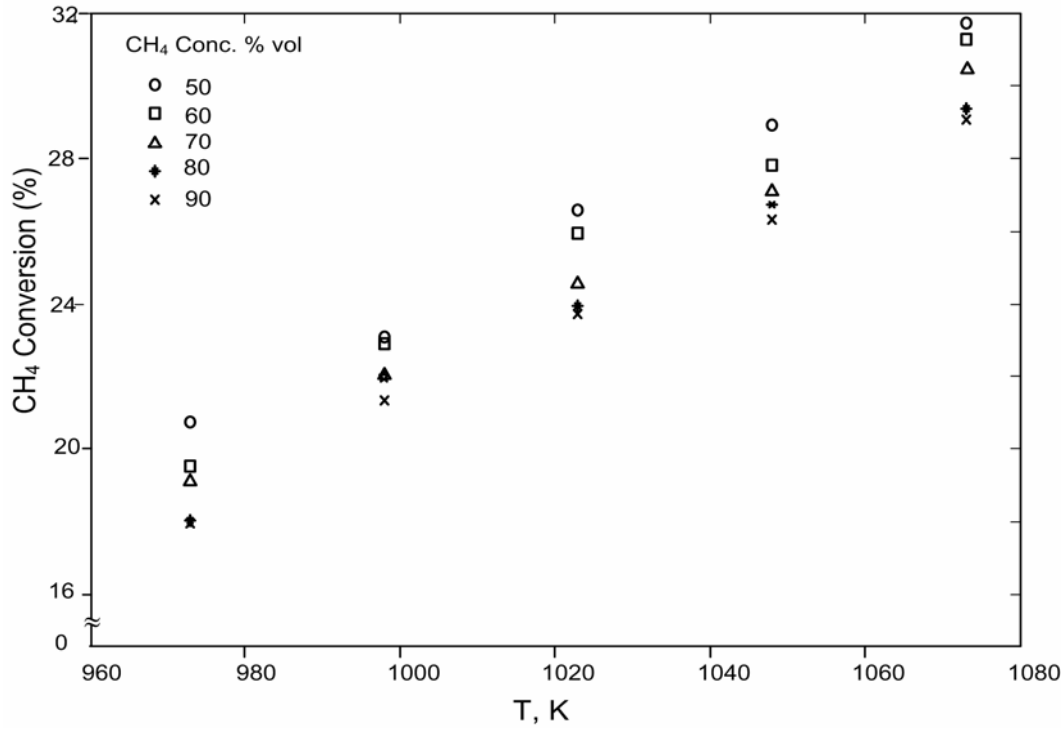

Figure 6.2: Effect of temperature on methane conversion under different methane concentrations.

6.3.2 Kinetic Parameters

Based on the experiments data shown in Fig. 6.3 and regression analysis, kinetic and equilibrium constants for the reaction of methane in the presence of co-feeding to produce gasoline hydrocarbons were obtained. From the regression results presented in Table 1, it can be seen that rate constant k_{rs} and equilibrium constant K_2 increased with increasing temperature whereas the adsorption constant K_1 showed a decreasing trend with an increase in temperature. The same findings were reported by Iliuta *et al.* [113]. The kinetic parameters in Table 6.1 were used to determine the activation energy (*Ea*), the frequency factor (k_0), the adsorption enthalpy (ΔH_{ads}), and entropy (ΔS_{ads}) using Arrhenius and Van't Hoff relationships as plotted in Figure 6.4.

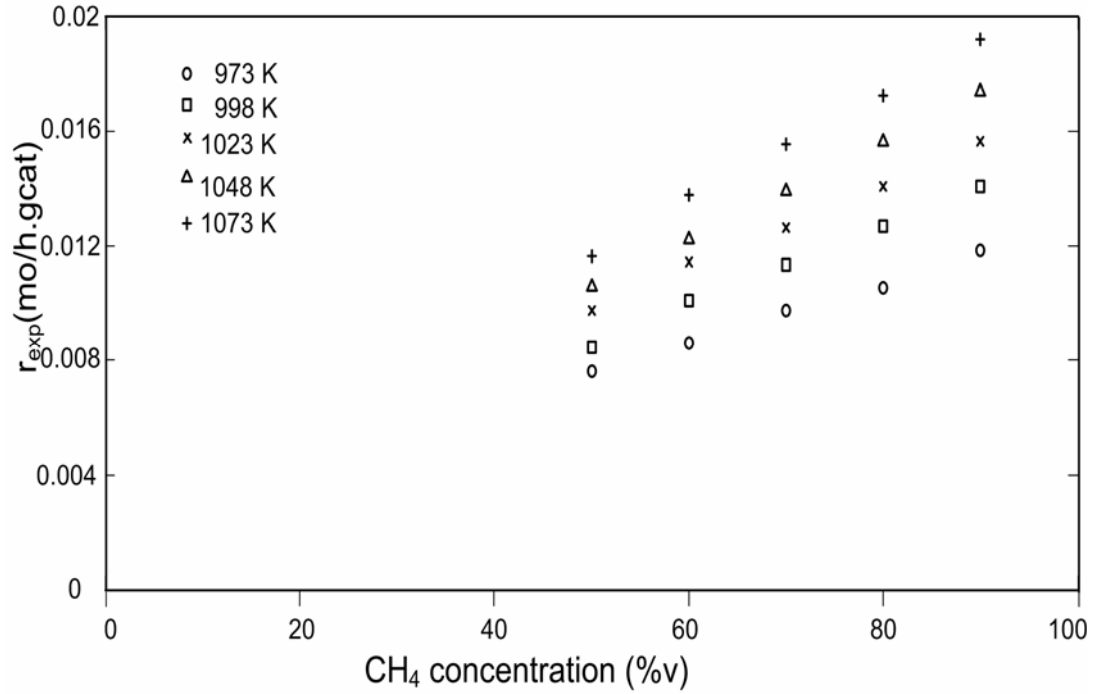

Figure 6.3: Experimental reaction rate as a function of methane concentration at different temperatures.

Table 6.1: Estimated Kinetic and Equilibrium Constants k_{rs}, K_1, and K_3 obtained from a non linear regression of the model.

Temperature	**k_{rs}, mol/g_{cat}.h.atm**	**K_1, atm^{-1}**	**K_2, $atm^{-1/2}$**
973	0.826	1.374	3.300
998	0.855	1.345	3.379
1023	0.908	1.275	4.000
1048	0.941	1.241	4.271
1073	0.976	1.211	4.728

The activation energy of the reaction was calculated by using Arrhenius:

$$k_{rs} = k_0 \exp\left(-\frac{E_a}{RT}\right) \qquad (6.23)$$

From the slope of the rate constant, ln k_{rs} against 1/T, the activation energy (E_a) and the frequency factor (k_0) were calculated to be 141.5 J/mol and 0.959 mol/g.cat.h, respectively. The entropy and the enthalpy were predicted by plotting ln K_1 vs 1/T based on the Van't Hoff equation:

$$\ln K_1 = \frac{\Delta S_{ads}}{R} - \frac{\Delta H_{ads}}{RT} \qquad (6.24)$$

The adsorption enthalpy for K_1 was -177.16 J/mol, and the corresponding adsorption entropy was -1.274 J/mol.K.

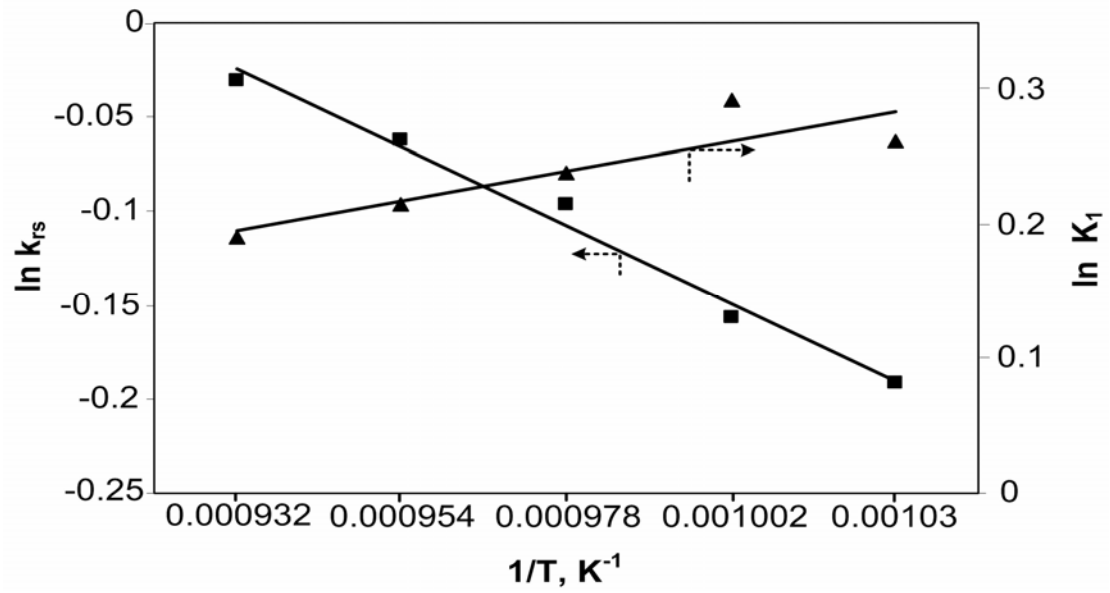

Figure 6.4: Van't Hoff and Arrhenius plots for equilibrium and rate constants.

By substituting the optimized kinetic parameters into equation (6.22), the rate of reaction was numerically calculated. The comparison between calculated and experimental reaction rate in Figure 6.5 indicates that simulated values do not deviate significantly from the experimental value and that the proposed kinetic model can be used to explain the observed data for methane conversion to C_5^+ hydrocarbons.

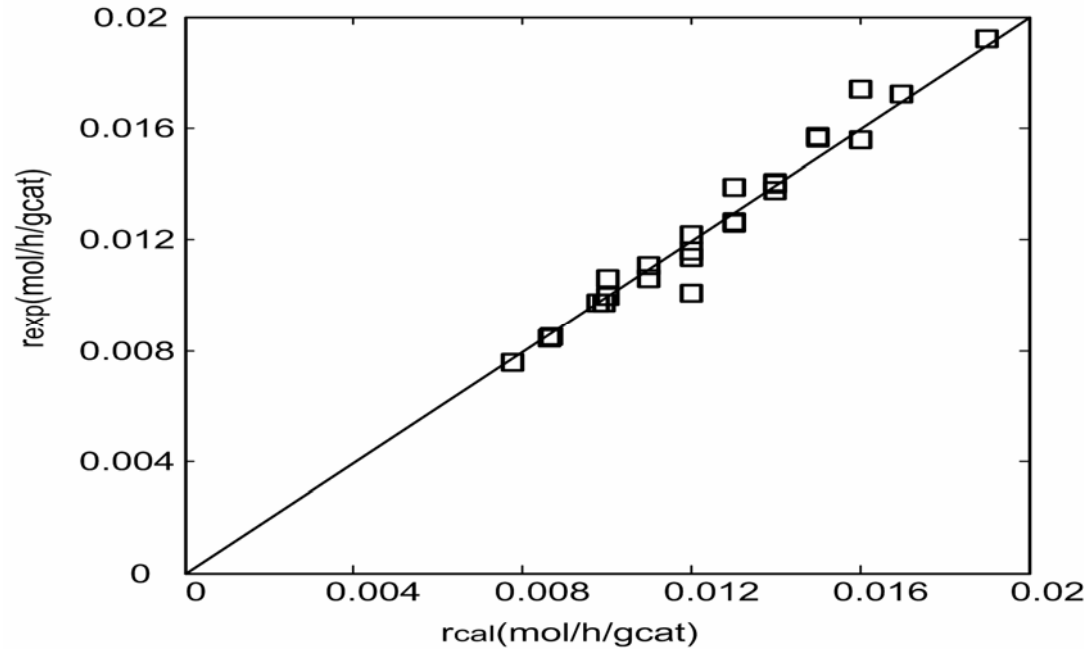

Figure 6.5: Experimental versus calculated reaction rate.

6.4 Conclusions

Kinetic studies of methane conversion in the presence of co-feeds ethylene and methanol to produce higher hydrocarbons in gasoline range has been performed over W/HZSM-5 catalyst. The reaction temperature was varied between 973-1073 K. The feed mixture consisted of methane-ethylene-methanol-nitrogen at different methane concentration. The reaction rate was strongly dependent on temperature and methane concentration. The reaction rate increased when methane concentration in the feed mixture was decreased. The kinetic model was proposed based on a Langmuir-Hinshelwood-Hougen-Watson mechanism for the reaction of methane in the presence of co-feeds ethylene and methanol. Based on the experimental data, the kinetic parameters were obtained. The activation energy (E_a), the frequency factor (k_0), the adsorption enthalpy (ΔH_{ads}), and entropy (ΔS_{ads}) were found to be 141.5 J/mol, 0.959 mol/g.cat.h, -177.16 J/mol, and -1.274 J/mol.K, respectively. The correlation between experimental and calculated reaction rate indicates that the model fits the data well.

CHAPTER 7

A THERMODYNAMIC EQUILIBRIUM ANALYSIS ON OXIDATION OF METHANE TO HIGHER HYDROCARBONS

Abstract

Thermodynamic chemical equilibrium analysis using total Gibbs energy minimization method was carried out for methane oxidation to higher hydrocarbons. For a large methane conversion and also a high selectivity to higher hydrocarbons, the system temperature and oxygen concentration played a vital role whereas, the system pressure only slightly influenced the two variables. Numerical results showed that the conversion of methane increased with oxygen concentration and reaction temperature, but decreased with pressure. Nevertheless, the presence of oxygen suppressed the formation of higher hydrocarbons that mostly consisted of aromatics, but enhanced the formation of hydrogen. As the system pressure increased, the aromatics, olefins and hydrogen yields diminished, but the paraffin yield improved. Carbon monoxide seemed to be the major oxygen-containing equilibrium product from methane oxidation whilst almost no H_2O, CH_3OH and HCOH were detected although traces amount of carbon dioxide were formed at relatively lower temperature and higher pressure. The total Gibbs energy minimization method is useful to theoretically analyze the feasibility of methane conversion to higher hydrocarbons and syngas at the selected temperature, pressure

Keywords *Thermodynamic chemical equilibrium, Gibbs energy minimization, Methane conversion, higher hydrocarbons*

7.1 Introduction

Following the oil crisis in the 1970s, there seems to be many efforts focusing on synfuel production [119]. Hence, the development of a simple and commercially advantageous process for converting methane, the major constituent of natural gas, to more valuable and easily transportable chemicals and fuels becomes a great challenge to the science of catalysis. However, methane is the most stable and symmetric organic molecule consisting of four C-H covalence bonds with bond energy of 440 kJ/mol [120]. Thus, effective methods to activate methane are desired.

Thermodynamic constraints on the reactions in which all four C–H bonds of CH_4 are totally destroyed, such as CH_4 reforming into synthesis gas is much easier to overcome than the reactions in which only one or two of the C–H bonds are broken under either oxidative or non-oxidative conditions. For this reason, only indirect conversions of CH_4 via synthesis gas into higher hydrocarbons or chemicals are currently available for commercialization [46]. Nonetheless, heat management issues are common to CH_4 reforming. With steam reforming, large quantities of heat must be supplied, whereas, with catalytic partial oxidation, a large amount of heat is released at the front end of the catalyst bed as CH_4 undergoes total oxidation ($CH_4 + 2O_2 \rightarrow CO_2 + 2H_2O$) [28].

Direct conversions of methane to the desired products circumvent the expansive syngas step, making it more energy efficient. These processes are thermodynamically more favorable in the oxidative than the non-oxidative conditions. For example, the partial oxidation of methane into C_1 oxygenates such as methanol and formaldehyde, is one such process. Many studies on the catalytic oxidation of methane to methanol at high temperature reported low conversion and selectivity [121-124]. Typically, the selectivity of methanol is below 50% while the conversion of methane is below 10%

[123]. The results indicated that the yield of methanol by direct oxidation of methane is too low to be economically attractive.

The study on oxidative coupling of methane (OCM) has drawn much attention after the pioneering work [125]. Similar to partial oxidation of methane to methanol, after intensive efforts from researchers involved with catalysis, no catalysts could achieve a C_2 yield beyond 25% and a selectivity of C_2 higher than 80% [126].

As an alternative approach, transformation of methane to aromatics has also attracted great interests from many researchers [127-129]. They reported that only trace amount of aromatics could be detected if CH_4 reacted with O_2 or NO over HZSM-5 zeolite, and the main products would be CO_x and H_2O. In an attempt to avoid the use of oxygen, several researches tried to transform methane into higher hydrocarbon in the absence of oxygen. Mo supported on HZSM-5 zeolite has been reported as the most active catalyst for non-oxidative aromatization of methane [46, 126, 130] but its activity and stability are still inadequate for the aromatization process to be commercialized. Previous work have also shown that the conversion of methane to liquid fuels is promising by using metal modified ZSM-5 (or with MFI structure) zeolite as catalysts [131-132].

The study on thermodynamic equilibrium composition has been used in investigating the feasibility of many types of reaction e.g. simultaneous partial oxidation and steam reforming of natural gas [133-136]. Meanwhile, the minimization of Gibbs free energy using Lagrange's multiplier was applied by Lwin *et al*. [137], Douvartzides *et al*. [138], Chan and Wang [133, 139], and Liu *et al*. [140] for solving thermodynamic equilibrium analysis of autothermal methanol reformer, solid oxide fuel cells, natural-gas fuel processing for fuel cell applications, and catalytic combustion of methane, respectively.

The main objective of this paper is to perform a thermodynamic chemical equilibrium analysis of possible equilibrium products formed in a methane reaction under oxidative and non-oxidative conditions. In this analysis, the effect of various conditions, i.e. temperature, CH_4/O_2 feed ratio and system pressure, on chemical equilibrium are discussed. The thermodynamics analysis is important to study the feasibility of reactions in a reacting system, and also to determine the reaction conditions and the range of possible products that can be formed.

7.2 Experimental Procedure

The total Gibbs energy of a single-phase system with specified temperature T and pressure P, $(G^t)_{T,P}$ is a function of the composition of all gases in the system and can be represented as,

$$(G^t)_{T,P} = g(n_1, n_2, n_3, \ldots, n_N) \tag{7.1}$$

At equilibrium condition the total Gibbs energy of the system has its minimum value. The set of n_i's which minimizes $(G^t)_{T,P}$ is found using the standard procedure of the calculation for gas-phase reactions and is subject to the constraints of the material balances. The procedure, based on the method of Lagrange's undetermined multipliers, is described in detail by Smith et al. [141].

In this paper, the gas equilibrium compositions of a system which contains CH_4, C_2H_6, C_2H_4, C_3H_8, C_3H_6, C_4H_{10}, C_4H_8, C_5H_{12}, C_5H_{10}, C_6H_6, C_7H_8, C_8H_{10}, CO, CO_2, H_2, H_2O, CH_3OH and HCOH species at 900-1100K, various oxygen/methane mole ratio and 1-10 bar are calculated. These products are chosen as they are likely to be produced from

the reaction between CH_4 and O_2. The oxygen/methane mole ratio is set to be 0.04, 0.05, 0.1 and 0.2. The condition without oxygen is also simulated. In the preliminary calculations, the compositions of O_2 and C_{6+} aliphatic hydrocarbons are always less than 1E-10 mol% and for that reason the subsequent calculations only involved the C_1-C_5 aliphatic hydrocarbons.

By applying Lagrange's undetermined multipliers method for total Gibbs free energy minimization, the following equations need to be solved simultaneously:

$$\frac{\Delta G°_{fi}}{RT} + \ln(y_i \Phi_i P / I_i P°) + \sum_k \frac{\lambda_k}{RT} a_{ik} = 0 \qquad (i = 1,2,\ldots,N) \tag{7.2}$$

$$\sum_i y_i a_{ik} = \frac{A_k}{n} \qquad (k = 1,2,\ldots,w) \tag{7.3}$$

$$\sum_i y_i = 1 \tag{7.4}$$

Where,

a_{ik} = the number of atoms of the kth element presents in each molecule of the chemical species i.

A_k = total number of atomic masses of the kth element in the system, as determined by the initial constitution of the system.

$\Delta G°$ standard Gibbs energy change of reaction

$\Delta G°_{fi}$ = standard Gibbs-energy change of formation for species i

$(G^t)_{T,P}$ = total Gibbs energy of a single-phase system with specified temperature and pressure

P = system pressure

P° = pressure in the standard state, in this case, is 1 bar.

R = universal gas constant.

T = system temperature

w = total number of element in the system

y_i = mole fraction of species i at equilibrium condition.

n = total number of moles at equilibrium condition.

I_i the number of isomers of species i.

Since there are 18 species and three elements (C, H, and O) in the system, a total of 22 equations (18 equations for Equation (7.2), 3 equations for Equation (7.3) and 1 equation for Equation (7.4)) are solved simultaneously in order to calculate the 22 unknowns in the formulae (mole fraction of 18 species, Lagrange multiplier of three elements and one total number of mole). All calculations are performed using Mathcad 2001i Professional software. The iterative modified Levenberg-Marquardt method, called and applied during the solving process, is taken by Mathcad from the public-domain MINPACK algorithms developed and published by the Argonne National Laboratory in Argonne, Illinois. The values of $\Delta G°_{fi}$ used in the calculation are obtained from the literature [142-145]. The flowchart of the methodology is depicted in Figure 7.1.

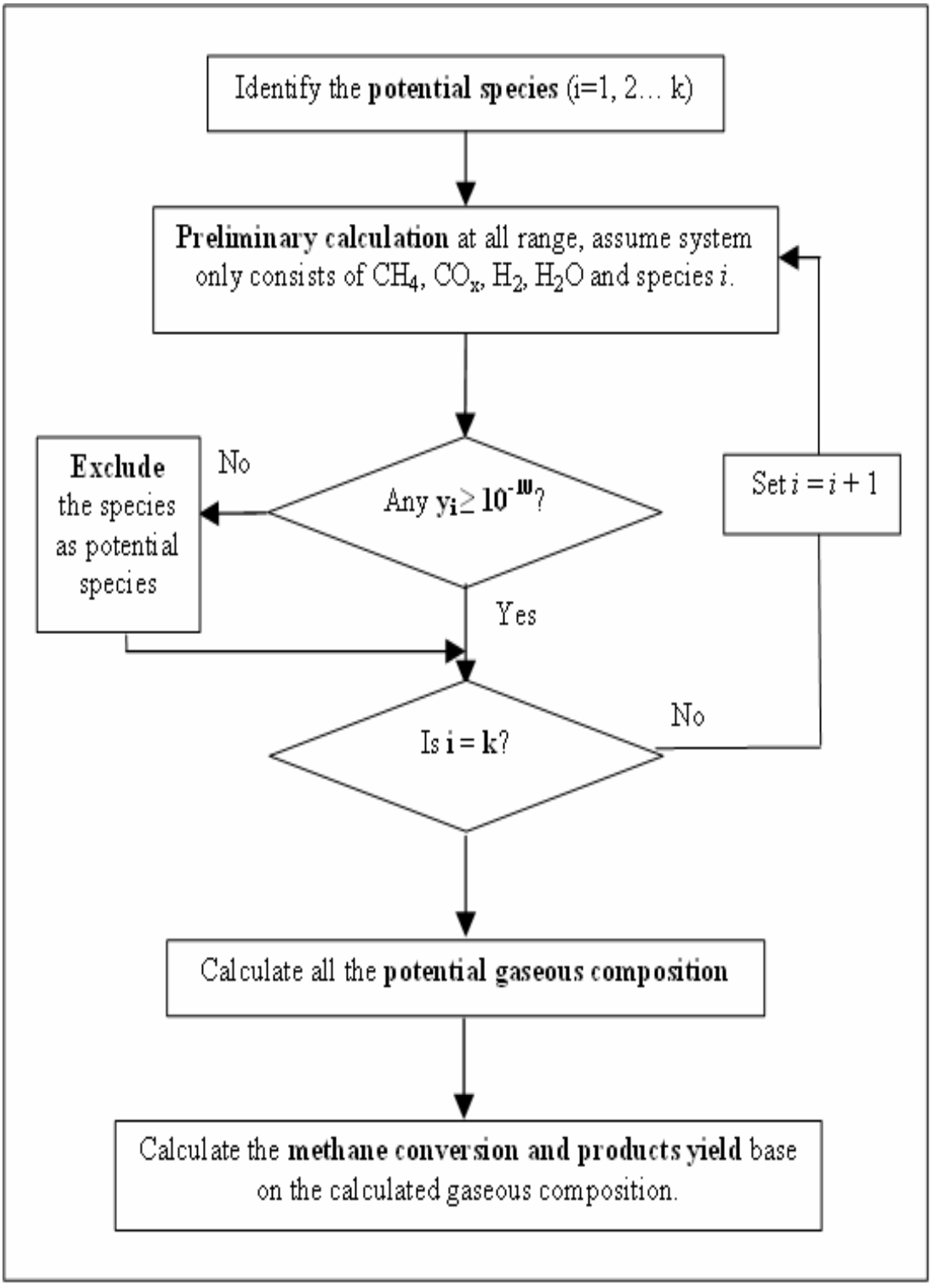

Figure 7.1: Flow diagram for computation of the equilibrium composition.

7.3 Results and Discussion

7.3.1 Methane Conversion

The methane conversion, based on carbon number basis, and the equilibrium compositions, shown in Tables 7.1 and 7.2 increase with system temperature at all conditions. The results are in agreement with the equilibrium conversion of methane calculated by Zhang et al. [146] based on reaction (5):

$$6CH_4 \rightarrow C_6H_6 + 9H_2 \qquad (7.5)$$

The equilibrium methane conversions at temperatures 973K, 1023K, 1073K, 1123K and 1173K are reported as 11.3%, 16%, 21%, 27% and 33% respectively but lower than the result calculated in this work for non-oxidative conditions since they considered only benzene as the hydrocarbon product.

Table 7.1: The effect of oxygen/methane mole ratio on methane equilibrium conversions at 900K - 1100K and 1 bar.

Temperature	**CH4 Conversion (%)**				
(K)	**0.00***	**0.04***	**0.05***	**0.10***	**0.20***
900	6.64	8.21	10.02	19.08	33.74
1000	14.07	13.65	13.82	20.22	39.41
1100	25.07	25.29	25.28	26.29	40.24

*** : O2/CH4 ratio**

Table 7.2: The effect of system pressure on methane equilibrium conversions at 900K – 1100K and oxygen/methane mole ratio = 0.1.

Temperature (K)	CH4 Conversion (%)				
	1 bar	**2 bar**	**3 bar**	**5 bar**	**10 bar**
900	19.08	17.61	16.35	14.54	12.41
1000	20.22	19.86	19.72	19.04	17.40
1100	26.29	22.07	20.83	20.23	19.89

The effect of oxygen/methane ratio on methane conversion is tabulated in Table 7.1. The conversion of methane is enhanced by increasing the oxygen/methane ratio as methane can be easily oxidized to carbon oxides in the presence of oxygen. Nevertheless, the methane conversion decreases as the system pressure increased. By examining the calculated equilibrium compositions, it is apparent that the conversions of methane involve the following reactions:

$$\text{Partial Oxidation}: CH_4 + ½O_2 \rightarrow CO + 2H_2 \quad (\upsilon = 1½) \tag{7.6}$$

$$\text{Total oxidation}: CH_4 + 2O_2 \rightarrow CO_2 + 2H_2O \quad (\upsilon = 0) \tag{7.7}$$

$$\text{To aromatic}: xCH_4 \leftrightarrow C_xH_{(2x-6)} + (x+3)H_2\,,\ x \geq 6 \quad (\upsilon = 4) \tag{7.8}$$

$$\text{To paraffins}: xCH4 \leftrightarrow C_xH_{(2x+2)} + (x-1)H_2\,,\ x = 2 \quad (\upsilon = 0) \tag{7.9}$$

$$\text{To olefins}: xCH4 \leftrightarrow C_xH_{2x} + xH_2\,,\ x = 2 \quad (\upsilon = 1) \tag{7.10}$$

Except for equations (7.7) and (7.9), Equations (7.6), (7.8) and (7.10) have positive υ value. The increase in the system pressure shifts the reaction with the positive υ to the

left [141], resulting in the decrease of methane equilibrium conversion in consistent with the results reported in the literature [140, 147].

7.3.2 Aromatic Yield

The effects of initial oxygen/methane ratio and system pressure on the equilibrium aromatics yield are shown in Tables 7.3 and 7.4, respectively. As expected, the yield of aromatics (benzene, toluene and xylene) at higher temperature exceeds that at lower temperature. Conversely, the increment of oxygen content in the feed suppresses the formation of higher hydrocarbons. Table 7.4 shows that the aromatic yield decreases with increasing system pressure as according to Equation (7.8) the increment of the system pressure shifts the reaction to the left, and suppresses the formation of aromatics due to the positive υ in the stoichiometric reaction.

Table 7.3: The effect of oxygen/methane mole ratio on aromatic equilibrium yield at 900K - 1100K and 1 bar.

Temperature (K)	**Aromatics yield**				
	0.00*	**0.04***	**0.05***	**0.10***	**0.20***
900	6.47	0.0991	0.0158	0.000425	0.000000245
1000	13.8	5.29	3.52	0.0643	0.0000769.
1100	24.9	16.7	14.6	5.61	0.0455

*** : O2/CH4 ratio**

Table 7.4: The effect of system pressure on aromatic equilibrium yield at equilibrium at 900K - 1100K and oxygen/methane mole ratio = 0.1.

Temperature (K)	Aromatics yield				
	1 bar	**2 bar**	**3 bar**	**5 bar**	**10 bar**
900	≈0	≈0	≈0	≈0	≈0
1000	0.0643	0.00456	0.00104	≈0	≈0
1100	5.61	1.55	0.478	0.0776	0.00604

7.3.2 Paraffin and Olefin Yields

The equilibrium calculations indicate that the formations of paraffins and also olefins are not favorable in the temperature range between 900K and 1100K and pressure between 1 and 10 bar. Most of the paraffins and olefins formed are C_2 hydrocarbons, i.e. ethane and ethylene. Tables 7.5 and 7.6 show that except for the paraffin yield in non-oxidative condition, the paraffin and olefin yields at higher temperature are always greater than the yields at lower temperature.

Table 7.5 and (b): The effect of oxygen/methane mole ratio on (a)paraffin and (b)olefin equilibrium yields at 900K - 1100K and 1 bar.

(a)

Temperature (K)	Paraffin yield				
	0.00*	**0.04***	**0.05***	**0.10***	**0.20***
900	0.125	0.0074	0.577	0.0245	0.00968
1000	0.137	0.119	0.113	0.615	0.0184
1100	0.132	0.122	0.119	0.100	0.0402

*** : O2/CH4 ratio**

(b)

Temperature (K)	Olefin yield				
	0.00*	**0.04***	**0.05***	**0.10***	**0.20***
900	0.0784	0.0307	0.0202	0.00516	0.00144
1000	0.267	0.218	0.199	0.0785	0.015
1100	0.725	0.667	0.633	0.513	0.156

*** : O2/CH4 ratio**

Meanwhile both the paraffin and olefin yields decrease with the increment of oxygen. The equilibrium yields of paraffin and olefin are also affected by the system pressure. The paraffin yield increases with pressure, but the olefin yield decreases as the system pressure increases. The results may be attributed to the positive υ as shown in Eq 7.10. Similar trends have also been observed in the literature [147].

Table 7.6: The effect of system pressure on (a) paraffin and (b) olefin equilibrium yields at equilibrium at 900K - 1100K and oxygen/methane mole ratio = 0.1.

(a)

Temperature (K)	Paraffin yield				
	1 bar	**2 bar**	**3 bar**	**5 bar**	**10 bar**
900	0.0245	0.0283	0.0322	0.0392	0.0531
1000	0.0615	0.0627	0.064	0.0677	0.0792
1100	0.100	0.129	0.139	0.143	0.148

(b)

Temperature (K)	Olefin yield				
	1 bar	**2 bar**	**3 bar**	**5 bar**	**10 bar**
900	0.00516	0.00325	0.00267	0.0022	0.00187
1000	0.0785	0.0405	0.0279	0.0183	0.0118
1100	0.513	0.381	0.284	0.175	0.00929

7.3.4 Hydrogen and Oxygen-containing Product Yields

Tables 7.7 and 7.8 show the dependency of hydrogen equilibrium yield, based on hydrogen number basis, on oxygen/methane mole ratio and system pressure, respectively. It can be clearly seen that hydrogen can be produced at remarkable level even in non-oxidative condition. However, the hydrogen yields increases with system temperature and oxygen but decreases with the system pressure. Hydrogen yield up to 40% can be achieved at system temperature of 1100K, oxygen/methane mole ratio of 0.2 and pressure of 1 bar.

Table 7.7: The effect of oxygen/methane mole ratio on hydrogen equilibrium yield at 900K –1100K and 1 bar.

Temperature	**Hydrogen yield**				
(K)	**0.00***	**0.04***	**0.05***	**0.10***	**0.20***
900	4.90	8.06	9.89	18.78	32.04
1000	10.43	12.08	12.73	20.02	39.14
1100	18.98	20.75	21.25	24.47	40.05

*** : O2/CH4 ratio**

Table 7.8: The effect of system pressure on hydrogen equilibrium yields at equilibrium at 900K - 1100K and oxygen/methane mole ratio = 0.1.

Temperature	**Hydrogen yield**				
(K)	**1 bar**	**2 bar**	**3 bar**	**5 bar**	**10 bar**
900	18.78	16.88	15.31	13.10	10.22
1000	20.02	19.75	19.48	18.69	16.64
1100	24.47	21.39	20.50	20.08	19.57

Meanwhile, the reacted oxygen is converted to mostly CO with trace amounts of CO_2. Yields of CH_3OH and HCOH can be neglected for the fact that the yields are below 3.0 x 10^{-5} % at the given conditions.

Figures 7.2 and 7.3 illustrate the effect of oxygen/methane ratio at T, P constant and the effect of system pressure on carbon oxide (CO_x) yield at fixed T and oxygen/methane ratio respectively. Overall, the total CO_x yield increase with increasing oxygen content in the system as oxygen conversion is 100% in all cases. As shown in Figure 7.3, at methane to oxygen ratio equal to 0.2, some of the oxygen is converted to CO_2 at 900K causing a slight reduction in the total CO_x equilibrium yield. The CO_x yield does not seem to be greatly affected by the reaction temperature, except for the conditions where the oxygen concentration and the pressure are high. When the system pressure increases, lowering the system temperature would increase the CO_2 yield, but the CO and overall CO_x yields would be reduced.

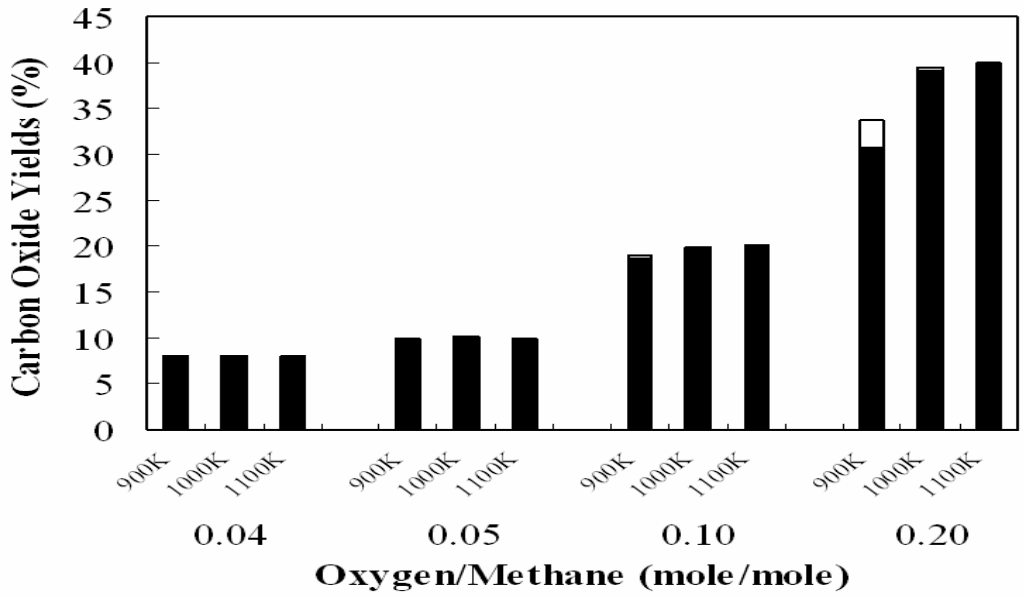

Figure 7.2: The effect of oxygen/methane mole ratio at initial unreacted state and system temperature on carbon monoxide (■) and carbon dioxide (□) yields.

Numerical equilibrium results that methane conversion is greatly enhanced but the aromatic yield is suppressed as more oxygen is added. Nevertheless, a small amount of oxygen is still needed to improve the stability of the catalyst. The study by Tan et al. [148] revealed that the addition of appropriate amount of oxygen to methane would increase the aromatic yield over Mo/HZSM-5 due to the improved catalyst stability. However, they have also shown that further increment in the oxygen concentration resulted in a reduced aromatic yield, and that trend is also observed in this work.

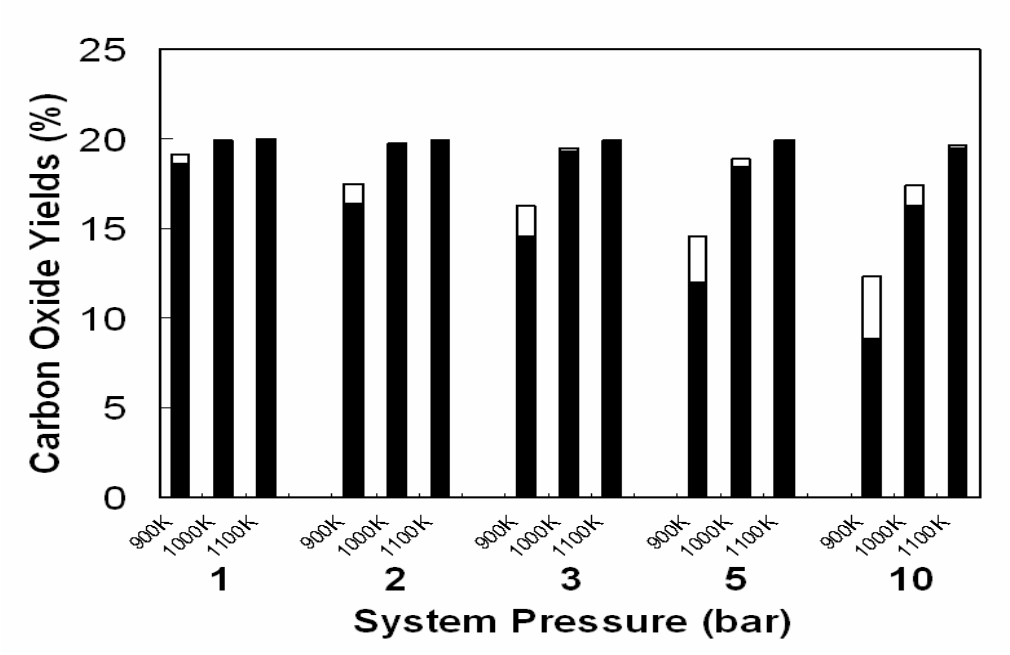

Figure 7.3: The effect of system pressure and system temperature on carbon monoxide (■) and carbon dioxide (□) yields. Oygen/methane mole ratio =0.2

Table 7.9 shows the distribution of products with concentrations > 0.01mol% as a function of system temperature and oxygen/methane mole ratio. It is interesting to note that no aromatics are formed when the levels of CO_2 and H_2O yields became noticeable. The observation is consistent with the literature report on methane oxidation over Mo/HZSM-5 [148, 149] and La_2O_3 + Mo_3/HZSM-5 [150] catalysts. The existence of CO_2 and H_2O not only suppressed the active carbon surface species on the catalysts, but the

aromatics are converted to CO and H_2 via steam and carbon dioxide reforming, as shown in the following equations:

$$C_xH_{(2x-6)} + xH_2O \rightarrow xCO + (2x - 3)H_2 \quad (7.11)$$

$$CxH_{(2x-6)} + xCO_2 \rightarrow 2xCO + (x - 3)H_2 \quad (7.12)$$

The results in Table 7.9 clearly reveal that reactions (7.11) and (7.12) are thermodynamically favorable at the given conditions and are only retarded when CO_2 and H_2O concentrations are low.

Table 7.9: Distribution of product concentration > 0.01 mole% as a function of system temperature and oxygen/methane mole ratio.

Temperature	**O_2/CH_4**	**Concentration > 0.01 mole%**						
900K	0	-	-	H_2	-	C_2H_4	C_2H_6	Aromatics
	0.04	CO	CO_2	H_2	H_2O	-	C_2H_6	-
	0.05	CO	CO_2	H_2	H_2O	-	C_2H_6	-
	0.1	CO	CO_2	H_2	H_2O	-	-	-
	0.2	CO	CO_2	H_2	H_2O	-	-	-
1000K	0	-	-	H_2	-	C_2H_4	C_2H_6	Aromatics
	0.04	CO	-	H_2	-	C_2H_4	C_2H_6	Aromatics
	0.05	CO	-	H_2	-	C_2H_4	C_2H_6	Aromatics
	0.1	CO	CO_2	H_2	H_2O	C_2H_4	C_2H_6	-
	0.2	CO	CO_2	H_2	H_2O	-	-	-
1100K	0	-	-	H_2	-	C_2H_4	C_2H_6	Aromatics
	0.04	CO	-	H_2	-	C_2H_4	C_2H_6	Aromatics
	0.05	CO	-	H_2	-	C_2H_4	C_2H_6	Aromatics
	0.1	CO	-	H_2	-	C_2H_4	C_2H_6	Aromatics
	0.2	CO	-	H_2	H_2O	C_2H_4	-	-

In the study of the equilibrium compositions, the operating temperature needs to be kept as large as possible for high conversion and high aromatic yield. Nevertheless, coke formation, which is the main cause of the catalysts deactivation, is unavoidable at high temperature. To test for the presence of coke, the following reaction is considered:

$$C_6H_6(g) \rightarrow 6C(s) + 3H_2(g) \tag{7.13}$$

The equilibrium constant, K for this reaction is:

$$K = e^{\frac{-\Delta G^\circ}{RT}} = \frac{a_c{}^6 p_{H_2}{}^3}{p_{C_6H_6}} \tag{7.14}$$

Rearranging, we have

$$a_c = (e^{\frac{-\Delta G^\circ}{RT}} \cdot \frac{p_{C_6H_6}}{p_{H_2}{}^3})^{1/6} \tag{7.15}$$

where a_c = activity of coke

$p_{C_6H_6}$ partial pressure of benzene in system

p_{H_2} partial pressure of gas hydrogen in system

K equilibrium constant

The value for a_c is always larger than 1, indicating that coke will be formed in the entire operating range considered (900-1100K, oxygen/methane mole ratio of 0–0.2, and 1-10 atm). Therefore, it is essential to develop a catalyst not only with high catalytic activity, but with high heat and coke resistant as well.

From the analysis in this work, it is also shown that syngas is the other major product other than aromatics. The process seems promising as methane can be converted into aromatics and syngas in the same reactor. An example of the process is shown in Figure 7.4. The aromatic hydrocarbon products and hydrogen can be easily separated from the unreacted methane and carbon monoxide by membrane or any other separation methods. Methane and carbon monoxide will be good feedstocks for the second dehydroaromatization reactor. With carbon monoxide as the co-feed, benzene formation is promoted and the stability of the catalysts is improved [151]. Therefore, a good catalyst for this process must fulfill the following criteria: a) heat resistant, b) coke resistant, c) high methane oxidation and aromatic formation activity

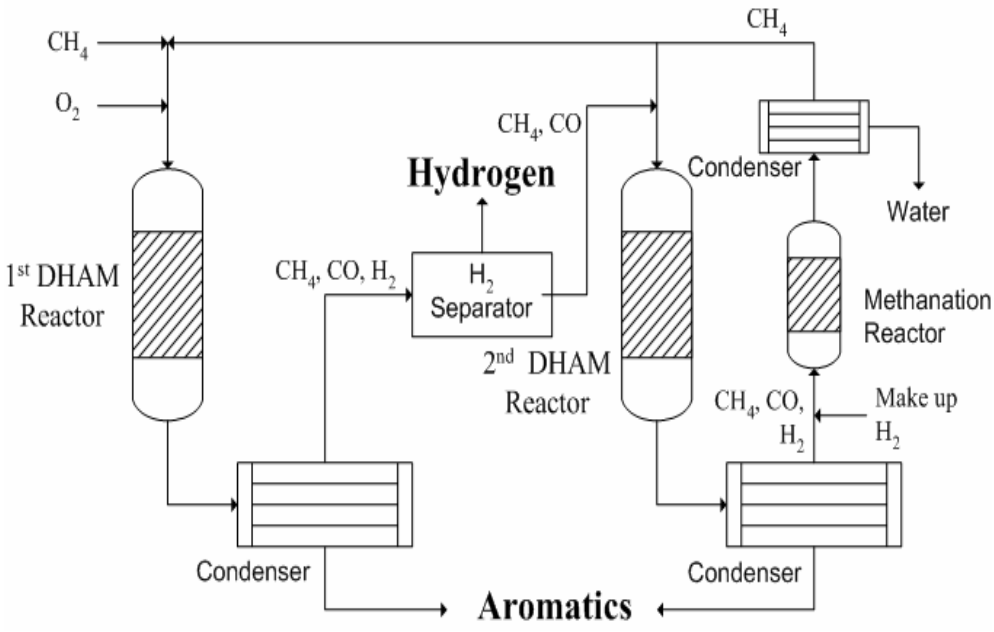

Figure 7.4: A schematic flow chart of proposed process configuration for methane conversion to aromatics and hydrogen.

7.4 Conclusions

The effects of system pressure, temperature and oxygen/methane mole ratio on the methane conversion and product distribution at equilibrium have been studied. The formations of CH_3OH, HCOH, CO_2, H_2O, paraffins and olefins are unfavorable at the selected temperature, pressure and oxygen/methane mole ratio. Meanwhile, CO, H_2 and aromatics are the major equilibrium products. In order to achieve high conversion and high aromatics yield, the system temperature should be kept as high as possible whilst the system pressure and oxygen/methane mole ratio should be low. The conversion of methane to aromatics and syngas is theoretically feasible at the selected temperature, pressure, and oxygen/methane ratio.

REFERENCES

[1] L. Wang, R. Ohnishi and M. Ichikawa, Catal. Lett. 62 (1999) 29.

[2] W. Liu and Y. Xu, 1999, J. Catal. 185 (1999) 386.

[3] V.T.T. Ha, L.V. Tiep, P. Meriaudeau, C. Naccache, J. Mol. Catal. A. 181 (2002) 283.

[4] J.L. Zeng, Z.T.Xiong, H.B.Zhang, G.D. Lin, K.R. Tsai, Catal. Lett. 53 (1998) 119.

[5] Z.T. Xiong, , H.B. Zhang , G.D. Lin and J.L. Zeng, Catal. Lett. 74 (2001) 233.

[6] Z.T. Xiong, L.L. Chen, H.B.Zhang, J.L. Zeng and G.D Lin, Catal. Lett. 74 (2001) 227.

[7] N.A.S. Amin and Kusmiyati, J. Nat. Gas Chem. 13 (2004) 148-159.

[8] Y. Shu, R. Ohnishi, M. Ichikawa, Appl. Catal. A 252 (2003) 315.

[9] H. Wang, G. H.u, H. Lei, Y. Xu, and X. Bao, Catal. Lett. 89 (2003) 1.

[10] S. Liu, L. Wang, R. Ohnishi, and M. Ichikawa, J. Catal 181 (1999) 175.

[11] J. Shu, A. Adnot, B.P.A. Grandjean, Ind. Eng. Chem. Res. 38 (1999) 3860.

[12] W. Zhang, D. Ma, X. Han, X. Liu, X. Bao, X. Guo, X. Wang, J. Catal. 188 (1999) 393.

[13] W. Liu, Y. Xu, S. Wong, L. Wang, J. Qiu, N. Yang, J. Mol. Catal. A. 120 (1997) 257.

[14] J. Yang, F. Deng, M. Zhang, Q. Luo, C. Ye, J. Mol. Catal. A. 202 (2003) 239.

[15] C.L. Zhang, S. Li, Y. Yuan, W.X. Zhang, T.H. Wu, and L.W. Lin, Catal. Lett. 56 (1998) 207.

[16] Y. Shu, Y. Xu, S.T. Wong, L. Wang, and X. Guo, J. Catal. 170 (1997) 11.

[17] P.L. Tan, Y.L. Leung, S.Y. Lai and C.T. Au, Catal. Lett. 78 (2002) 251.

[18] Y. Shu, R.Ohnishi, and M. Ichikawa, J. Catal. 206 (2002) 134.

[19] S. Yuan, J.Li, Z.Hao, Z.Feng, Q. Xin, P. Ying, and C. Lin, Catal. Lett. 63 (1999) 73.

[20] A. Lucas, J.L Valverde, P.Canizares and L.Rodriguez, Appl. Catal. A. 172 (1998) 165.

[21] A. Lucas, J.L.Valverde, P. Canizares and L. Rodriguez , Appl. Catal. A.184 (1999) 143.

[22] A. Lucas, J.L. Valverde, L. Rodríguez, P. Sanchez, M.T. Garcia, Appl. Catal. A. 203 (2000) 81.

[23] Aguiar, E. F. S., Appel, L. G. and Mota, C. (2005). Catal Today. 101, 3–7.

[24] Alkhawaldeh, A., Wu, X. and Anthony, R. G. (2003). Catal Today. 84, 43–49.

[25] Anunziata, O. A., Eimer, G. A. and Pierella, L. B. (1999). Catal Lett. 58, 235–239.

[26] Baba, T. and Abe, Y. (2003). Appl Catal A: Gen. 250, 265–270.

[27] Han, S., Palermo, R. E., Pearson, J. A. and Walsh, D. E. (1994). J Catal. 148, 134-137.

[28] Lunsford, J. H. (2000).*Catal Today*. 63, 165–174.

[29] Pierella, L. B., Wang, L. and Anunziata, O. A. (1997). React Kinet Catal Lett. 60,101-106.

[30] Szoke, A. and Solymosi, F. (1996) Appl Catal A: Gen.142, 361-374.

[31] Zaidi, H. A. and Pant, K. K . (2004). Catal Today. 96, 155–16

[32] K.A. Petersen, J.H. B. Hansen, T.S. Christensen, I. Dybekjaer, P.S. Christensen, C. S. Nielsen, S.E.L.W. Madsen, J.R.R. Nielsen, Appl. Catal. A, 221 (2001) 379.

[33] S. L. G. Cortes, J. Orozco, B. Fontal, Appl. Catal. A, 213 (2001) 259.

[34] V.R.Choudhary, S. Banerjee, D. Panjala, Microporous and Mesoporous Mater., 51 (2002) 203.

[35] H. Gonzalez, A. Rodriguez, L. Cedeno, J. Ramirez, J. Aracil, Ind. Eng. Chem. Res., 35 (1996) 3964.

[36] Y. S. Ooi, R. Zakaria, A. R. Mohamed, S. Bathia, Biomass and Bioenergy, 27 (2004) 477.

[37] D.C. Montgomery, Design and Analysis of Experiments, 5th ed., John Wiley and Sons Inc., New York, 2001.

[38] M.K. Mahat, R. M., Illias, R.A. Rahman, N.A.A. Rashid, N. A. N. Mahmood, O. Hassan, S.A. Aziz, K. Kamaruddin, Enzyme and Microbial Tech., 35 (2004) 467.

[39] Q.H. Chen, G.Q. He, M.A.M. Ali, Enzyme and Microbial Tech., 30 (2002) 667.

[40] B. Liu, Y. Yang, and A. Sayari, Appl. Catal. A: General 214, (2000) 95.

[41] Y. Lu, Z. Xu, Z. Tian, T. Zhang, and L. Lin. Catal. Lett. 62, (1999) 215

[42] S. Li, C. Zhang, Q. Kan, D. Wang, T. Wu,and L. Lin. Appl. Catal. A: General 187, (1999) 199.

[43] L. Chen, L. Lin, Z. Xu, X. Li, and T. Zhang, J. Catal. 157, (1995) 190.

[44] S. Wong, Y. Xu, W. Liu, L. Wang,and X. Guo, Appl. Catal. A: General 136, (1995)7.

[45] N.A. Saidina Amin and E. P. Soon, to be submitted to J. Tek, (2004).

[46] Y. Xu, X. Bao, and L. Lin, J. Catal. 216, (2003) 386.

[47] R.Ohnishi, S.Liu, Q.Dong, L.ang, and M. Ichikawa, J. Catal. 182, (1999) 93.

[48] N.A. Saidina Amin and D.D. Anggoro. Fuel 83, (2002) 83.

[49] N.A. Saidina Amin and Kusmiyati. To be published to J. Nat. Gas Chem.

[50] B.M. Weckhuysen, D. Wang, M. P. Rosynek, and H. Lunsford, J. Catal. 175, (1998) 347.

[51] L. Mleczko, M. Baerns, Fuel Process. Technol. 42 (1995) 217.

[52] J.P. Ramirez, J.M.G. Cortes, F. Kapteijn, M.J.I. Gomez, A. Ribera, C.S.M.D. Lecea, J.A. Moulijn, Appl. Catal. B 25 (2000) 191.

[53] J.H. Lee, J.G. Kim, J.K. Lee, J.H. Kim, Catal. Today 87 (2003) 35.

[54] M. Asadullah, T. Miyazawa, S.I. Ito, K. Kunimori, M. Yamada, K. Tomishige, Appl. Catal. A. 267 (2004) 95.

[55] J. Zhu, M.S.M.M. Rahman, J.G.V. Ommen, L. Lefferts, Appl. Catal. A 259 (2004) 95.

[56] M. Traykova, N. Davidova, J.S. Tsaih, Appl. Catal. A 169 (1998) 237.

[57] V.R. Choudhary, V.H. Rane, T. Chaudhari, Appl. Catal. A 158 (1997) 121.

[58] S. Lacombe, C. Geantet, C. Mirodatos, J. Catal. 151 (1994) 439.

[59] S. Kus, M. Otremba, M. Taniewski, Fuel 82 (2003) 1331.

[60] V.R. Choudhary, V.H. Rane, S.T. Chaudhari, Fuel 79 (2000) 1487.

[61] S. Lacombe, C. Geantet ,C. Mirodatos. J. Catal.155 (1995) 106.

[62] S. Kus, M. Otremba, A. Torz, M. Taniewski. Fuel 81 (2002) 1755.

[63] V.R. Choudhary, V.H. Rane, Catal Lett 4 (1990) 101.

[64] D.Z. Wang , X.D. Lu, X.Y. Dou, W.B. Li, C.H.Yang, Appl. Catal. 59 (1990) 75.

[65] S. Jeong, K.J. Fisher, R.F. Howe, G.D. Willett, Microporous Mesoporous Mater. 22 (1998) 369.

[66] P. Yarlagadda, C.R.F. Lund, E. Ruckenstein, Appl. Catal. 62 (1990) 125.

[67] T. Baba, Y. Abe. Appl. Catal. A 250 (2003) 265.

[68] A. Alkhawaldeh, X. Wu, R.G. Anthony, Catal. Today 84 (2003) 43.

[69] P. Tynjala, T.T. Pakkanen, Microporous Mesoporous Mater. 20 (1998) 36.

[70] X. Guo, J. Shen, L. Sun, C. Song, X. Wang. Appl. Catal. A 261 (2004) 183.

[71] F. Lonyi, J. Valyon, Microporous Mesoporous Mater. 47 (2001) 111.

[72] N.A.S. Amin, Kusmiyati, J. Nat. Gas Chem. 13 (2004) 148.

[73] S. Schwarz, M. Kojima, C.T. O'Connor, Appl. Catal. 56 (1989) 263.

[74] A. Corma, Chem. Rev. 95 (1995) 559.

[75] A.V. Ivanov, G.W. Graham, M. Shelef, Appl. Catal. B 21 (1999) 243.

[76] L.J. Lobree, I.C. Hwang, J.A. Reimer, A.T. Bell, J. Catal.186(1999) 242.

[77] E. Xing, Z. Mi, C. Xin, L. Wang, X. Zhang, J. Mol. Catal. A: Chem. 231 (2005) 161.

[78] S.M. Campbell, D.M. Bibby, J.M. Coddington, R.F. Howe, R.H. Meinhold, J. Catal. 161 (1996) 338.

[79] P.L. Tan, Y.L. Leung, S.Y. Lai, C.T. Au, Appl. Catal. A 228 (2002) 115.

[80] J. Erena, J.M. Arandes, J. Bilbao, A.G. Gayubo, H.I.D. Lasa, Chem. Eng. Sci. 55 (2000) 1845.

[81] V.R. Choudhary, S.A.R. Mulla, V.H. Rane, Appl. Energy 66 (2000) 51.

[82] R.D. Samarth, S.Y. Chen, K.M. Dooley, Appl. Catal. B 5 (1994) 71.

[83] P. Pareja, S. Molina, A. Amariglio, H. Amariglio, Appl. Catal. A 168 (1998) 289.

[84] M.Y. Sinev, Catal. Today 24 (1995) 389.

[85] V.I. Vedeneev, O.V. Krylov, V.S. Arutyunov, V.Y. Basevich, M.Y. Goldenberg, M.A.T. Boim, Appl. Catal. A 127 (1995) 51.

[86] R. Sethuraman, N.N. Bakhsi, S.P. Katikaneni, R.O. Idem, Fuel Process. Technol. 73 (2001) 197.

[87] E.P.J. Mallens, J.H.B.J. Hoebink, G.B. Marin, Catal. Today 24 (1995) 225.

[88] G.A. Martin, C. Mirodatos, Fuel Process. Technol. 42 (1995) 179.

[89] A. Corma, J.M.L., J. Mol. Catal. A: Chem. 123 (1997) 75.

[90] A.A. Davydov, M.L. Shepotko, A.A. Budneva, Catal. Today 24 (1995) 225.

[91] V.T.T. Ha, L.V. Tiep, P. Meriaudeau, C. Naccache, J. Mol. Catal. A: Chem. 181 (2002) 283.

[92] W.J.H. Dehertog, G.F. Fromen, Appl. Catal. A 189 (1999) 63.

[93] A.G. Anshits, E.V. Kondratenko, E.N. Voskresenskaya, L.I. Kurteeva, N.I. Pavlenko, Catal. Today 46 (1998) 211.

[94] T. Karasuda, K. Aika, J. Catal. 171 (1997) 439.

[95] H. Borchert, M. Baerns, J. Catal. 168 (1997) 315.

[96] V.R. Choudhary, S.A.R. Mulla, B.S. Uphade, Fuel 78 (1999) 427.

[97] S. Pak, P. Qiu, J.H. Lunsford, J. Catal. 179 (1998) 222.

[98] T. Sano, Y. Uno, Z.B. Wang, C.H Ann, K. Soga, Microporous Mesoporous Mater. 31 (1999) 89.

[99] O. Kresnawahjuesa, G.H. Kuhl, R.J. Gorte, C.A. Quierini, J. Catal. 210 (2002) 106.

[100] S.N. Vereshchagin, K.P. Dugaev, N.P. Kirik, N.N. Shishkina, A.G. Anshits, Catal. Today 24 (1995) 349.

[101] Z. Tian, Y. Xu, L. Lin, Chem. Eng. Sci. 59 (2004) 1745.

[102] O.A. Anunziata, G.A. Eimar, L.B. Pierella, Appl. Catal. A 190 (2000) 71.

[103] J.A. Barbero, M.A. Banares, M.A. Pena, J.L.G. Fierro, Catal. Today 71 (2001) 11.

[104] A.V. Kucherov, A.A. Slinkin, M.S. Kharson, T.N. Bondarenko, K.M. Minachev, J. Mol. Catal. 53 (1989) 293.

[105] Y.H. Hu, E. Ruckenstein, J. Catal. 158 (1996) 260.

[106] A.D. Lucas, J.L. Valverde, P. Canizares, L. Rodriguez, Appl. Catal. A 172 (1998) 165.

[107] Y. Xu and L. Lin:. Appl. Catal. A: Gen., **188**, 53 (1999).

[108] Wang, Y. Xu, S.T. Wong, W. Cui, X. Guo: Appl. Catal. A: Gen., **152**. 173 (1997).

[109] L. Wang, R. Ohnishi and M. Ichikawa: Catal Lett., **62**, 29 (1999).

[110] L. Wang, L. Tao, M. Xie, G. Xu, J. Huang, Y. Xu: Catal. Lett. , **21**, 35 (1993).

[111] L. Chen, L. Lin, Z. Xu, X. Li, T. Zhang: J. Catal., **157**, 190 (1995).

[112] R. Ohnishi, S. Liu, Q. Dong, L.Wang, and M. Ichikawa: J. Catal., **182**, 92 (1999).

[113] M. C. Iliuta, I. Iliuta, B. P. A. Grandjean, and F. Karachi: Ind. Eng. Chem. Res., **42**, 3203 (2003).

[114] V.R. Choudary, P. Devadas, S.B. Banerjee, A.K. Kinage,: Microporous and Mesoporous Materials, **47**, 253 (2001) .

[115] H. Lunsford and M.P. Rosynek, J. Catal. **169**, 347 (1997).

[116] B.M. Weckhuysen, D. Wang, M.P. Rosynek and J.H. Lunsford: J. Catal., **175**, 338 (1998).

[117] O. A. Anunziata, G. A. Eimer and L. B. Pierella: Catal. Lett , **58**, 235 (1999).

[118] Kusmiyati, N A S Amin: Catal. Today, **106**, 271 (2005).

[119] J. Hutching, M.S. Scurrell, Methane Conversion by Oxidative Processes, New York: Van Nostrand Reinhold, 1998.

[120] M.A. Banares, Catal. Today 51 (1999) 319.

[121] W. Ye, O.Kiyoshi, J. Catal. 155 (1994) 256.

[122] Q. Liu, J.Rogut, B.Chen, J.L. Falconer, R.D. Noble, Fuel 75 (1995) 1748.

[123] T.J.Hall, J.H.J. Hargreaves, G.J.Hutchings, R.W.Joyner, S.H.Taylor, Fuel Process. Technol. 42 (1995) 151.

[124] R.L. McCormick, B.A.Mohammad, G.O.Alptekin, Appl. Catal. A 226 (2001) 129.

[125] G.E. Keller, M.M. Bhasin, J. Catal. 73 (1982) 9.

[126] Y. Xu, L. Lin, Appl. Catal. A 188 (1999) 53.

[127] S.S. Shepelev, K.G. Ione, Reaction Kinetic. Catal. Lett. 23 (1983) 323.

[128] J.R. Anderson, P. Tsai, Appl. Catal. A 19 (1985) 141.

[129] S. Han, D.J. Martenak, R.E. Palermo, J.A. Pearson, D.E. Walsh, J. Catal. 148 (1994) 134.

[130] S. Li, C. Zhang, Q. Kan, D. Wang, T. Wu, L. Lin, Appl. Catal. A 187 (1999) 199.

[131] N.A.S. Amin, D.D. Anggoro, Fuel 83 (2002) 487.

[132] N.A.S. Amin, D.D. Anggoro, J. Nat. Gas Chem. 12 (2003) 123.

[133] S H Chan, H M. Wang. Int J Hydrogen Energy 25 (2000) 441.

[134] A E, Lutz, R. W. Bradshaw, J. O Keller Int J Hydrogen Energy 2003, 28: 159.

[135]Lutz A E, Bradshaw R W, Bromberg L et al. Int J Hydrogen Energy, 2004, 29: 809.

[136] J. Zhu, D. Zhang, K.D. King, Fuel 80 (2000) 899

[137] Y. Lwin, W.R. Daud, A.B. Mohamad, Z. Yaakob, Int. J. Hydrogen Energy 25 (2000) 47

[138] Douvartzides S L, Coutelieris F A, Demin A K et al. AIChE J, 2003, 49: 248.

[139] Chan S H, Wang H M. J Power Sources, 2004126:8.

[140] Liu W Ch, Xu Y P, Tian Z J et al., J Nat Gas Chem, 2003, 12:237

[141] J.M. Smith, H.C.V. Ness, M.M. Abbott, Introduction to Chemical Engineering Thermodynamics, 5th Edition. New York: The McGraw-Hill Companies, 1996.

[142] R.A. Alberty, C. A. Gehrig, J. Phys. Chem. 3 (1984) 1173.

[143] R.A. Alberty, C. A. Gehrig, J. Phys. Chem. 14 (1985) 803.

[144] R.A. Alberty, J. Phys. Chem. 14 (1985) 177.

[145] L.V. Gurvich, V.S. Iorish, V.S. Yungman, O.V. Dorofeeva, Thermodynamic Properties as a Function of Temperature, CRC Handbook of Chemistry and Physics, 75th Edition. Boca Raton: CRC Press, 1995.

[146] H. Zhang, J. Zeng, Z. Xiong, G. Lin, K.R. Tsai, J. Catal. Lett. 53 (1998) 119.

[147] Istadi and N.A.S.Amin, J. Nat. Gas Chem, 14, (2005) 140.

[148] P.L. Tan, Y.L. Leung, C.T. Au, Catal. Lett. 78 (2002) 251.

[149] S. Yuan, J. Li, Z. Hao, Z. Feng, Q. Xin, P. Ying, C. Li, Catal. Lett. 63 (1999) 73.

[150] Y. Liu, J. Lin, K.L. Tan, Catal. Lett. 50 (1998) 165.

[151] R. Ohnishi, S. Liu, Q. Dong, L. Wang, M. Ichikawa, J. Catal. 182 (1999) 92.